The role of CD39 in cardiovascular disease

by

Matthew Craig Hyman

A dissertation submitted in partial fulfillment
of the requirements for the degree of
Doctor of Philosophy
(Molecular and Integrative Physiology)
in The University of Michigan
2009

Doctoral Committee:

       Professor David J. Pinsky, Chair
       Professor Steven L. Kunkel
       Professor Daniel A. Lawrence
       Professor Richard M. Mortensen
       Assistant Professor Daniel E. Michele

For Mom, Dad, Jon, Jeremy, Nana and Pop
who have always pushed me to excel
and never wavered in their support

And most of all,
for Kristin,
whose friendship and love
have made me a better person

ACKNOWLEDGEMENTS

Throughout these last four years I have become indebted to numerous people. I have invested a lot of my heart and time in this thesis, but each of these people has given of themselves to help me throughout this process.

My mentor David Pinsky has been critical to my development as a scientist. He has led by example, showing me that you are never old enough to stop learning. Very early on David set the precedent that my training was his highest priority and it is that support that has profoundly shaped and nurtured my scientific growth. More importantly, David is one of the few people I know that seems to sincerely care more about the success of those around him than his own personal advancement, which I find incredibly unique. Above all of these other things, I would like to thank David for his friendship over these last 4 years and hopefully into the future.

To the Pinsky Lab as a whole, you have impacted me more than I can describe. Whether it be socially as a new group of friends or scientifically as an invaluable repository of scientific knowledge and techniques, I am not quite sure where this thesis would be without each of you. In particular I would be remiss in not thanking Hui Liao for his patience in teaching me almost every molecular biology technique I know (and many of them twice). I also must thank the incomparable Danica Petrovic-Djergovic without whom I never would have finished the cerebral ischemia project.

Finally to my family, Mom, Dad, Jon, Jeremy, Nana, and Pop, you have seen me through not just the last four years, but also the last 28 years. I owe you so much more than anyone else on these pages. Together, you have a raised me and molded me into the person that I am today and for that I am forever in your debt. Thank you for your support and thank you for your faith, which have instilled a confidence in me to pursue whatever I want in life.

And last, but very far from least, Kristin, you are the love of my life. There are too many things to say, and too many things I should acknowledge, so I will just say thank you.

TABLE OF CONTENTS

LIST OF FIGURES

Figure

ABSTRACT

The role of CD39 in Cardiovascular Disease

by

Matthew C. Hyman

Chair: David J. Pinsky

While ATP and ADP are traditionally thought of as energy intermediaries in the intracellular space, these nucleotides primarily act as signaling molecules in the extracellular space. By engaging purine receptors on the surface of leukocytes and endothelium in the vasculature, ATP and ADP can elicit inflammatory and pro-thrombotic responses. CD39, an ecto-enzyme, rapidly metabolizes extracellular nucleotides to suppress purinergic signaling cascades. Though it is well established that CD39 regulates ADP-driven thrombosis, it remained unclear whether CD39 participates in ATP/ADP driven inflammation. This led to the hypothesis that CD39 is a critical regulator of inflammation through the catabolism of extracellular nucleotides. Studies of macrophage and neutrophil flux into post-ischemic brain tissue and of atherosclerotic plaque development revealed a novel role for CD39 in the regulation of leukocyte activation. Leukocyte surface CD39 degrades ATP that would otherwise activate the $P2X_7$ receptor, leading to a suppression of both the adhesion molecule

$\alpha_M\beta_2$-integrin and the scavenger receptors SRA-1 and CD36. In the setting of ischemic stroke, CD39's mediated-reduction of adhesion molecule expression manifests as a profound suppression of leukocyte recruitment into the ischemic brains, and a concordant decrease in ischemic tissue damage. In the setting of atherosclerosis, CD39's inhibition of scavenger receptor expression limits foam cell formation and ultimately atherogenesis. In addition to modulation of leukocyte function, CD39 was shown to regulate platelet activation in both ischemic stroke and atherogenesis. Further exploration of atherosclerotic plaques revealed that laminar shear stresses, imparted by flowing blood, potently induce the expression of CD39 on the vascular endothelium in a mechanism partially dependent on Kruppel-Like Factor 2. These laminar shears create regionalization to CD39 expression and may impart certain vascular regions with either a resistance or predisposition to thrombosis and inflammation. In total, this thesis has identified extracellular nucleotide metabolism as a novel endogenous regulator of acute and chronic inflammation with implications for a variety of cardiovascular and other disease processes.

CHAPTER I

CD39: MEDIATOR OF EXTRACELLULAR NUCLEOTIDE METABOLISM

Introduction

ATP and ADP are commonly viewed as intracellular energy intermediaries, yet in the extracellular space adenine nucleotides play a different role. While intracellular nucleotides primarily serve as energy depots, extracellular nucleotides primarily function as signaling molecules[1]. These nucleotides act by engaging cell surface purine sensitive receptors, where they elicit tailored and precise responses ranging from immune cell activation, to lamellipodial extension, to heterotypic cellular adhesion[2-4]. Thus purine signaling cascades coordinate the activation of neighboring cells in an autocrine and paracrine fashion.

Purine signaling is similar in many ways to other forms of extracellular communication, yet with one key distinction. Classic cell-cell signaling by cytokines and chemokines continue for the duration of the cognate receptor-ligand interaction, with downregulation of signaling dictated by passive on-off kinetics of this interaction. In contrast, nucleotide-driven signaling can be rapidly quenched by cell surface nucleotidases which dissipate ambient levels of purinergic signaling agonist. The half life of ATP and ADP in the blood is on the order of seconds, due to the activity of cell surface apyrases[5]. In the vasculature, CD39 is the dominant nucleotidase[6-9], where due to its expression on the cell

surface characterizes it as an "ecto-enzyme." The ecto-enzyme CD39 quenches purine signals by catalyzing the terminal phosphohydrolysis of both ATP and ADP, yielding AMP, and thus dissipating the tri- and di-phosphorylated agonists for purine receptor activation. Thomboregulation[10], ischemic tissue injury[11-13], and inflammation[14] are each mediated in part by extracellular nucleotides; and in each, CD39 could modulate these conditions by quickly metabolizing ATP and ADP. Thus, CD39 may be protective in pathologic situations driven by the signaling of extracellular nucleotides.

From a teleologic standpoint, it is somewhat counter-intuitive that an enzyme evolved on the surface of cells to degrade extracellular nucleotides. Phosphorylated nucleotides are a precious, high-energy intracellular resource, which are generated following great effort by a cell. Once generated, these intracellular nucleotides accumulate at micromolar quantities establishing a steep concentration gradient between the outside and inside of the cell. This serves two purposes: 1) Acting as an intracellular energy depot for driving cellular metabolism; 2) Providing a ready source of nucleotide signaling molecules to mediate autocrine and paracrine signaling. This second function likely evolved as a response to cellular lysis or apoptosis where large intracellular stores of nucleotides were released into the extracellular space. Neighboring cells likely developed receptors to sense this local damage establishing the earliest forms or purinergic signaling. In addition to cell death, adenine nucleotides are released by other more regulated methods such as in response to cell-surface receptor engagement, flickering of ligand and ion gated channels, and even a slow basal leakage that is thought to occur in most cells.

A diversity of processes are regulated by purine signaling, and each of their cascades converge upon a few common agonists, i.e. ATP and ADP. This suggests the existence of critical adaptive functions of extracellular nucleotides, the levels of which must be tightly regulated. Given this commonality, CD39 and other ecto-enzymes are poised to regulate purine signaling and vascular homeostasis as a whole in a highly efficient manner. One example of this would be endothelial CD39, which can regulate not only the activation of platelets by ADP[6,11,15], but also the activation of the endothelial cell itself by ATP[16,17]. This suggests an inherently elegant signaling scheme wherein purine signals on the surface of a cell are rapidly dissipated by an enzyme on that very same cell's surface. For these reasons, we and others have used this concept to harness nature's own tools using recombinant CD39 peptides to provide exogenous supplementation of nucleotidase activity when the integrity of the endogenous nucleotidase system is insufficient, such as in the setting of ischemic stroke, thrombotic disorders, and transplant-associated ischemic tissue injury.

This thesis will explore the cytoprotectant role of the nucleotidase CD39. In doing so, I will address the intersection between CD39 and purinergic signaling in the areas of thromboregulation, cerebroprotection, immunomodulation, atherogenesis, and ischemic injury.

CD39 Background

CD39 is a glycoprotein, found on the surface of various cells[18], that was originally identified as a marker of B-cell activation[19,20]. Since that time, CD39 has been identified on numerous cells in addition to B cells ranging from natural killer cells[21], T cells[21],

monocytes[21], neutrophils[22], endothelium[21], cardiomyoctes, neurons, smooth muscle cells[23], Langerhan's cells[14], and mesangial cells. When initially cloned, a strong sequence similarity was noted between CD39 and the guanosine diphosphatase *GDAI* from yeast (*Saccharomyces cerevisiae*)[18]. This suggested that CD39 was not only a phenotypic marker, but also an enzyme. Wang and Guidotti later demonstrated that lymphocyte CD39 is an E-type ecto-apyrase, i.e. CD39 metabolizes both ATP and ADP in a Ca^{2+}- and Mg^{2+}-dependent fashion to yield AMP[24]. CD39's affinity for ATP and ADP is not equal, though, as ATP is metabolized slightly faster than ADP $(1.7:1)$[24]. It is important to note that when CD39 sequentially metabolizes ATP to AMP, it does so in a concerted step. At no point is the ADP intermediate thought to be released and then recaptured by CD39, despite the difference in phosphohydolysis rates for ATP and ADP[25]. CD39 is the predominantly expressed vascular apyrase, and consequently is thought to play a principal role in the regulation of the blood streams nucleotide milieu.

CD39 is situated in the cell plasmalemma, with intracellular amino- and carboxy-terminal ends, two transmembrane domains, and an extracellular loop[18]. The exact function of the intracellular amino and carboxy-terminal ends is unclear, but the amino-terminal Cys^{13} of CD39 can be palmitoylated. This thioester-linked lipid modification is important for localizing CD39 to microdomains of the cell membrane called caveolae[26]. Caveolae are pouch-like, membrane invaginations that act as specialized signaling domains which integrate external stimuli into internal activation through clustering of various components of a signaling cascade. In caveolae, CD39 is colocalized with the AMPase CD73[27,28]. This is thought to coordinate the transfer of AMP, the final product of CD39, to the AMPase CD73,

allowing efficient generation of adenosine. Purine sensitive receptors such as the $P2Y_1$ receptor can be found in the very same caveolae, in close proximity to both CD39 and CD73[28]. This implies that the action of CD39 and CD73 could be occuring in concert to regulate purinergic signaling at the surface of a cell – CD39 through consumption of receptor agonists and CD73 through production of receptor agonist. It is of note that ATP and ADP responsive receptors (P2) tend to elicit pro-inflammatory and pro-thrombotic cellular responses[29], whereas adenosine responsive receptors (P1) tend to elicit anti-inflammatory cellular responses[30]. Thus, CD39 is able to take a pro-inflammatory stimulus and sequentially convert it into a homeostatic, anti-inflammatory signal. These actions of CD39 are graphically illustrated in **Figure 1.1**.

CD39: Structure and Function

CD39 is structurally homologous to numerous nucleotidases throughout the plant and animal kingdoms. In addition to high sequence similarity with yeast GDPase[18], CD39 shares similarity with mutiple protozoan NTPases (*Toxoplasma gondii*)[31], mosquito saliva apyrase (*Aedes aegypti*)[32], potato tuber apyrase (*Solanum tuberosum*)[33], garden pea NTPase (*Pisum sativum*)[33], and fruit fly NTPase (*Drosophila melanogaster*)[34]. Looking specifically at humans, CD39 is only one member of a family of ectonucleotidases known as ecto-nucleoside triphosphate diphosphohydrolases (E-NTPDases). Each member of the E-NTPDase gene family has a unique distribution of expression and enzymatic capability. CD39, for example, degrades ATP only slightly more efficiently then ADP (1.7:1), whereas CD39L1, another E-NTPDase family member, degrades ATP much more efficiently than ADP (6:1)[35]. Even so, despite functional differences between E-NTPDase family members,

they each retain the five highly conserved domains, known as apyrase conserved regions (ACRs I-V)[33]. This conservation led to the theory that these domains are necessary for CD39's enzymatic function[36,37].

To understand how the amino acid sequence of CD39 enables it to cleave phosphates and simultaneously confers it with substrate specificity, multiple labs have used site-directed mutagenesis to explore the structure of CD39. As the ACRs are a common motif of ectonucleotidases, initial mutational studies were focused here. The amino acid sequences of ACR I and ACR IV contain a 'DXG' phosphate binding motif, a motif common to the actin family of NTPases[37]. The 'DXG' motif in actin is thought to bind and stabilize phosphyorylated nucleosides. Accordingly, mutation of the aspartate residue or the glutamate residue within the ACRs of CD39 resulted in a molecule with severely diminished or absent catalytic activity[37]. This suggests that ACRs I and IV are critical for stabilizing the interaction of CD39 and ATP at ATP's β- and γ-phosphates, respectively, during phosphate cleavage[37,38]. Two other ACR residues, Glu[174] (ACR III) and Ser[218] (ACR IV) (in a soluble form of CD39), are also necessary for enzyme function[39]. Although the role of these residues in CD39's enzymatic activity is unknown, it has been noted that the homologous glutamate in ACR III and serine in ACR IV are critical for enzymatic function in other E-NTPDase family members as well[40]. Not all ACR mutations resulted in loss of function, though, as transmutation of Ser[57] to Ala (ACR I) resulted in a 100% increase in ADPase activity[39]. Conserved amino acids, outside of the ACRs also have been mutated, but these experiments have produced dichotomous results. Substitution of Trp[187] with alanine resulted in a loss of protein folding, and consequent reduction in CD39 protein export and surface expression. In

contrast, substitution of Trp[459] with alanine resulted in heightened ATPase activity with simultaneous loss of ADPase activity[41].

Taken together these studies demonstrate that the conserved amino acid sequences of ectonucleotidases do play a role in enzyme function. However, these studies have been unable to explain how homologous ectonucleotidases with nearly identical amino acid sequences have such varied affinity for individual nucleotides. The first study to shed light on this question involved the mutation of His[59] in rat CD39. Mutation of His[59] resulted in a near total loss of enzyme activity. Significantly, if the transmembrane domains of CD39 were removed, this effect was abrogated.[42]. These results implied that the transmembrane domains of CD39 (and thus the tertiary and quaternary structure) play a large role in its functional activity.

Having two transmembrane domains is a common motif of numerous pores and channels but unique for an ecto-apyrase[43]. Most ecto-aspyrases possess only one transmembrane domain, yet when either or both of CD39's transmembrane domains are removed there is a greater than 90% loss of apyrase activity[44]. This is partly attributed to the fact that native CD39 is found in tetramers that are coordinated by the intramolecular and intermolecular interactions of their transmembrane domains (though CD39 is shown as a monomer for the sake of simplicity in **Figures 1.1** and **1.2**) [44,45]. These interactions are important for the arrangement of the individual CD39 subunits, but also for allowing free rotation of the transmembrane helices upon each other. This rotational mobility is thought to allow for accommodation of the incoming nucleotide and its subsequent catalysis by

CD39[35,45]. Furthermore, when multimerized, the CD39 subunits synergize to produce greater enzymatic activity than four monomers would alone[44]. Of great interest is the concept that the specificity of CD39 for ATP and ADP is also dictated by the transmembrane helices. In fact, transfer of CD39's transmembrane domains to another ecto-apyrase yields protein a with identical ATPase and ADPase activity as native CD39, despite a different extracellular loop[35,46]. These studies show that both the activity and specificity of CD39 are dependent upon the tertiary and quaternary protein structure of CD39, including transmembrane domain structure and interaction with adjacent CD39 molecules.

The transmembrane interactions of CD39 are further responsive to the lipid bilayer itself, as well as its membrane constituents. Membrane cholesterol composition directly correlates with the elasticity and fluidity of the lipid bilayer. By modulating transmembrane helix movement and interactions, membrane cholesterol depletion results in a loss of CD39 activity[47,48]. In a scheme similar to the activation of integrins, CD39 can switch between a less active conformational state and a more active conformational state. In the case of CD39, membrane flexibility and fluidity is thought to preferentially stabilize different conformational states. Other membrane constituents such as free fatty acids can also modulate the ATPDase activity of CD39. Monounsaturated and saturated fatty acids increase ATPDase activity of endothelial cells, whereas polyunsaturated fatty acids diminish the ATPDase activity of endothelium[49]. Similar to the studies with cholesterol, fatty acids are though to modulate CD39 activity through changes in membrane flexibility. Finally, the intracellular signaling molecule Ran Binding Protein M (RanBPM) can also regulate CD39 activity. RanBPM is a broadly expressed nuclear and cytosolic protein that was originally

cloned as a protein bound to Ran. Ran is classically appreciated for its role in nuclear pore translocation and binding of GTP. It is thought that RanBPM can bind to the amino-terminus of CD39, thereby altering the structural conformation to decrease ecto-apyrase activity[50].

The extracellular loop of CD39 contains 7 *N*-glycosolation sites that allow for substantial post-translational modification of the protein. Deglycosylation with *N*-glycanase reduces the molecular weight of CD39 to a molecular mass of 54 kD; in contrast the glycosylated form has a size ranging from 70 to 100 kD [21]. These substantial glycosolations are thought to serve two main purposes. First, the *N*-linked glycosolations are critical for facilitating export from the endoplasmic reticulum and trafficking to the surface of the cell[51,52]. Second, some *N*-glycosolation sites (1, 4, and 7) have been shown to be critical for conferring specific activity to CD39, i.e. they affected protein structure but not surface expression. It is not surprising, therefore, that these sites (1, 4, and 7) are conserved in the CD39 of humans, mice rats, cows, pigs and chickens[53]. Other N-linked glycosolation sites (2, 3, 5, 6) are not as well conserved between species.

The apyrase CD39 has been postulated to play additional roles in cell physiology beyond its ability to metabolize nucleotides. As mentioned previously, the intracellular protein RanBPM can associate with the amino-terminal end of CD39. The association of these two proteins has led to speculation that CD39 may actually play a role in signal transduction[50]. This idea has been reinforced by experiments showing that engagement of B cell surface CD39 with an antibody leads to homotypic B cell adhesion events[21,54]. The

signaling events that transmit the extracellular engagement of CD39 to the intracellular space remain unclear, but it is known that the B-cell clustering phenomenon is tyrosine kinase-dependent[54]. One additional, potential function of CD39 is as a cell membrane ATP channel. CD39 is structurally unique as an apyrase for having two transmembrane domains with one extracellular loop, features which make it similar to numerous cell membrane pores and channels [43]. As CD39 multimerizes in the plasmalemma in tetrameric groupings, this suggests the possibility of ATP pore formation. Furthermore, hyperpolarization of *Xenopus* oocytes transfected with human CD39 promotes the release of intracellular ATP [55].

CD39 and Thromboregulation

Adenosine diphosphate (ADP) was the first molecule identified as an activator of circulating platelets[56]. Subsequently, other agonists such as collagen and thrombin have been shown to activate platelets as well[57]. Yet, for each of these agonists, the auto-activation that characterizes platelet thrombus formation is dependent upon ADP signaling. ADP, released from the α–granules of activated platelets, is the primary means by which one platelet communicates with another to initiate a secondary wave of platelet activation and stabilize thrombus formation[58,59]. For many years, the precise platelet receptor(s) agonized by ADP remained unknown, but recent work has identified the $P2Y_1$ and $P2Y_{12}$ receptors as mediators of ADP's effects[60]. Both of these receptors are G-protein coupled receptors: the $P2Y_1$ receptor stimulates the G_q subunit to mediate platelet calcium flux[61,62], and the $P2Y_{12}$ receptor stimulates the G_i subunit to lower intra-platelet cAMP levels[60]. The signaling pathways initiated by these two receptors synergize to facilitate platelet aggregation. The $P2Y_{12}$ receptor is also important for

sensitizing platelets to activation by other agonists[58,59]. An entire class of anti-platelet therapies, known as thienopyridines (e.g., clopidigrel and ticlopidine), targets the $P2Y_{12}$ receptor and has proven to be one of the most effective anti-thrombotic medicines available, particularly for platelet-dependent thromboprophylaxis.

It was noted many years ago that when a platelet comes within the proximity of an endothelial cell, the platelet's sensitivity to ADP-induced activation was severely muted[6,7]. At the time it was also known that endothelia release numerous factors such as nitric oxide and prostaglandin that can suppress platelet reactivity. However, closer examination revealed that inhibition of both of these pathways did not abrogate the endothelia's ability to prevent ADP-induced platelet aggregation[7]. Moreover, endothelial cells could prevent platelet activation without coming in direct contact with the platelets so long as the ADP agonist was pre-incubated with the endothelial cells. The explanation for this phenomenon was revealed by thin layer chromatography showing that radiolabelled ADP is rapidly degraded in the presence of endothelial cells to AMP, adenosine, inosine, and finally hypoxanthine[6,7]. The factor responsible for the catabolism of ADP was later cloned by two different groups and identified as the ecto-enzyme CD39[6,8].

Once identified, CD39 was shown to directly regulate platelet function in numerous studies. Transfection of CD39 into COS-7 cells (a cell line without native CD39) imbued these cells with the ability to not only rapidly degrade ATP and ADP, but also inhibit the activation of platelets[6,8]. Targeted ablations of CD39 in mice, however,

yielded a paradoxical phenotype. Though it was theorized that an abundance of accumulated ADP would lead to enhanced aggregation and spontaneous thrombosis, CD39-null mice exhibited prolonged bleeding times and a resistance to clotting [11,15]. Subsequent experiments showed that this unexpected phenotype mice was due to desensitization of the ADP sensitive receptors on the surface of platelets [11,15]. Furthermore, the desensitization of ADP receptors in CD39-null mice could be recued transiently by intra-peritoneal injection of a soluble potato homolog of CD39[15,33]. In other studies, CD39-null mice, when challenged with cerebral ischemia CD39-null mice exhibit an underlying pro-thrombotic phenotype that results in enhanced platelet deposition in the brains of ischemic mice[11].

Currently there are several pharmacotherapeutics that are highly effective at suppressing thrombosis and platelet-activation, but with limitations. In general, these limitations arise because the anti-thrombotic medications work by directly preventing activation of the platelet itself. Clopidogrel and abciximab, for example, act by preventing ADP induced platelet at the platelet surface P2Y12 receptor or platelet aggregation by blocking the function of the adhesion molecule GPIIb/IIIa respectively. These drug strategies that target the platelet itself are highly effective in preventing unwanted platelet activation, yet they are confounded by simultaneously preventing the normal platelet function that is a part of maintaining vascular homeostasis. CD39 is unique in this regard as it is able to limit platelet activation without acting on the platelet itself. In contrast to clopidigrel which blocks the ADP receptor on the platelet's surface, CD39 dissipates the ADP before it can even encounter the platelet. Thus platelet

function is not affected and hemorrhagic complications should be reduced.   revelation that CD39 is an endogenous regulator of both of these things has led to Clinically thrombosis and aberrant platelet activation can complicate numerous conditions such as ischemic stroke and transplantation, which has led to the development of . and Though numerous other *in vivo* agents regulate thrombosis and maintain vascular homeostasis, CD39 is unique in that it does can accomplish these roles without interacting directly with the platelet itself. In other words, if a patient were treated with a recombinant form of CD39, a denuded section of endothelium would still be able to attract and bind platelets through collagen activation, thus homeostasis is maintained. CD39 would only begin to exert its effects on the subsequent and explosive accumulation of platelets at that site. To this end, a recombinant form of CD39 (solCD39), missing the transmembrane domains, was developed and shown to dissipate ADP and prevent platelet activation[63]. When applied therapeutically, solCD39 was able to significantly diminish the post-ischemic accumulation of platelets (and thereby diminish infarct volume) in the brains of both mice and rats[11,64]. In addition, solCD39's post-ischemic limitation of thrombosis did not come at the expense of increased risk of hemorrhage as was the case with aspirin[11].

CD39 and Immunomodulation

One of the first signs that CD39 may be involved in the regulation of immune responses was the identification of CD39 on B cells[21,54]. In addition to its constitutive low level expression, activation of B cells, such as by infection with Epstein-Barr virus, resulted in a profound upregulation of CD39 on their surface[21]. Furthermore, antibody

engagement of CD39 on lymphocytes induced homotypic adhesions between immune cells[21,54]; though the physiologic relevance of this phenomenon remains to be determined.

Despite its initial uses as a leukocyte activation marker, a functional role for CD39 on leukocytes remained unclear. One of the first clear signs of CD39's functional importance came from Langerhans cell biology. In the field of dermatology, CD39 is used as a marker to identify Langerhans cells in skin biopsies[65]. When *Cd39-/-* mice were examined in a model of contact dermatitis, CD39 was shown to limit ATP signaling between Langerhan's cells and keratinocytes[14,66]. This communication is critical to leukocyte recruitment, and when unchecked leads to a significant exacerbation of inflammation. In contrast to contact dermatitis, a different set of experiments showed that allergy-induced dermatitis was reduced in *Cd39-/-* mice due to desensitization of immune cells[14].

CD39 is highly expressed on other cells of the innate immune system ranging from monocytes to neutrophils[67]. In models of ischemia and reperfusion, the response of the innate immune system was increased in *Cd39-/-* mice as determined indirectly by a whole tissue myeloperoxidase assay[13]. The mechanism for the inflammation in this model was unclear, though it was noted that ischemic *Cd39-/-* mice had enhanced vascular permeability potentially allowing for greater leukocyte extravasation[13]. CD39 has been noted to regulate endothelial activation and cytokine release in addition to vascular permeability providing several potential mechanisms by which CD39 may suppress inflammation[16,17]. In a matrigel based tumor model, however, *Cd39-/-* macrophages were

unable to invade a foreign plug[68]. The authors attributed this to a desensitization to ATP dependent chemotaxis, though the proteolytic component of this model was never explored.

Some of the most exciting work in the field of CD39 and immunity has come in the field of T cell biology. T cells are know to release ATP during antigen presentation. Subsequent conversion of this ATP to adenosine is thought to play an immunosuppressive role involving T cells. CD39 is expressed on only a few subsets of T cells. One of the subsets with very high CD39 expression is a population of regulatory T cells called T_{regs}[4]. Interestingly, T_{reg} cells are the only T cell population known to express both CD39 and CD73 suggesting a coherent mechanism by which ATP released during antigen presentation is converted by T_{reg} cells into adenosine to foster immunosuppression[4]. Concordantly, $Cd39^{-/-}$ T_{reg} cells have impaired immunosuppressive capabilities and $Cd39^{-/-}$ mice and are unable to prevent allograft rejection[4].

Statement of major thesis themes

While a greater understanding of CD39's role in regulating extracellular nucleotide signaling has begun to emerge in recent years, there are still many questions that remain to be answered. First among them is the role CD39 plays on individual cell types and subpopulations. Individual cells can be tested in the isolation of an *in vitro* system, but *in vivo* there are a multitude of CD39 bearing cells which can interact. This raises such simple questions as if one cell has CD39, but another does not, how close must they be before one begins to influence the other? To this point, most studies have

looked at animals that were either completely CD39-competent or completely CD39-null. This has made attribution of critical CD39 bearing subpopulations difficult. In addition, most inflammatory research has focused on acute injury and insults such as ischemia-reperfusion or contact dermatitis. What remains unclear is whether ecto-enzyme catabolism of nucleotides can play a role in a more chronic injury setting where the opportunity for receptor desensitization and other forms of physiologic compensation is much greater. Finally, very little is known about the regulation of CD39's cell surface expression. This begs the question of how can the environment, specifically a pro-inflammatory one, influence the expression of CD39? The commonality amongst each of these gaps in knowledge is one of the underlying themes this thesis will seek to address: *What is the importance of CD39's cellular location and how does this influence it's vascular homeostatic role?*

Specific Aim 1: To determine which CD39 bearing subpopulation provides critical protection from cerebral ischemia. As endothelial cells are the largest repository of intravascular CD39, most of the literature in this field attributes CD39's protective and anti-inflammatory effects to this source. In Chapter II, I test this idea by separating CD39's contribution from resident tissues, such as vascular endothelium, and CD39 contribution from circulating bone marrow-derived cells. Furthermore, I explore the innate immune response in a more rigorous fashion than has been previously done using a highly sensitive flow cytometric technique. *The underlying hypothesis of this aim is that resistance to cerebral ischemia is conferred by CD39 expressed tissue resident cells, particularly the vascular endothelium.*

Specific Aim 2: To elucidate the role of CD39 in a hyperlipidemia induced model of atherogenesis, and determine the cellular/humoral mediators involved. Current cardiovascular therapies target the synthesis of lipids to suppress atherogenesis. In Chapters III and IV, I explore if purine metabolism by ecto-enzymes is atherosuppressive through its regulation of platelet reactivity and lipid deposition. *The hypothesis of this aim is that increased platelet reactivity due to a lack of CD39, coupled with a basal state in which macrophages are primed for activation and recruitment, will lead to an exacerbation of atherosclerosis in CD39-null mice.*

Figure 1.1 Schematic of CD39 in the vasculature. CD39 is found on the surface of the endothelium where it catalyzes the breakdown of the purinergic signaling moieties ATP and ADP, ultimately generating AMP. AMP is subsequently degraded to adenosine by the enzyme CD73, which co-localizes with CD39.   When not broken down, ATP and ADP can activate leukocytes, endothelial cells, and platelets which release more ATP and ADP in an amplifying cascade. In this thesis, I suggest that the shear stress generated by blood flowing through vessels induces anti-inflammatory and anti-coagulant vessel properties by inducing CD39 expression.

Figure 1.1

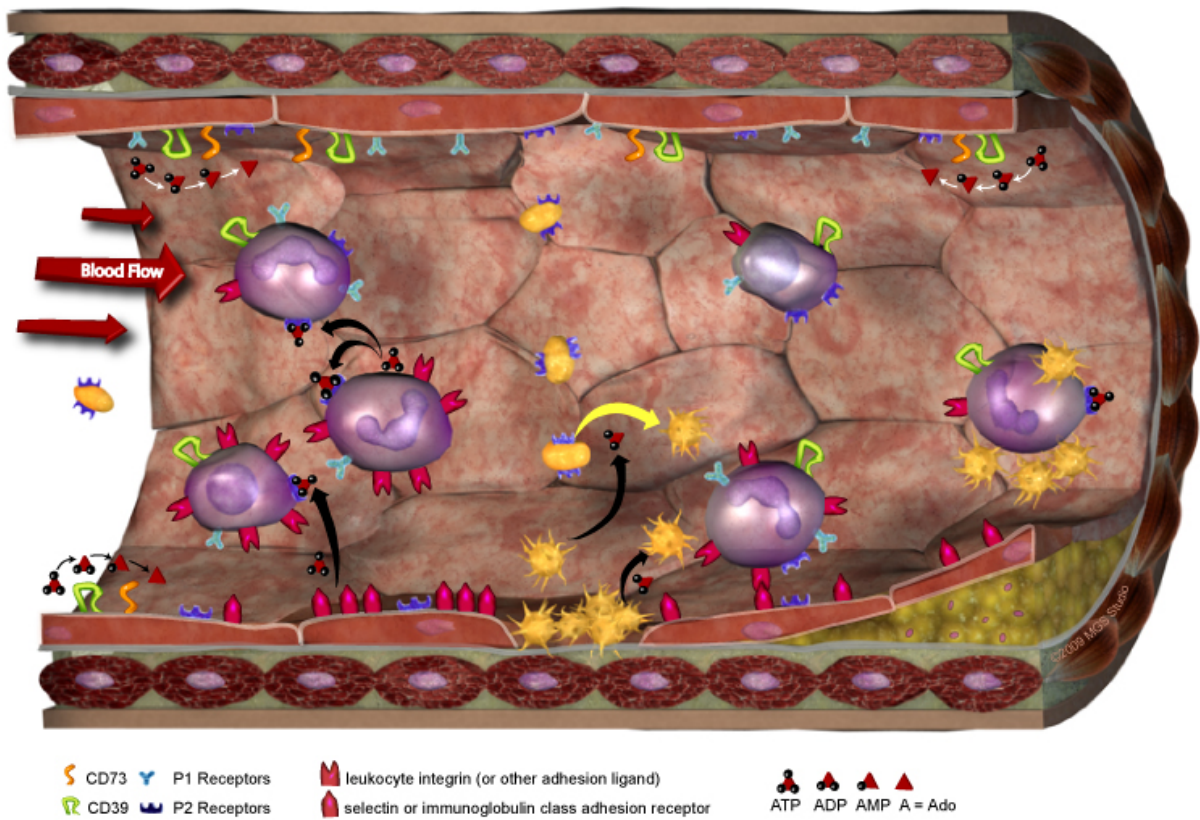**Figure 1.2** CD39 structure. The enzymatically functional domain of CD39 resides in the extracellular loop. The five apyrase conserved regions (ACRs) in this protein (highlighted in red) are necessary for the full enzymatic activity of CD39. RanBPM is the only known intracellular binding partner for CD39 and can interact with its N-terminus to modify enzyme activity as well.
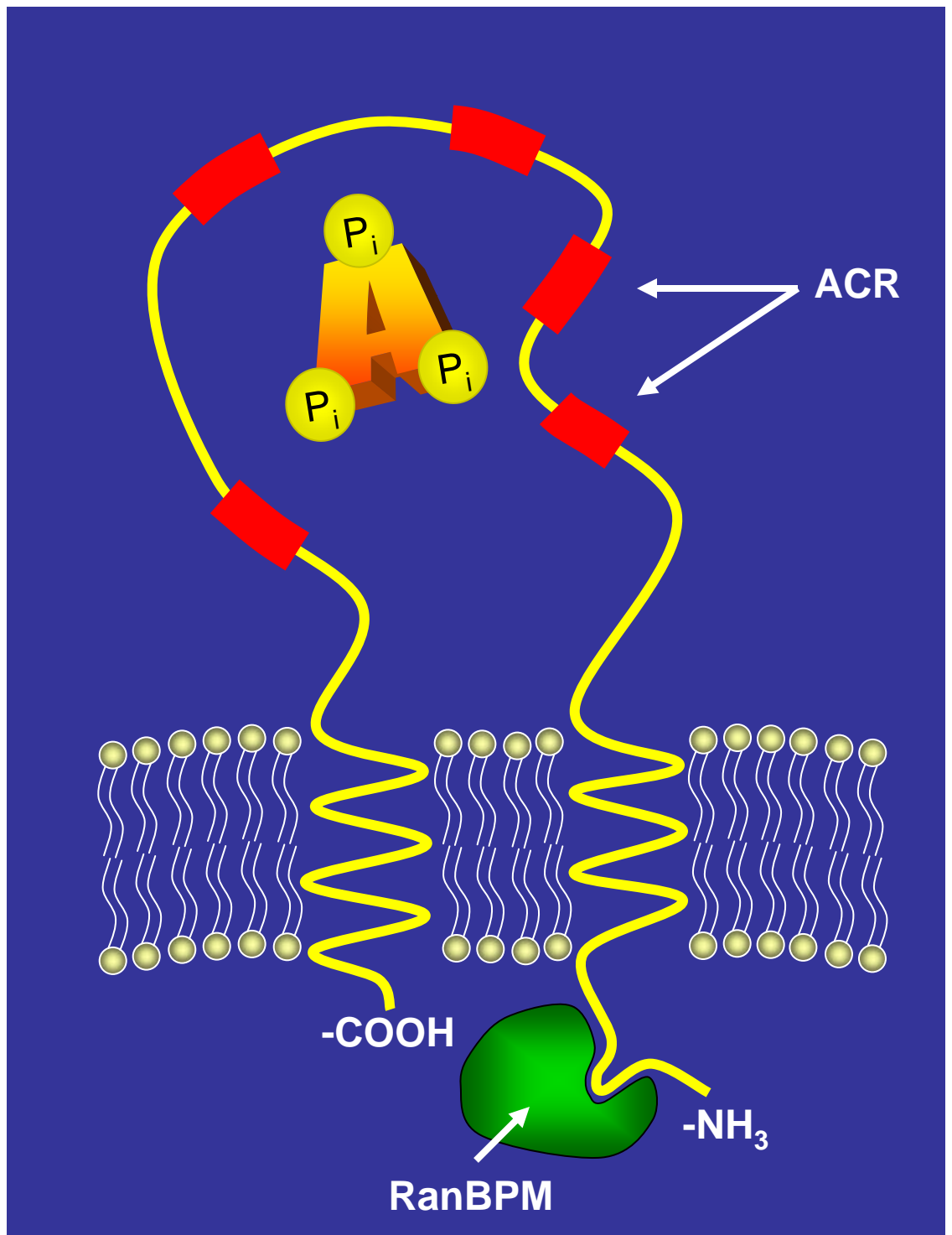
Figure 1.2

CHAPTER II

SELF-REGULATION OF INFLAMMATORY CELL TRAFFICKING IN MICE

BY A LEUKOCYTE SURFACE APYRASE

Abstract

The ectonucleotidase ENTPDase1 (CD39) on the plasmalemma of endothelium metabolizes ADP to suppress platelet accumulation. In the setting of tissue ischemia, the role for leukocyte surface ATPDase in regulating monocyte and neutrophil trafficking is not known. Here we demonstrate a novel mechanism by which CD39 on monocytes and neutrophils regulate their own sequestration into ischemic tissue, by catabolizing nucleotides released by injured cells, inhibiting their chemotaxis, adhesion, and transmigration. Bone marrow-reconstitution or provision of apyrase normalized ischemic leukosequestration and cerebral infarction in CD39-deficient mice. Leukocytes purified from $Cd39^{-/-}$ mice have markedly diminished capacity to phosphohydrolyze adenine nucleotides and regulate platelet reactivity, suggesting that leukocyte ectoenzymes critically modulate the ambient vascular nucleotide milieu. Dissipation of ATP by CD39 reduced $P2X_7$ receptor stimulation and thereby suppressed baseline leukocyte $\alpha_M\beta_2$-integrin expression. As $\alpha_M\beta_2$-integrin blockade reversed the post-ischemic, inflammatory phenotype of $Cd39^{-/-}$ mice, these data suggest that phosphohydrolytic activity on the leukocyte surface suppresses cell-cell interactions which would otherwise promote thrombosis or inflammation. These studies add a new dimension to

understanding how CD39, not just on endothelium, but on leukocytes themselves, regulates inflammatory cell trafficking and platelet reactivity, with a consequent reduction in tissue injury following ischemic challenge.

Introduction

The early consequences of cerebral ischemia are often amplified by local leukocyte and platelet accumulation. This cellular accrual exacerbates cerebral damage by impeding distal microvascular flow [69,70] and promoting local inflammation, tissue destruction and regional edema. Although purinergic signaling is a critical mediator of platelet and leukocyte accumulation, endogenous mechanisms regulating these events are poorly understood [71-74]. We have shown previously that platelet accumulation in the ischemic brain is suppressed by the endothelial ectonucleoside triphosphate diphosphohydrolase 1 (CD39), as well as by a soluble engineered fragment [64,75], which catalyzes the terminal phosphohydrolysis of ADP and ATP [6,7]. However platelet reactivity and accumulation cannot fully account for the sequelae of cerebral ischemia [70]. Though CD39 regulates platelet activation and adhesion through catabolism of ADP [75-77], it is not known whether CD39 modulates trafficking of inflammatory cells in ischemic tissue. Emerging evidence has highlighted a crucial role for autocrine and paracrine purinergic signaling in the activation and chemotaxis of leukocytes [78]. This led us to hypothesize that ectonucleotidases, which can dissipate adenine nucleotides and generation of adenosine, may regulate inflammation in ischemic tissues.

Extracellular ATP and ADP, biomarkers of cellular injury [79], amplify inflammatory cascades by attracting additional leukocytes to sites of tissue damage. Thus, purine-mediated leukocyte trafficking, like ATP-directed neutrophil activation and chemotaxis, may exacerbate collateral tissue destruction following hypoxia-induced neuronal cell death [2,78,80]. Adenine nucleotides, however, are unique in that an endogenous and highly specific mechanism exists by which these signaling moieties could be degraded. Quenching of purinergic signaling would be a novel means to temper inflammation distinct from classical chemokine and cytokine signals. Furthermore, AMP, generated by CD39-mediated phosphohydrolysis of ATP/ADP, is subsequently converted to adenosine [81-83]. In this schema, nucleotide metabolism and nucleoside generation mediate a critical balance between inflammatory and quiescent signals, with vascular apyrases such as CD39 mediating the fulcrum/pivot point between the two.

In the present study, we tested the hypothesis that CD39 regulates leukocyte trafficking by rapidly dissipating ATP and ADP from the leukocyte microenvironment in the ischemic brain. Experiments were designed to determine whether CD39 alters leukocyte accumulation in the ischemic brain, and if so, whether the mechanism is dependent upon endothelial or leukocyte CD39 expression. Previous studies focused primarily on endothelial CD39 and thrombosis; however the role of CD39 on the leukocyte cell surface in ischemic tissue is unknown. Employing an experimental strategy of bone marrow transplantation and selective-reconstitution, we now demonstrate CD39-dependent leukocyte trafficking into an ischemic tissue, and elucidate the relative contributions of CD39-bearing cell subpopulations to ischemic

leukosequestration. Furthermore, the P2X$_7$ receptor is identified as a regulator of $\alpha_M\beta_2$-integrin expression, with CD39 downregulating $\alpha_M\beta_2$-integrin by suppressing stimulation of leukocyte P2X$_7$. These studies show that leukocytes, through CD39, regulate their own recruitment to post-ischemic tissue.

Results

Cd39 genotype and clinical sequelae of cerebral ischemia

Permanent cerebral ischemia was induced in CD39-deficient and wild-type mice with the use of a photothrombotic model of middle cerebral artery occlusion [84]. Forty-eight hours later, T2 weighted cortical MRIs were performed to assess infarct volume (**Figure 2.1A**). Infarct volumes in CD39-deficient mice were 78.7% larger than those in wild type controls (**Figure 2.1B**). The larger infarct volumes in *Cd39*$^{-/-}$ mice were of functional significance since they also demonstrated greater neurological deficits than wild type mice (**Figure 2.1C**). The data obtained with this model of stroke parallel those previously reported with intraluminal MCA occlusion using a nylon monofilament: studies in which larger cerebral infarct volumes were observed in *Cd39*$^{-/-}$ mice 24 hours after ischemia [75].

CD39 modulation of ischemic leukosequestration

CD39-deficient mice are characterized by enhanced platelet deposition in ischemic cerebral tissue, yet platelet activation alone cannot account for all of the sequelae of cerebral infarction. For instance, when a short acting GPIIb/IIIa antagonist was given to mice in the setting of stroke, though platelet deposition was markedly

diminished, there was reduction in, but not complete rescue from cerebral infarction [70]. In addition to release by platelets of granular contents, exposure of platelet surface adhesion molecules such as P-selectin, and provision of a procoagulant phospholipid surface, we hypothesized that the ischemia-susceptibility of $Cd39^{-/-}$ mice could be partly attributed to increased post-ischemic leukocyte infiltration. Histologic examination revealed that large numbers of macrophages and neutrophils are recruited to ischemic cortex, and suggested that absence of CD39 in particular exaggerates macrophage recruitment into the ischemic zone (**Figure 2.2, A-L**). Using flow cytometry to quantify leukocyte infiltration, we analyzed ischemic and non-ischemic hemispheres of mice 48 hours post-ischemia induction. Antibodies to CD45 and LY-6G characterized the neutrophil (CD45^{hi}LY-6G$^+$) subpopulation of the infiltrating cells (green in **Figure 2.2M**); F4/80 positivity in combination with CD45 staining identified macrophages (CD45^{hi}F4/80$^+$) (blue in **Figure 2.2N**) [85,86]. The CD45$^{low/negative}$F4/80$^+$ cells observed could represent activated microglial cells, which are known to express F4/80 [87,88]. Ischemic hemispheres of untransplanted CD39-deficient mice demonstrated 61% more total infiltrating nucleated cells as compared to the ischemic hemispheres of untransplanted wild type mice. Conversely, the non-ischemic hemispheres of controls did not show significant differences with regard to infiltrating cell numbers between genotypes (data not shown). This implied that CD39 does not affect baseline numbers of resident leukocytes in the brain. Subpopulation analysis demonstrated a 2-fold enrichment in number of infiltrating neutrophils and macrophages in each ischemic hemisphere of CD39-deficient vs. control mice ($259 \times 10^3 \pm 24 \times 10^3$ vs. $134 \times 10^3 \pm 4 \times 10^3$ neutrophils per hemisphere and $108 \times 10^3 \pm 5 \times 10^3$ vs. $46 \times 10^3 \pm 3 \times 10^3$ macrophages per hemisphere) (**Figure 2.2, O-P**).

Circulating apyrase protects Cd39$^{-/-}$ mice from cerebral ischemia

We hypothesized that the heightened leukocyte flux seen in *Cd39$^{-/-}$* mice was due in part to an absence of vascular CD39 activity, and also in part due to a loss of CD39 circulating on the leukocytes themselves. To examine this, we assessed the ability of wild type and CD39-deficient leukocytes to metabolize ATP and ADP in their extracellular milieu. Purified buffy coats were incubated with either [8-^{14}C] ADP or [8-^{14}C] ATP, after which phosphohydrolysis was assessed by thin layer chromatography (**Figure 2.3, A-B**). CD39-deficient leukocytes were deficient in ATPase and ADPase activity (**Figure 2.3, A-B**). To demonstrate that the loss of ecto-apyrase activity in *Cd39* null mice was driving their leukosequestration phenotype, a soluble apyrase was administered prior to ischemic induction. Apyrase is a functional analog of CD39 which has been shown to restore normal vascular homeostasis (mitigate platelet desensitization) in *Cd39$^{-/-}$* mice [76]. CD39 null mice treated with apyrase, but not saline, were protected with a diminished cerebral infarct size (42.8 ± 7.6 mm^3 vs. 68.6 ± 2.1 mm^3, p<0.04), (**Figure 2.3C**). This finding is concordant with previous studies using solCD39 in murine [75] and rat [64] models of cerebral ischemia. Data also showed a concordant decrease in the number of neutrophils and macrophages in the ischemic brain of apyrase-treated mice when compared to saline controls (apyrase: 176x10^3 ± 23x10^3 neutrophils per hemisphere vs. saline: 331x10^3 ± 40x10^3 neutrophils per hemisphere, p<0.02; apyrase: 60x10^3 ± 6x10^3 macrophages per hemisphere vs. saline: 144x10^3 ± 10x10^3 macrophages per hemisphere, p<0.0001) (**Figure 2.3, D-E**). These data show that

inhibition of ischemia-driven leukocyte accumulation can be achieved through administration of a functional CD39 analog.

Restoration of normal leukocyte mobilization in Cd39$^{-/-}$ mice by bone marrow transplantation

To determine whether CD39 on circulating cells or on vascular tissue was contributing to the increased cerebral ischemia-susceptibility of CD39-deficient animals, a series of bone marrow transplantations were performed between *Cd39* gene null and wild type animals [89]. *Cd39$^{-/-}$* or WT bone marrow was transplanted into myeloablated *Cd39$^{-/-}$* (KO→KO) and WT (WT→WT) mice respectively (Donor→Recipient). These mice served as transplantation controls. Similarly, *Cd39$^{-/-}$* or WT bone marrow was also transplanted into WT (KO→WT) or *Cd39$^{-/-}$* (WT→KO) myeloablated recipients to generate chimeric mice with either CD39 on the resident tissue alone (KO→WT), or on bone marrow-derived cells (BMDCs) alone (WT→KO).

To confirm the efficiency of the marrow reconstitution, we developed a new quantitative PCR methodology with probe and primer sets designed against both neomycin (cassette used in generating the *Cd39* knockout) and neural growth factor (as an internal control). This allowed assay of the percentage of cells in a population that were CD39-deficient (containing neomycin) or wild type (no neomycin) (**Figure 2.4A**). Fluorescence-activated cell sorting was used to collect individual neutrophil and monocyte populations for DNA isolation. The Neo/NGF assay was used to genotype the cells in each of our four chimeras and revealed that circulating neutrophils and

monocytes were fully reconstituted (**Figure 2.4, B-C**). In a separate set of experiments, flow cytometry (**Figure 2.4, D-G**) was used to examine both the circulating neutrophil and monocyte protein expression of CD39. These methods demonstrated that at both the DNA and protein levels, neutrophils and monocytes were completely reconstituted in the chimeric mice. Further staining of tissue homogenates demonstrated that the resident endothelial populations retained recipient phenotype following bone marrow transplantation (**Figure 2.4I**), with endothelial cells having approximately two times the surface CD39 expression of either the resident neutrophil or macrophage populations.

Eight to ten weeks were allowed for full bone marrow reconstitution, after which the chimeras were subjected to photothrombotic middle cerebral artery occlusion. MRIs of the homologously transplanted (i.e., WT→WT or KO→KO) and infarcted mice demonstrated that bone marrow transplantation does not alter the susceptibility to cerebral injury in ischemic stroke of wild type and $Cd39^{-/-}$ mice. Mice without CD39 (KO→KO) had significantly larger infarct volumes than mice with CD39 (WT→WT) (65.6 ± 2.3 mm^3 vs. 30.5 ± 5.1 mm^3, p<0.001) (**Figure 2.5A**). Chimeric mice with CD39-bearing BMDCs were largely rescued from infarction when compared to KO→KO mice (65.6 ± 2.3 mm^3 vs. 42.2 ± 4.7 mm^3, p<0.01). Conversely, expression of CD39, on only the vascular-tissue surface provided limited protection from cerebral ischemia (KO→WT 59.0 ± 3.4 mm^3). Furthermore, the increased infarct volumes of the KO→KO mice proved to be functionally important as they had significantly greater neurologic deficits than WT→WT or WT→KO mice (data not shown). KO→WT chimeras had an intermediate neurologic deficit.

Given the susceptibility of CD39-deficient mice to ischemia-driven leukosequestration, we examined which CD39-bearing tissues confer protection to wild type mice using the same marrow reconstitution strategy. The total number of cells infiltrating the contralateral, non-ischemic hemisphere was similar across all chimeric strains (data not shown). Subpopulation analysis of ischemic hemispheres showed CD39 on BMDCs strongly suppressed leukocyte recruitment to ischemic tissue. The total number of infiltrating neutrophils was significantly higher ($p<0.01$) in KO$\rightarrow$KO mouse brain ($390\times10^3 \pm 18\times10^3$) compared to all other groups (WT$\rightarrow$WT $217\times10^3 \pm 16\times10^3$; KO$\rightarrow$WT $273\times10^3 \pm 28.6\times10^3$; WT$\rightarrow$KO $255\times10^3 \pm 21\times10^3$) (**Figure 2.5B**). The number of macrophages recruited to the ischemic brain correlated closely with the presence or absence of CD39 on BMDCs. The absolute number of infiltrating macrophages was significantly increased, almost 2-fold, in the KO$\rightarrow$KO and KO$\rightarrow$WT mouse brains when compared to either WT$\rightarrow$WT or WT$\rightarrow$KO mice (**Figure 2.5C**). This implies that though a transient rescue from CD39-deficiency can be obtained through administration of a soluble CD39 analog, a permanent rescue can be obtained via bone marrow reconstitution.

CD39 bearing subpopulations contribute to platelet reactivity

CD39 has previously been shown to be a prime regulator of platelet activation and recruitment *in vivo* [75,76,90] and *ex vivo* [90,91], yet the role of CD39 loss from a subpopulation has not been explored. We hypothesized that CD39 on the surface of leukocytes could be regulating platelet activation and recruitment, thereby contributing to the sequelae of

cerebral ischemia in this fashion. To determine how a change in leukocyte phosphohydrolytic activity might modulate platelet reactivity, we employed whole blood aggregometry. In contrast to platelet-rich plasma aggregometry, this assay mimics platelet-leukocyte interactions. In keeping with previous published observations in platelet-rich plasma aggregometry [75,76], non-transplanted *Cd39*^{-/-} mice demonstrated platelet desensitization when compared to wild type control mice (**Figure 2.5D**). We sought to examine whether this was attributable to the catabolism of platelet-activating nucleotides by endothelial- or leukocyte-bound CD39 using bone marrow reconstitution studies. Two weeks following reconstitution, mice with either tissue CD39 alone (KO→WT) or BMDCs with CD39 (WT→KO) demonstrated only partial desensitization of platelets demonstrating a role for both of these subpopulations in the maintenance of vascular homeostasis (**Figure 2.5, E-F**). This is complimentary to previous work in which human CD39 was overexpressed on either the leukocyte or endothelial populations. These experiments showed that CD39 can regulate platelet activation from either the endothelial or leukocyte compartment [90].

CD39 deficiency and leukocyte $\alpha_M\beta_2$-integrin surface expression

ATP is known to upregulate expression of $\alpha_M\beta_2$-integrin (MAC-1, CD11b/CD18), a critical glycoprotein adhesion receptor expressed on human neutrophils [2,92]. To discern whether a lack of CD39 resulted in stimulation of CD39-deficient leukocytes via basal nucleotide release, we examined peripheral blood monocyte and neutrophil populations by flow cytometry. Histologic analysis performed to confirm the cell gates reveals 92% and 97% purity of the sorted monocytes and neutrophils,

respectively (data not shown). There was a 50% increase in the number of high expressing $\alpha_M\beta_2$-integrin monocytes (measured by the α_M/CD11b subunit) in $Cd39^{-/-}$ mice when compared to WT controls (**Figure 2.6, A-C**). In contrast, neutrophils did not display differences in cell surface $\alpha_M\beta_2$-integrin expression at baseline (**Figure 2.6D**). Treatment of $Cd39^{-/-}$ animals with a soluble apyrase restored a near wild-type expression of $\alpha_M\beta_2$-integrin on monocytes (**Figure 2.7**). By comparison, treatment of wild-type animals with apyrase resulted in a ~40% reduction in the number of $\alpha_M\beta_2$-integrin high expressers relative to vehicle.

CD39 overexpression reduces cell surface $\alpha_m\beta_2$-integrin

RAW 264.7 murine macrophages were transfected with either "empty" pCDNA3.1 vector or pCDNA3.1 containing murine CD39, to explore the relationship between CD39 and $\alpha_M\beta_2$-integrin in vitro. Stable CD39 transfectants expressed 15-fold more *Cd39* mRNA than vector control cells with a concurrent increase in membrane protein (**Figure 2.8A**). Following media exchange with serum-free media, RAW cells overexpressing CD39 were found to have 71% less ATP in their media when compared to vector transfectants, likely reflecting the difference in CD39 protein expression (**Figure 2.8B**). The source of this ATP was presumed to be leakage or release from the macrophages themselves. When the CD39-overexpressing cells were analyzed by flow cytometry, they maintained a resting state with 40% less cell surface $\alpha_m\beta_2$-integrin than empty vector transfectants (**Figure 2.8C**). We hypothesized that basal ATP released from cells was metabolized more efficiently in CD39-overexpressing cells. This implies that the reduced $\alpha_M\beta_2$-integrin expression phenotype is derived either through reduced

stimulation of P2 receptors, or via increased adenosine generation. To distinguish between these two possibilities, APCP was used to block conversion of CD39-generated AMP into adenosine by CD73 [83,93]. In the presence of APCP, only a small, insignificant increase in the expression of $\alpha_m\beta_2$-integrin was observed, implying this phenotype is not dependent upon the generation of adenosine (**Figure 2.8D**).

As the suppression of $\alpha_M\beta_2$-integrin expression by CD39 appears to be independent of adenosine generation, experiments were next directed towards elucidating a role for ambient ATP. ATP binds to and activates purinergic receptors. To investigate a direct role for purinergic receptor engagement by adenine nucleotide phosphates, purinergic signaling was blocked using the inhibitors suramin (inhibits $P2X_{1-3, 5}$ and $P2Y_{1, 11}$) [72,94-96], TNP-ATP (inhibits $P2X_{1-4}$) [97,98], or ox-ATP (inhibits $P2X_7$) [99,100]. Little change in $\alpha_M\beta_2$-integrin expression was seen in either CD39-overexpressing or vector-transfected cells when treated with suramin or TNP-ATP. However, strong suppression of $\alpha_M\beta_2$-integrin expression was conferred by the specific $P2X_7$ inhibitor, ox-ATP (**Figure 2.8D**). Blockade of the $P2X_7$ receptor in vector-transfected macrophages brought $\alpha_M\beta_2$-integrin expression to levels below those of CD39-overexpressing macrophages. Not surprisingly, as CD39 dissipates ATP and hence itself should indirectly reduce $P2X_7$ receptor stimulation, $P2X_7$ receptor blockade had a less significant effect on $\alpha_M\beta_2$-expression in mCD39 transfectants. Finally, the specific $P2X_7$ receptor agonist bzATP dose-dependently induced $\alpha_M\beta_2$-integrin expression in both cell lines (**Figure 2.8E**). This suggested that suppression of $\alpha_M\beta_2$-integrin expression in CD39

transfectants is due to diminished $P2X_7$ receptor stimulation in CD39 over-expressing cells.

To confirm that the changes in integrin expression were not due to pharmacologically-induced off-target effects, a gene silencing approach was employed. Using an shRNA that targeted the $P2X_7$ receptor as well as an empty vector control, the $P2X_7$ receptor was silenced at mRNA and protein levels in both control and CD39-overexpressing macrophage cell lines (**Figure 2.8F**). These cell lines were subsequently examined by flow cytometry for $\alpha_M\beta_2$-integrin expression. The cells each carried two plasmids, one containing mCD39 or corresponding control vector; the other $P2X_7$ shRNA or corresponding control vector. These experiments confirm the earlier transfection experiments shown in **Figure 2.8C**, i.e., when the single transfectants are additionally transduced with a control shRNA, overexpression of mCD39 still results in a significant diminution of α_M-integrin expression. In contrast, transduction with a $P2X_7$ silencing shRNA completely abolished the difference in integrin expression seen between CD39-overexpressing and control cells (**Figure 2.8G**). In essence, $P2X_7$ suppression uncouples CD39 levels from regulation of α_M-integrin levels. This implies that CD39 can regulate the expression of $\alpha_M\beta_2$-integrin by dissipating ATP that would otherwise activate the $P2X_7$ receptor.

CD39 regulates leukocyte trafficking via $\alpha_M\beta_2$-integrin in vitro and in vivo

Our in vitro studies suggest that the amplified leukocyte recruitment in *Cd39*-null mice is a consequence of upregulated $\alpha_M\beta_2$-integrin expression in *Cd39*-null leukocytes.

To further explore this, leukocyte transmigration assays were performed on fibrin(ogen) coated transwells. Fibrin(ogen) is a known cognate binding partner for $\alpha_M\beta_2$-integrin. In this assay, $Cd39^{-/-}$ peritoneal macrophages migrated 300% more than wild type controls (**Figure 2.9, A-B**). Further, CD39-overexpressing macrophages had a greater than 90% reduction in leukocyte transmigration compared to control cells (**Figure 2.9C**). Antibody blockade of the α_M-subunit demonstrated that the enhanced leukocyte migration seen in vector-transfected cells was dependent upon $\alpha_M\beta_2$-integrin. We further sought to determine whether $\alpha_M\beta_2$-integrin might affect leukosequestration in our cerebral ischemia studies. CD39 null and WT mice were treated with α_M-blocking or isotype control antibody. Isotype-treated $Cd39^{-/-}$ mice had 61% more infiltrating neutrophils and 104% more infiltrating macrophages than isotype-treated wild type mice, similar to our prior data (**Figure 2.2**) showing increased cerebral leukosequestration after ischemia in untreated $Cd39^{-/-}$ mice. This demonstrates that the leukocyte infiltration phenotype was not affected by an isotype-matched antibody ($p<0.001$, **Figure 2.9, D-E**). In sharp contrast, treatment of ischemic $Cd39^{-/-}$ mice with α_M-blocking antibody yielded a striking decrease in the number of infiltrating macrophages and neutrophils when compared to ischemic $Cd39^{-/-}$ mice treated with isotype control antibody (**Figure 2.9, D-E**). Furthermore, antibody blockade in $Cd39^{-/-}$ mice restored levels of leukocyte trafficking to those seen in isotype antibody-treated wild type mice. Analysis of peripheral blood showed that this abrogated leukocyte trafficking was not due to pan-leukodepletion following intravenous antibody administration (data not shown). When antibody-treated mice were examined by MRI, both wild type and CD39-deficient mice were significantly protected by treatment with an α_M-integrin blocking antibody (**Figure 2.9F**). The fact

that α_M blockade was incompletely protective in *Cd39⁻ᐟ⁻* mice (i.e., α_M-blockade did not reduce infarct volumes to the extent seen in α_M-antibody-treated WT mice) suggests other injury mechanisms at play beyond α_M-dependent leukosequestration alone.

To investigate whether heterotypic monocyte-platelet interactions could be contributing, monocyte-platelet aggregates were measured; these data showed no significant differences in monocyte-platelet aggregates between WT and *Cd39⁻ᐟ⁻* mice, though there was a trend for there to be more in the CD39-deficient mice (data not shown). Together, these data demonstrate a critical role for $\alpha_M\beta_2$-integrin-dependent leukosequestration in the tissue injury in ischemic stroke, especially in *Cd39⁻ᐟ⁻* mice.

Discussion

Disruption of blood flow to metabolically active tissues which depend on an uninterrupted supply of oxygen and other nutrients elicits a sequence of events which can ultimately lead to cell death. The initial injury, triggered by substrate deprivation, is amplified by thrombotic occlusion and infiltration of activated leukocytes [101]. Under quiescent conditions, CD39, an ecto-apyrase expressed on endothelium and leukocyte subpopulations [67], rapidly metabolizes ADP and ATP released by activated platelets, thereby inhibiting platelet recruitment into an evolving thrombus. To date, this nucleotidase has not been recognized as a modulator of post-ischemic inflammatory cascades. We herein identify a novel paradigm by which CD39 expressed on the leukocyte surface autoregulates the leukocyte's own ambient nucleotide milieu, thereby controlling its adhesive properties for inflamed vasculature and for circulating cells.

Our previous work demonstrated that CD39-deficient mice developed worse clinical outcomes than CD39-bearing controls following challenge by cerebral ischemia [75]. This resulted in increased local platelet activation and thrombus formation in mice lacking CD39. In addition to amplifying previous observations, our new data highlight additional mechanisms by which CD39 protects against post-ischemic cerebral injury. This adds a new dimension to our understanding of the role of CD39 on leukocytes in regulation of tissue injury in response to ischemic stress. The present studies, using a cell population-specific CD39 deletion strategy, demonstrate a critical role for leukocyte CD39 in regulation of platelet reactivity. This extends previous work in which human CD39 overexpressed in marrow-derived cells enhances the endogenous inhibitory effects of CD39 on platelet reactivity [90].

Earlier investigations could not fully attribute the sequelae of stroke to either the leukocyte or platelet populations, leading to the hypothesis that they may interact in a synergistic manner [70]. Our prior data showed that platelet inhibition alone (with GPIIb/IIIa blockade) is incompletely protective in the setting of stroke [70]. Our current data indicates that accumulated leukocytes contribute to ischemic cerebral injury as well. Blockade of α_M-integrin is protective in our model of cerebral ischemia in part by preventing leukocyte trafficking. In the CD39 knockout mice, α_M-integrin blockade reduced leukosequestration to levels equal to those in WT mice. This suggests that the increased leukosequestration in $Cd39^{-/-}$ mice was related to the increased $\alpha_M\beta_2$-integrin expression on circulating $Cd39^{-/-}$ leukocytes. When infarct volumes are examined,

protection by α_M-integrin blockade is incomplete, likely attributable to the fact that mechanisms other than leukosequestration are also in play and contribute to tissue injury in ischemic cerebral infarction. One potential explanation for the incomplete protection afforded by α_M-integrin blockade is that thrombosis and inflammation intersect through the formation of leukotrienes [102] and leukocyte-platelet aggregates [103]. Though we did not see a statistically significant increase in the percentage of circulating monocytes that were bound to platelets in $Cd39^{-/-}$ mice (vs WT), there was a trend in that direction. The possibility remains that interactions of monocytes and platelets directly at the vascular surface is an important contributory mechanism to ischemic tissue injury. Interestingly, other models of intestinal [104] and renal [12] ischemia revealed a global susceptibility to ischemic injury in $Cd39$ null animals. In each of these studies, the protective effects of CD39 were attributed to its location on endothelial cells, where it modulated platelet activation and recruitment as well as vascular permeability. Although CD39 expression is recognized on certain leukocyte populations (B cells, monocytes, neutrophils [22,67]), the present investigation may the first to definitively attribute resistance to ischemic injury to leukocytes bearing CD39 apyrase.

The current bone marrow transplantation studies demonstrate that CD39 on leukocytes (particularly monocytes) critically regulated leukocyte influx into ischemic tissue, as well as tissue injury itself. Using a different gene-targeting strategy, $Cd39^{-/-}$ peritoneal macrophages exhibited less invasive potential in matrigel chemotaxis or tumor models compared to wild-type controls [68]. Our work demonstrates a clear predisposition for enhanced leukocyte sequestration in CD39-deficient mice derived with a strategy that

deleted the conserved apyrase domain. However, these two models are quite different: Ischemia-driven cell infiltration is guided by a well-organized sequence of events leading from cell adhesion to diapedesis, whereas the matrigel models involve proteolysis of the matrix as well as a potentially different set of diapedesis cues. Nevertheless, both *Cd39*-deletional mutants are susceptible to ischemic injury and both could be rescued by treatment with apyrase [12] or solCD39 [64,75]. In general, the protective effects of solCD39 have been attributed to its ability to block platelet activation and recruitment. However, our current study's apyrase-treatment experiments demonstrate that the protective effects of this enzyme may also lie in its ability to inhibit leukocyte recruitment to ischemic tissues.

The classic paradigm of inflammatory signaling has focused upon recruitment and activation of leukocytes with concomitant release of soluble mediators which amplify and accelerate the process. It is possible that some of the anti-inflammatory properties of CD39 are related to adenosine generated by the sequential phosphohydrolysis of ATP to ADP, AMP, and adenosine, the terminal reaction being catalyzed by CD73. We examined the role for adenosine generated downstream of CD39 in our in vitro model by utilizing APCP, which blocks the function of CD73 thereby preventing the generation of adenosine from AMP. As there was no difference in macrophage surface integrin expression irrespective of CD73 activity, this suggests that the major contribution of CD39 to suppress ischemic leukosequestration lies in the dissipation of ADP and ATP rather than downstream generation of adenosine. Given the high abundance of CD39 on the surface of myeloid lineage cells, one can envision leukocytes regulating not only the

activation of each other, but also themselves in a cell-autonomous fashion, by catabolizing pro-inflammatory agonists.

This scheme of catabolism-mediated, autonomous-control of activation is seen in CD39's regulation of $\alpha_M\beta_2$-integrin. Though $\alpha_M\beta_2$-integrin is normally found in sub-membrane, preformed storage granules [105], in CD39-deficient animals, leukocytes appear to have a basal state of heightened $\alpha_M\beta_2$-integrin expression. One potential explanation for this observation is that ATP, known to upregulate $\alpha_M\beta_2$-integrin expression [2,92], would be at higher levels in the microenvironment of $Cd39^{-/-}$ cells due to their lack of ATP phosphohydrolase activity. Although basal levels of plasma nucleotides may not vary between $Cd39^{-/-}$ and wild type animals [75], treatment of $Cd39$ null monocytes with soluble apyrase does restore a wild-type $\alpha_M\beta_2$-integrin surface expression pattern, indicative of differences in local concentrations of ATP and ADP as also shown by downregulation of platelet ADP responses [75,76]. This could be important as extracellular ATP has been shown to play an important role in signaling intracellular events. Extracellular purinergic nucleotides, such as ATP and ADP, are known to activate families of receptors; these include ligand gated receptors (P2X family) as well as G-protein coupled receptors (P2Y family). Among the P2X family, there are 7 known receptor subunits which multimerize to form receptors of varying specificities. Our data demonstrate that the homomeric $P2X_7$ receptor regulates expression of $\alpha_M\beta_2$-integrin in unstimulated macrophages, and that $\alpha_M\beta_2$-integrin expression in these cells is inversely correlated with cell surface CD39 [106]. This is complimentary to previous work which established a putative role for CD39 in the regulation of the $P2X_7$ receptor on endothelial

cells [16]. The $P2X_7$ receptor, although not previously linked to integrin expression, is known to play a role in regulation and function of the inflammasome, a multiprotein complex that regulates production and release of pro-inflammatory cytokines [74,107]. Thus, in the setting of ischemia, where ATP and ADP are released as a consequence of tissue destruction, CD39-deficient mice would be less able to metabolically control ATP-driven inflammatory cascades. $Cd39^{-/-}$ leukocytes would become primed for adhesion and diapedesis across an activated endothelium. By contrast, wild type leukocytes, at baseline, would be less ready to initiate transmigration and induce subsequent tissue damage. A decrease in α_M-integrin expression has already been shown to be profoundly protective in the setting of cerebral ischemia [101,108]. Furthermore, the importance of this CD39-mediated integrin regulation is supported by our data showing normalization of leukocyte-trafficking in $Cd39^{-/-}$ mice by $\alpha_M\beta_2$-integrin blockade. Thus CD39 is likely to inhibit leukosequestration via its repression of $P2X_7$-driven $\alpha_M\beta_2$-integrin expression. This finding is particularly important given that $\alpha_M\beta_2$-integrin is a critical adhesion receptor in the formation of leukocyte-platelet heteroaggregates, and in light of our previous finding that CD39-deficient mice have heightened platelet deposition in the ischemic brain [75].

In summary, our experimental results demonstrate the first direct link between CD39 and control of leukocyte migration into ischemic tissue. This occurs via a previously unrecognized mechanism by which leukocytes regulate their own flux through metabolism of agonists released into local vascular microenvironments by cellular activation or leakage from dying cells. Previously, CD39 has been demonstrated to be the major control system for blood fluidity [6,7,75]; these new data add to the pleiotropic

properties of CD39 on platelet activation and recruitment, demonstrating that both CD39 bearing leukocyte and endothelial subpopulations can suppress platelet activation. Furthermore these new data indicate a prime role for CD39 in modulating the expression of glycoprotein adhesive receptors on the surface of leukocytes, particularly cells of the monocyte lineage. As such, CD39 resides at the critical nexus of inflammation, coagulation and thrombosis as a vital regulator of vascular homeostasis.

Materials and Methods

Animal experiments were approved by and carried out in accordance with the University of Michigan Institutional Animal Care and Use Committee. All reagents, unless otherwise noted, were obtained from Sigma. Mice deficient for the *Cd39* gene (generated by replacement of the enzymatically active extracellular portion of the CD39 molecule (exons 4–6; apyrase-conserved regions 2–4) with a PGKneo cassette) were used for the indicated experiments [75].

Photo-thrombotic Model of Middle Cerebral Artery Occlusion

Cerebral ischemia was induced as previously described [84] by an operator blinded to experimental conditions. The experiment was performed with mice aged 15-16 weeks in both untransplanted and transplanted mice. In brief, mice were anesthetized with ketamine/xylazine; body temperature was maintained at 37ºC using a heating pad. The skin overlaying the calvarium was incised, exposing the temporalis muscle. The temporalis was incised, after which a burr hole was drilled to visualize the middle cerebral artery (MCA). The exposed MCA was placed under a 542 nm neon laser and

the mouse was injected intravenously with Rose Bengal dye (1 mg/25 g of body weight) dissolved in normal saline (10 mg/ml). MCA blood flow was monitored with a laser Doppler flow probe (Transonic System) to determine occlusion, defined as a >80% reduction in blood flow sustained for 10 minutes. Following occlusion, the laser and flow probe remained in place for an additional 15 minutes, after which the probe was removed, the skin incision closed, and the mice allowed to recover.

Magnetic Resonance Imaging

Forty-eight hours following induction of cerebral ischemia, infarct volumes were assessed by magnetic resonance imaging. Mice were anesthetized with 2% isoflurane/air mixture throughout MRI examination. Mice were placed prone in a 7.0 T Varian MR scanner (183-mm horizontal bore, Varian) with body temperature maintained at 37ºC using circulated heated air. A double-tuned volume radiofrequency coil was used to scan the head region of the mice. Axial T_2-weighted images were acquired using a spin-echo sequence with the following parameters: repetition time (TR)/effective echo time (TE), 4000/40 ms; field of view (FOV), 30x30 mm; matrix, 128x128; slice thickness, 0.5 mm; slice spacing, 0 mm; number of slices, 25; and number of scans, 1 (total scan time ~8 min.). Infarct volumes for each animal were quantified by an observer blinded to experimental conditions.

Neurologic Deficit Scoring

Evaluations were made by an operator blinded to experimental conditions using a previously described 5 point scoring system [109]: 1 = normal motor function, 2 = flexion of

the torso and contralateral forelimb upon lifting of the animal by the tail, 3 = circling to the contralateral side with normal posture at rest, 4 = leaning to the contralateral side at rest, 5 = no spontaneous motor activity.

Immunohistochemistry of ischemic brains

Contralateral and ischemic hemispheres of infarcted mice were fixed in 4% paraformaldehyde and embedded in Tissue-Tek OCT (Sakura Finetek) prior to sectioning. Neutrophils were identified by their expression of LY-6G (Southern Biotech). Macrophages were identified by their expression of F4/80 (Caltag Laboratories). Primary antibody was detected with a VECTASTAIN® ABC-Peroxidase Kit (Vector Labs) and developed using a TSA™ Fluorescein Tyramide Reagent Pack (Perkin-Elmer). Nuclei were stained with 4',6-diamidino-2-phenylindole (DAPI). Images were acquired with a 4x objective (1.614 μm/pixel) using MetaMorph v7.0r3 software (Molecular Devices) on an Eclipse TE2000-E microscope (Nikon Instruments).

Flow Cytometric Analysis of Infiltrating Leukocyte Populations

Following euthanasia, the cerebrum was removed and divided into ischemic and non-ischemic hemispheres. The hemispheres were mechanically dissociated with a scalpel and an 18 gauge syringe to yield single cell suspensions. A Percoll (density 1130g/ml) (GE Healthcare) gradient was used to separate the infiltrating cell population from myelin and neuronal debris. Erythrocyte contaminants were lysed using FACs Lyse (BD) per the manufacturer's protocol. Infiltrating cells were counted using a hemocytometer prior to flow cytometric analysis on a FACSCalibur (BD) using

CellQuest software (BD). Viable cells were identified by the absence of propidium iodide (PI) (BD) staining. Nonspecific antibody interactions were inhibited using Fc Block (BD). Leukocytes were initially identified as PE-conjugated CD45^{hi} (BD). CD45^{hi} cells were further identified as neutrophils based on FITC-conjugated LY-6G (BD) positivity or macrophages by FITC-conjugated F4/80 (Serotec) positivity. Ten thousand cells from the cellular-fraction of each hemisphere were acquired per data set.

Thin layer chromatography analysis of leukocyte AT(D)Pase activities

Mouse blood was drawn from the retro-orbital plexus into heparinized capillaries and was subsequently layered onto Histopaque 1119 (Sigma) before centrifugation according to the manufacturer's protocol. Purified buffy coats were washed and resuspended in RPMI-1640 (Gibco) containing 5 mM β-glycerophosphate (Sigma) [110]. To assess enzymatic function, cell suspensions of either CD39-deficient or wild-type leukocytes were mixed 1:1 with 1.0 mM [8-^{14}C] ADP (Perkin Elmer) or 1.0 mM [8-^{14}C] ATP (MP Biomedicals, Inc.) and incubated at 37°C for 30 minutes. The incubation time was chosen to ensure linearity of the reaction with time, i.e., a maximum of 30% of the initially introduced substrate was metabolized. The reaction was stopped using 8 M formic acid [111]. The reaction mixture was spotted on silica gel/TLC plates (Fluka) along with a ladder (a mixture of [8-^{14}C] AMP (GE Healthcare), [8-^{14}C] ADP, and [8-^{14}C] ATP). The nucleotides were separated by TLC with isobutanol/isoamyl alcohol/2-ethoxyethanol/ammonia/H20 (9:6:18:9:15) as previously described [7,110]. TLC plates were then exposed to a phosphoimaging screen (Kodak) and analyzed using a Typhoon Trio+ (GE Healthcare).

Apyrase rescue of CD39-deficient mice

CD39 null mice were treated with either vehicle or grade VII potato apyrase (4 U/g) one hour prior to induction of cerebral ischemia. This dose has been used previously to rescue CD39 null mice [76]. Three hours later mice were treated a second time with either vehicle or apyrase. After 48 hours, mice were examined via either magnetic resonance imaging or flow cytometry.

Bone-marrow Transplantation

At seven weeks of age, *Cd39*^{-/-} and wild-type mice underwent bone marrow transplantation as previously described [112]. In brief, mice were myeloablated via a 12.5 Gy radiation exposure administered in two doses three hours apart. Mice were reconstituted with approximately $4x10^6$ bone marrow-derived cells administered intravenously as follows: *Cd39*-deficient mice were reconstituted with *Cd39*^{-/-} bone marrow (to generate global knock-out controls) or with wild type bone marrow (to generate mice with "tissue-only CD39 ablation"). Wild-type (WT) mice were reconstituted with wild type bone marrow (to generate wild-type controls), or *Cd39*^{-/-} bone marrow (to generate mice with CD39 in established tissue, but not in bone-marrow-derived cells; "leukocyte CD39 ablation"). These chimeras are referred to as KO→KO, WT→KO, WT→WT, and KO→WT respectively. Mice were allowed to recover for eight to ten weeks prior to stroke induction or phenotype examination.

Chimerism assay

Citrated murine blood (150 μl) was drawn from the retro-orbital plexus of chimeric mice and the leukocyte fraction isolated using a Histopaque 1099 (Sigma) density gradient in a method previously described for human blood [2,92]. Cells were subsequently sorted based on their characteristic forward and side scatter properties to identify monocyte and neutrophil populations [113]. Neutrophils were secondarily gated for LY-6G positivity. Sorted monocyte and neutrophil populations were then collected and stained using HEMA 3 (Fisher) to confirm leukocyte purity (data not shown). Other collected cells were kept for DNA isolation. Probe and primer sets targeting both the neomycin cassette present in *Cd39^{-/-}* mice and NGF were used in a duplex format. The probes and primers were synthesized by Applied Biosystems with the following sequences: Neomycin Probe – 5'– CATCGCATCGAGCGAGCACGTACT – 3', Neomycin Primer 1 – 5' – CGGCTGCATACGCTTGAT – 3', Neomycin Primer 2 – 5' - CGACAAGACCGGCTTCCAT – 3', NGF Probe – 5' – ACGGTTCTGCCTGTACGCCGATCA – 3', NGF Primer 1 – 5' – TGCATAGCGTAATGTCCATGTTG – 3', NGF Primer 2 – 5' – TCTCCTTCTGGGACATTGCTATC – 3' [114,115]. DNA from purified leukocytes was amplified with the above probe and primers sets using TaqMan Gene Expression Master Mix (Applied Biosystems) in an ABI Prism7000 Sequence Detection System.

Whole blood analysis of cell surface CD39 expression in bone-marrow reconstituted mice

Citrated murine blood (150 μl) was drawn from the retro-orbital plexus of bone marrow reconstituted mice and sorted into neutrophil and monocyte populations as

above. In addition to LY-6G, these cell populations were concurrently stained for Propidium iodide, to exclude dead cells, and PE-conjugated CD39 (eBioscience) before analysis by flow cytometry.

Analysis of CD39 expression in tissue homogenates

Whole lungs of bone marrow-reconstitued mice were digested in 0.1% collagenase B (Roche Applied Science, Indianapolis, IN, USA) prior to dissociation with a gentleMACS™ Dissociator (Miltenyi Biotec). Cells were divided 10^6 per tube before staining with either: FITC-conjugated CD31 (BD), PE-cojugated CD39 (eBioscience), APC-conjugated CD45 (BD) to identify $CD31^+CD45^-$ endothelial cells; FITC-conjugated LY-6G (BD), PE-cojugated CD39 (eBioscience), APC-conjugated CD45 (BD) to identify $LY-6G^+CD45^+$ resident tissue neutrophils; or FITC-conjugated CD45, PE-cojugated CD39 (eBioscience), APC-conjugated F4/80 (Serotec) to identify $F4/80^+CD45^+$ resident tissue macrophages. For each of these stains 7-AAD was used to exclude dead cells (BD).

Whole blood aggregometry

Heparinized murine blood was drawn from the retro-orbital plexus of mice 2 weeks following bone marrow reconstitution. Whole blood impedance aggregometry was then performed using a Chrono-log 560CA with the AGGROLink 810. Whole blood was diluted 4-fold with physiologic saline before stimulation with 2 μM ADP (Chronolog).

Whole blood analysis of $\alpha_m\beta_2$-integrin surface expression

Heparinized murine blood (600 μl – 800 μl) was drawn from the inferior *vena cava* and the leukocyte fraction isolated using a Histopaque 1099 density gradient in a method previously described for human blood [2,92]. A subset of mice was injected intravenously with either vehicle (saline) or apyase (2 U/g) two hours prior to blood isolation. Following centrifugation, cells were washed with Hank's balanced salt solution (GIBCO), prior to cell labeling with propidium idodide, Fc block (BD), anti-CD11b Ab (the α_M subunit of $\alpha_M\beta_2$-integrin) conjugated to FITC (BD), or anti-LY-6G Ab conjugated to PE (BD) (15 min, 37°C). Neutrophils were identified by LY-6G positivity and their forward and side scatter properties. Monocytes were identified by their characteristic forward and side scatter properties [113].

Overexpression of CD39 in RAW 264.7 macrophages

RAW 264.7 macrophages were transfected with murine CD39 or vector control and clonally selected as an in vitro correlate to the whole blood studies. The CD39 open reading frame of full length mouse CD39 (mCD39) cDNA (ATCC) was PCR amplified using as 5'-primer, 5'- aaaagGtAccccttatggaagatataaagg-3' and as 3'-primer, 5'-gccgctcGAgctatactgcctctttccag-3'. This was subcloned into the pCDNA3.1 overexpression vector (Invitrogen, Carlsbad, CA). RAW cells were transfected with either the CD39 overexpression construct or empty pCDNA3.1 vector (control) using Superfect Transfection Reagent (Qiagen). The day before transfection, RAW cells were plated on 6-well plates (Corning) with 1 x 10^6 cells per well, and grown in RPMI 1640 (Invitrogen) containing 10% FCS (Invitrogen) (37°C, humidified atmosphere containing

5% CO_2) until they reached 50-80% confluence. Transfection complexes were generated using 2 μg of mCD39 overexpression plasmid and 10 μl of SuperFect in 100 μl of serum-free RPMI 1640 medium. The SuperFect mixture was incubated (room temperature, 10 min), after which the complexes were added to RAW cells (0.6 mL RPMI 1640 medium containing 10% FBS). Following incubating (37°C, 5% CO_2, 3 hours), cells were washed 3 times with HBSS (Invitrogen) and then incubated with RPMI with 10% FBS. After 72 hours, transfected cells were selected using hygromycin (300 μg/ml).

Membrane protein isolation

RAW cell transfectants were washed twice with phosphate-buffered saline (Gibco) and membrane protein was isolated as previously described [116]. In brief, 2 ml of ice-cold hypotonic lysis buffer (50 mM sucrose, 10 mM Hepes, pH 7.4, with 1 μg/ml aprotinin, 1 μg leupeptin, 1 mM PMSF) was added to each plate before cells were scraped from the dish bottom. Cells were homogenized by 25 strokes of a Dounce homogenizer (Kontes Glass) with a tight pestle. Following the addition of 132 μl of 65% sucrose [(w/w) in 10 mM Hepes, pH 7.4], 4 μl of 0.5 M $MgCl_2$ into 2 ml of hypotonic lysis buffer, the homogenate was subjected to two 20-min spins at 2,000 x g at 4°C to pellet nuclei, mitochondria, and unlysed cells. Crude membranes were pelleted from the resulting supernatant by centrifugation at 100,000g for 30 min at 4°C, washed quickly in 2 ml of hypotonic lysis buffer, and resuspended in the same buffer. The membranes were flash frozen in aliquots and stored at -80°C. Protein concentration was determined by Bio-Rad protein assay (Bio-Rad).

Free ATP measurement

RAW cell transfectants were washed 2 times with phenol red-free RPMI 1640 (Invitrogen) and then serum starved for 24 hours. Cell free media was then analyzed for endogenous ATP using an ATP bioluminescent assay kit (Sigma). Bioluminescent activity was measured using a VICTOR LIGHT luminometer (PerkinElmer).

$\alpha_m\beta_2$-integrin expression in transfected RAW 264.7 macrophages

RAW cell transfectants were serum starved overnight prior to stimulation for 5 hours with either 10 μM 2',3'-O-(2,4,6-trinitrophenyl) adenosine 5'-triphosphate (TNP-ATP) [97,98], 50 μM suramin [72,94-96], 50 μM adenosine 5'-(α,β-methylene)diphosphate (APCP) [83,93], or 150 μM periodate oxidized adenosine 5′-triphosphate (ox-ATP) [99,100]. Cells were treated (30 minutes) with 2′(3′)-O-(4-benzoylbenzoyl)adenosine 5′-triphosphate (bzATP, a specific P2X$_7$ receptor agonist). Macrophages were analyzed with flow cytometry following staining with an antibody directed against $\alpha_M\beta_2$-integrin.

Silencing the P2X$_7$ receptor in transfected RAW 264.7 macrophages

RAW cell transfected with murine *Cd39* or the control vector pcDNA3.1 were infected with lentivirus containing either a shRNA targeting the P2X$_7$ receptor or the control silencing vector pLKO.1. The sequence of the the P2X$_7$ shRNA construct within the pLKO.1 vector was 5' – CCGGGTCTTGCACATGATCGTCTTTCTCGAGAAAGACGATCATGTGCAAGACT TTTG – 3'. Both constructs were purchased as lentiviral particles from Sigma. Macrophages were subquently selected with puromycin to kill non-transfected cells.

Following 24 hours of serum starvation each of the four cell lines was analyzed by flow cytometry for cell surface $\alpha_M\beta_2$-integrin expression.

Macrophage transmigration assay

Primary peritoneal macrophages were elicited by injecting 3 ml of 4% thioglycolate medium (Sigma) into wild type and *Cd39$^{-/-}$* mice. Five days later peritoneal macrophages were isolated via peritoneal lavage and rinsed of debris with PBS. Primary macrophages were then used in a previously described transmigration assay [117]. Cells in serum free RPMI 1640 were added onto the upper well of a 24-well transwell plate (5μm pore, Costar) which had RPMI 1640 with 5% fetal bovine serum in the lower well. The inserts were precoated on both sides with fibrinogen (100mg/ml) and then blocked in bovine serum albumin. After 12 hours at 37°C, the number of cells that had transmigrated into the lower well was counted. The identity of transmigrating macrophages was confirmed by staining for F4/80. Images were acquired with a 20x objective (0.325 μm/pixel) using MetaMorph v7.0r3 software (Molecular Devices) on an Eclipse TE2000-E microscope (Nikon Instruments, Inc). RAW cell transfectants were serum starved in RPMI 1640 for 24 hours prior to being used in the same transmigration assay. Additional wells were simultaneously treated with either $\alpha_m\beta_2$-integrin functional blocking antibody (M1/70) or rat IgG2b, κ isotype control antibody after which the cells were allowed to transmigrate as before.

In vivo $\alpha_M\beta_2$-integrin blockade

An $\alpha_M\beta_2$-integrin functional blocking antibody (M1/70) or rat IgG2b, κ isotype control antibody was diluted in saline and administered intravenously (2 mg/kg) one hour prior to induction of cerebral ischemia [118]. Additional antibody (1 mg/kg) was administered 3 and 24 hours following ischemic induction [118]. All antibodies used were sodium azide-free and low endotoxin (NA/LE) preparations to minimize cytotoxicity. Single cell suspensions derived from ischemic and non-ischemic brain hemispheres from antibody-treated mice were analyzed by flow cytometry as described above, 48 hours following ischemic induction. Additional antibody-treated mice were analyzed by magnetic resonance imaging as described above.

Data analysis

Values are expressed as mean ± standard error of the mean, with the numbers of experiment performed provided in the figure legends. For experiments in which two variables were compared, two-tailed unpaired Student's *t* tests were used. For experiments in which more than two variables were compared, one-way ANOVA was used, with Fisher's exact test used to test for significant differences. For experiments involving a nominal variable and a measurement variable, the Mann-Whitney U-test was used for nominal variables with two values, while the Kruskal-Wallis test was used for nominal variables with three or more values. Data were considered significantly different when $p < 0.05$.

Acknowledgments

Figure 2.1 Effect of *Cd39* genotype on resistance to cerebral ischemia 48 hours after MCA occlusion. (**A**) Representative magnetic resonance images of WT and *Cd39*$^{-/-}$ brains after cerebral ischemia. (**B**) Quantification of average cerebral infarct volume in ischemic WT and *Cd39*$^{-/-}$ brains. (**C**) Functional effects of cerebral infarction were assessed using a neurologic deficit score, with higher scores indicating a greater deficit. The horizontal bars indicate the average neurologic deficit score for each group. *n* = 6 per group; *P* < 0.03, **P* < 0.01.
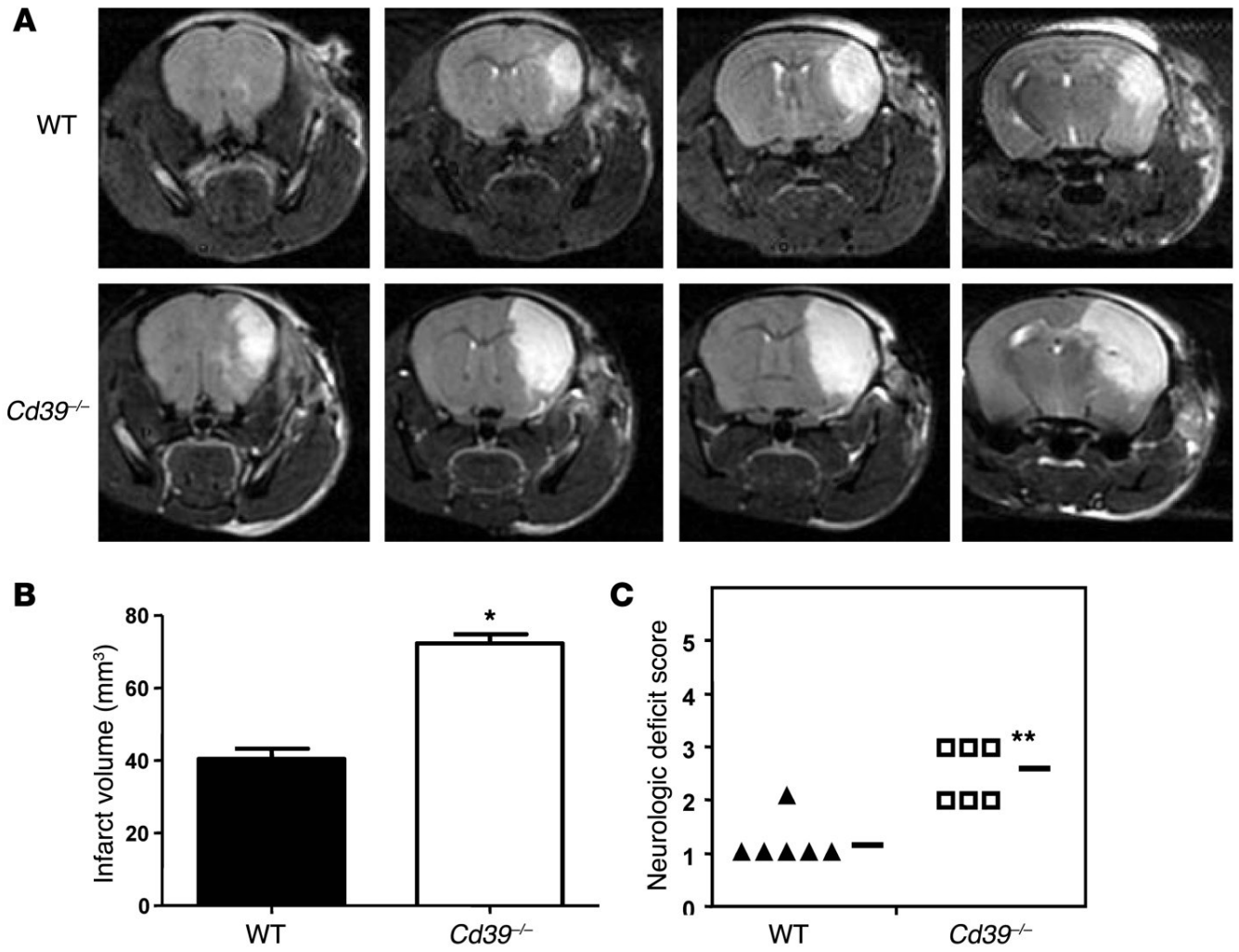
Figure 2.1

Figure 2.2 Role of CD39 in leukocyte sequestration in the ischemic cerebrum. The ischemic brains of WT (**A–C**) and *Cd39*$^{-/-}$ (**D–F**) mice were stained for nuclei (**A** and **D**) and neutrophils (**B**, **C**, **E**, and **F**). Scale bars: 1,000 μm (**A**, **B**, **D**, and **E**), 100 μm (**C** and **F**). Adjacent sections of WT (**G–I**) and *Cd39*$^{-/-}$ (**J–L**) ischemic mouse brains were stained for nuclei (**G** and **J**) and macrophages (**H**, **I**, **K**, and **L**). Scale bars: 1,000 μm (**G**, **H**, **J**, and **K**), 100 μm (**I** and **L**). The white boxes in the center panels show the magnified area in the right panels. (**M**) Representative scattergrams of LY-6G–stained neutrophil populations (green) within the ischemic and contralateral hemispheres of WT and *Cd39*$^{-/-}$ mice as well as isotype control. (**N**) Representative scattergrams of F4/80-stained macrophage populations (blue) within the ischemic and contralateral hemispheres of WT and *Cd39*$^{-/-}$ mice as well as isotype control. The effect of CD39 on the infiltration of leukocyte subpopulations was assessed using flow cytometry: neutrophils (**O**) and macrophages (**P**). $n = 6$ per group in **M–P**; *$P < 0.005$, **$P < 0.0001$.
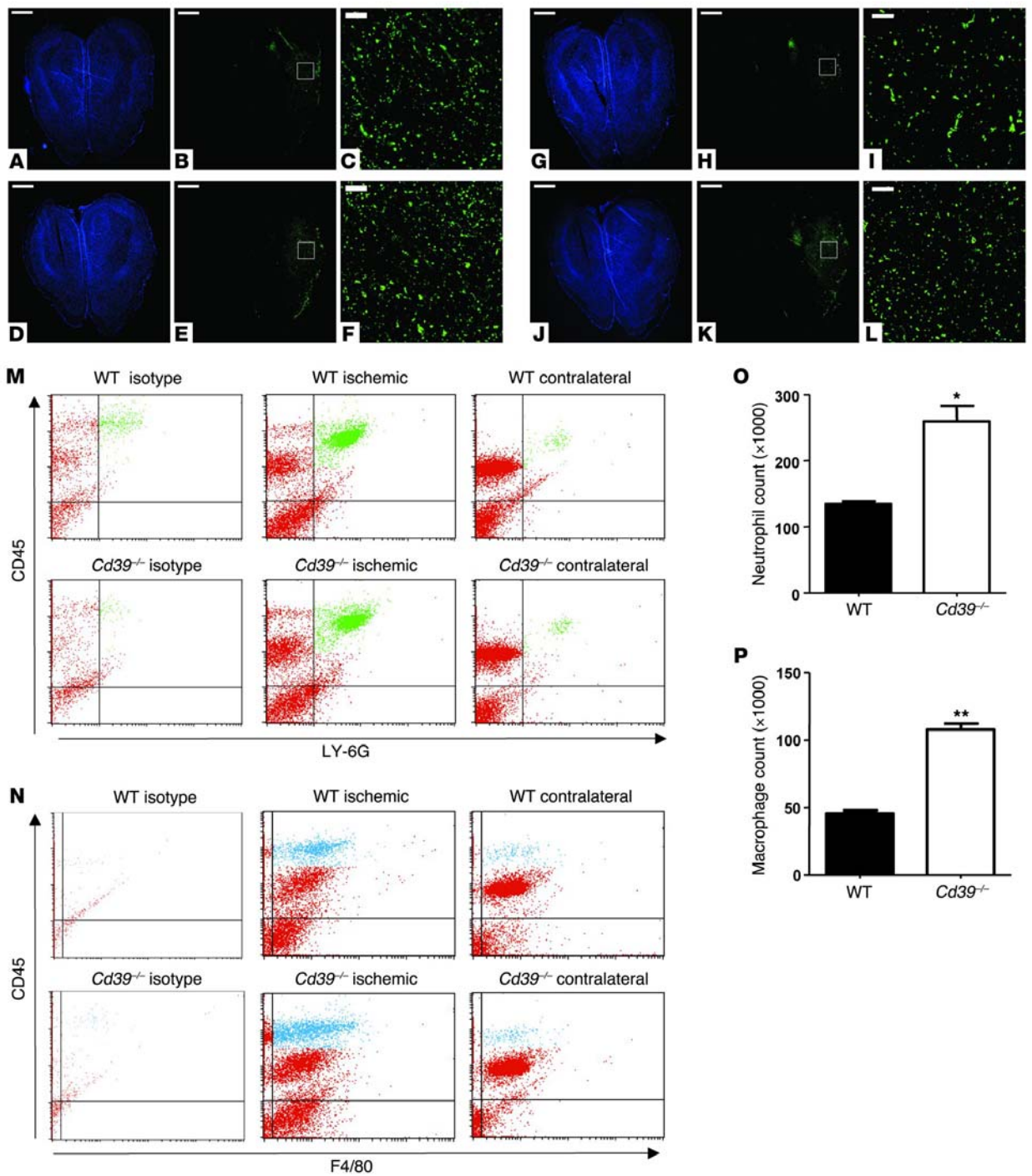
Figure 2.2

Figure 2.3 Circulating ectoapyrase activity confers resistance to cerebral ischemia. Leukocytes purified from WT and $Cd39^{-/-}$ mice were coincubated with [8-^{14}C]ATP or [8-^{14}C]ADP to assess the functional importance of leukocyte CD39. Metabolic products were resolved via TLC, and representative radioactivity histograms are shown for ATP (**A**) and ADP (**B**) (L, ladder comprising radiolabeled ATP, ADP, and AMP). Forty-eight hours after ischemia induction, MRI was performed to assess the therapeutic potential of soluble apyrase in diminishing cerebral infarction. Crosses (†) indicate the metabolite added to the reaction (**C**) Multiple strokes were scored to generate aggregate cerebral infarct volumes. Additional mice were subjected to flow cytometric analysis to determine neutrophil (**D**) and macrophage (**E**) infiltration following apyrase administration. $n = 4$ per group in **C**–**E**; *$P < 0.04$, **$P < 0.02$, ***$P < 0.001$.
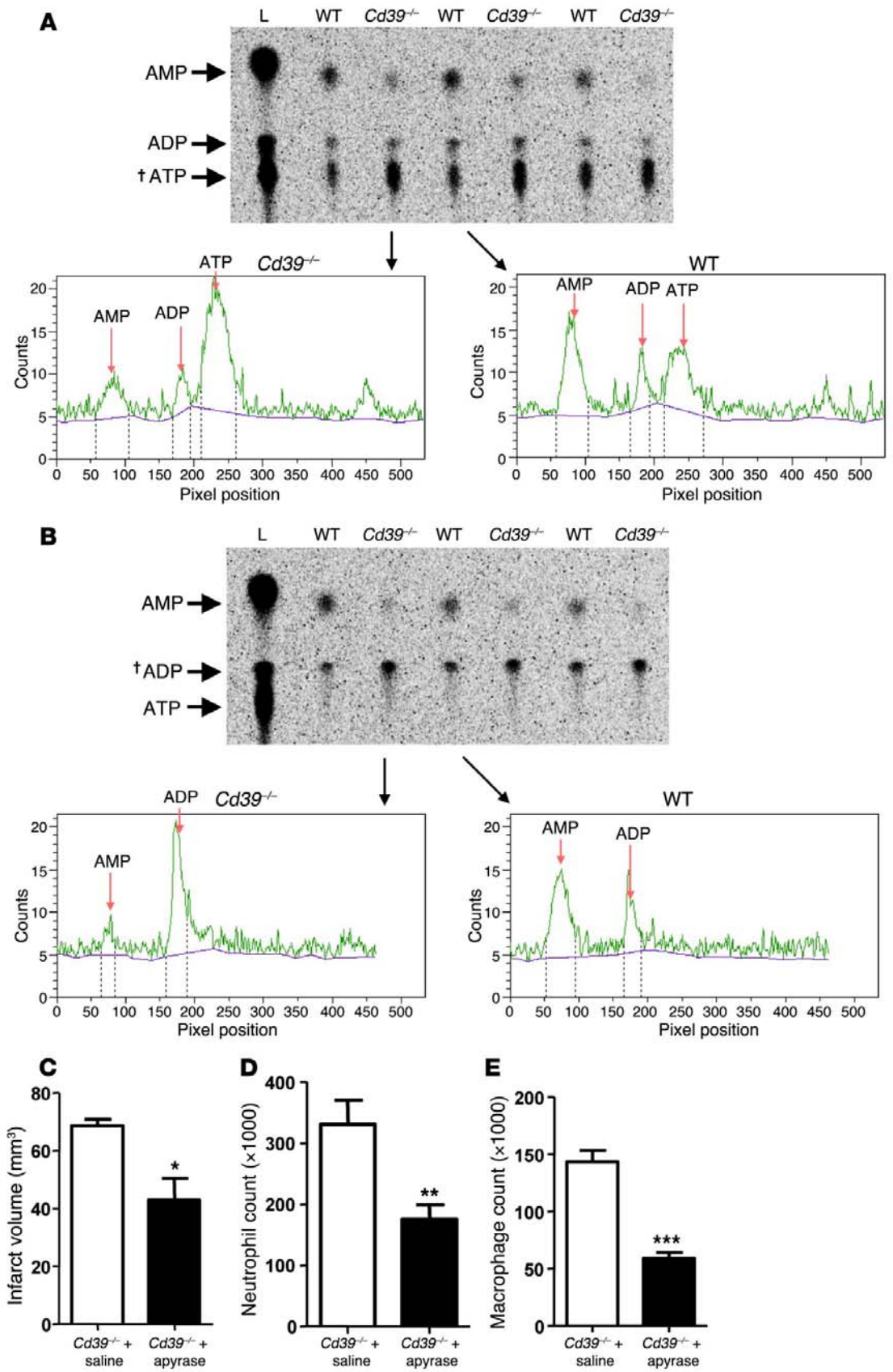
Figure 2.3

Figure 2.4 CD39 deficiency does not impair bone marrow reconstitution. To determine the contribution of donor and recipient cells to the neutrophil and monocyte subpopulations, we developed a quantitative PCR that measured neomycin gene dosage. (**A**) Mixtures of WT and *Cd39*$^{-/-}$ peripheral blood leukocytes (*x* axis indicates cell number × 10,000) were used to validate this assay. Leukocyte buffy coats from bone marrow–transplanted mice were sorted by flow cytometry to isolate the neutrophil and monocyte subpopulations. The neutrophils (**B**) and monocytes (**C**) were then quantified for relative neomycin DNA. Peripheral blood from untransplanted WT (green) and *Cd39*$^{-/-}$ (black) mice was separated into neutrophil (**D**) and monocyte (**E**) populations by flow cytometry and then examined for CD39 expression. Isotype control is shown in orange. Peripheral leukocytes from bone marrow chimeric mice were sorted into neutrophil (**F**) and monocyte (**G**) populations and stained for CD39: WT→WT (green), WT→KO (red), KO→WT (magenta), and KO→KO (black). Whole-lung homogenates from bone marrow chimeric mice were sorted for endothelial cells (**H**) and stained for CD39: WT→WT (green), WT→KO (red), KO→WT (magenta), and KO→KO (black). (**I**) Whole-lung digests from bone marrow–transplanted mice were analyzed for relative CD39 expression on endothelial, neutrophil, and macrophage subpopulations. $n = 4$ or 5 per group; $*P < 0.001$, $**P < 0.01$, $***P < 0.05$.

Figure 2.4

-62-

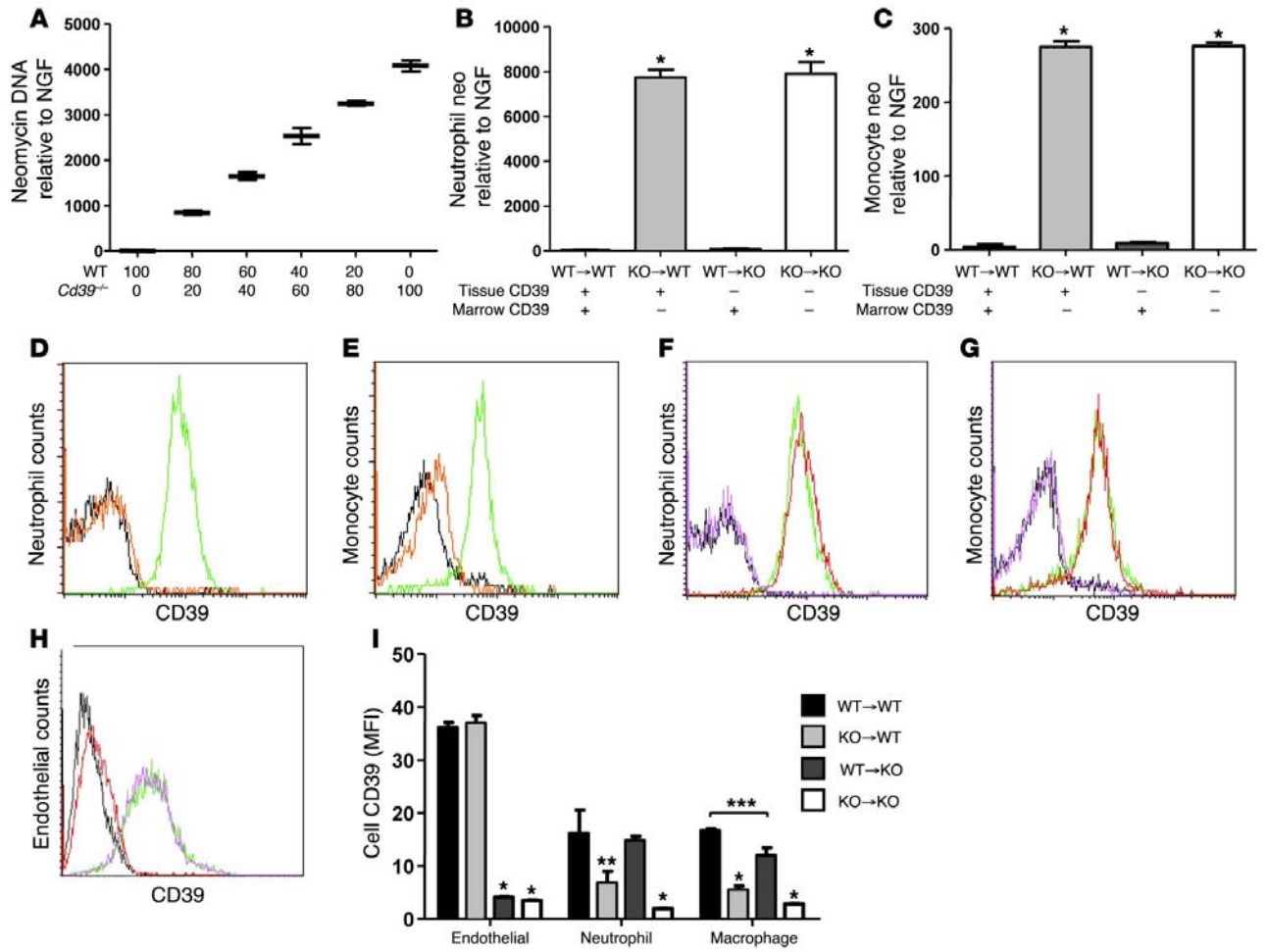**Figure 2.5** Role of CD39-bearing subpopulations in resistance to cerebral ischemia and regulation of platelet reactivity. WT and *Cd39*$^{-/-}$ mice underwent bone marrow reconstitution to generate chimeric mice, as a means to explore selective ablation of CD39 in endothelial and leukocyte subpopulations. (**A**) Quantification of average cerebral infarct volume determined by MRI in ischemic chimera brains. The contribution of CD39 on endothelium and leukocytes to leukosequestration of neutrophils (**B**) and macrophages (**C**) was examined in chimeric mice. (**D**) Whole-blood platelet aggregometry with ADP stimulation was performed on WT and *Cd39*$^{-/-}$ mice. Marrow-reconstituted mice were used to explore platelet reactivity following selective ablation of CD39 in endothelial and leukocyte subpopulations. (**E**) Representative whole-blood platelet aggregation profiles of each of the 4 chimeric subpopulations 2 weeks after transplantation. (**F**) Quantification of average platelet aggregation profiles. *n* = 5 or 6 per group in **A**–**D**; *n* = 4 or 5 per group in **E** and **F**. *$P < 0.01$; **$P < 0.001$; ***$P < 0.005$; $^{†}P < 0.01$ versus all other columns; $^{‡}P < 0.02$; $^{§}P < 0.001$ versus all other groups.
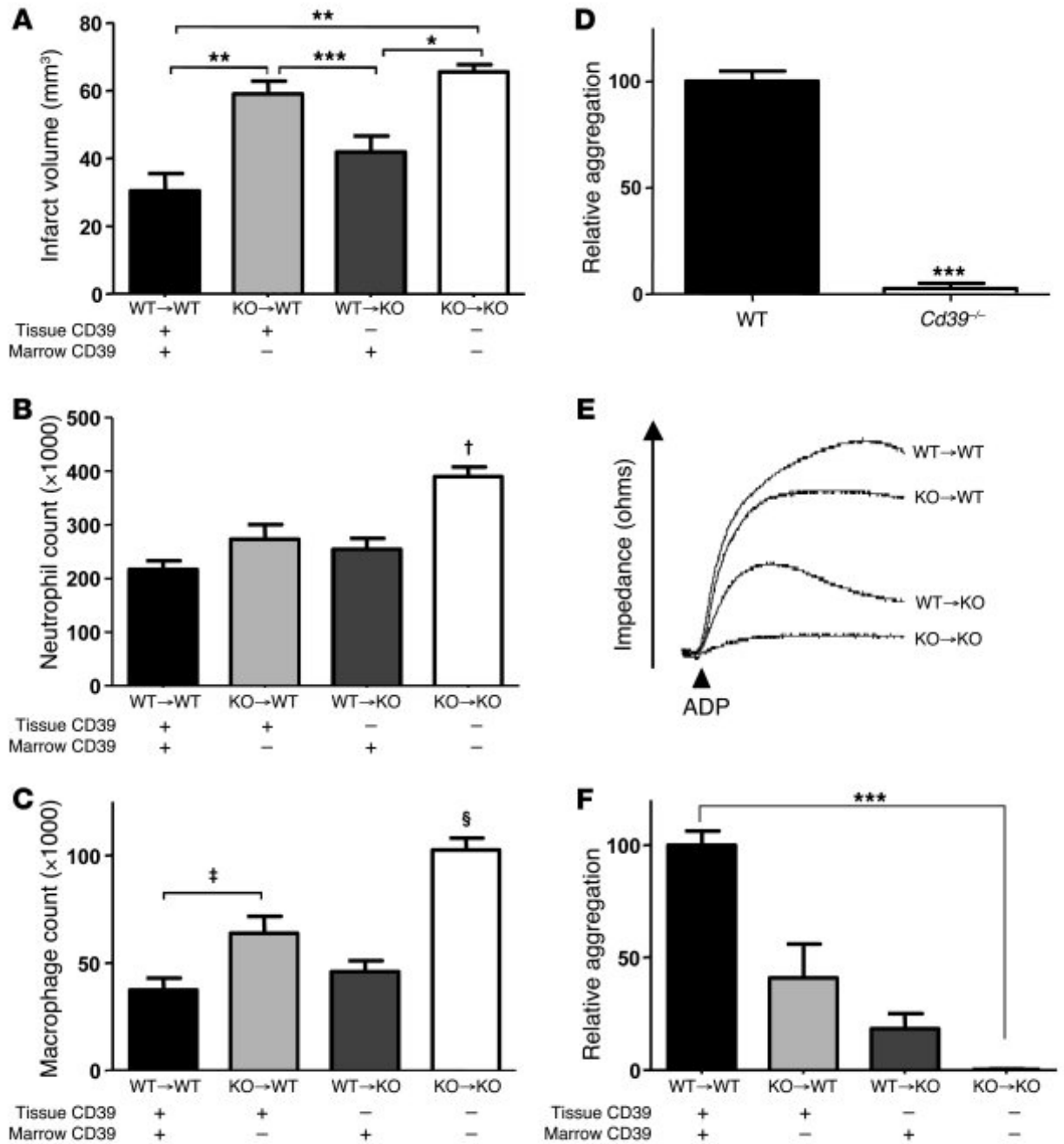
Figure 2.5

Figure 2.6   CD39 modulates circulating leukocyte $\alpha_M\beta_2$-integrin expression. Unstimulated whole blood of WT (black) and $Cd39^{-/-}$ (gray) mice was examined for $\alpha_M\beta_2$-integrin expression by staining the α_M subunit in the monocyte (**A**) and neutrophil (**B**) populations. The relative expression of α_M on the monocyte (**C**) and neutrophil (**D**) populations in WT and $Cd39^{-/-}$ mice is shown. $n = 9$ per group; *$P < 0.01$.
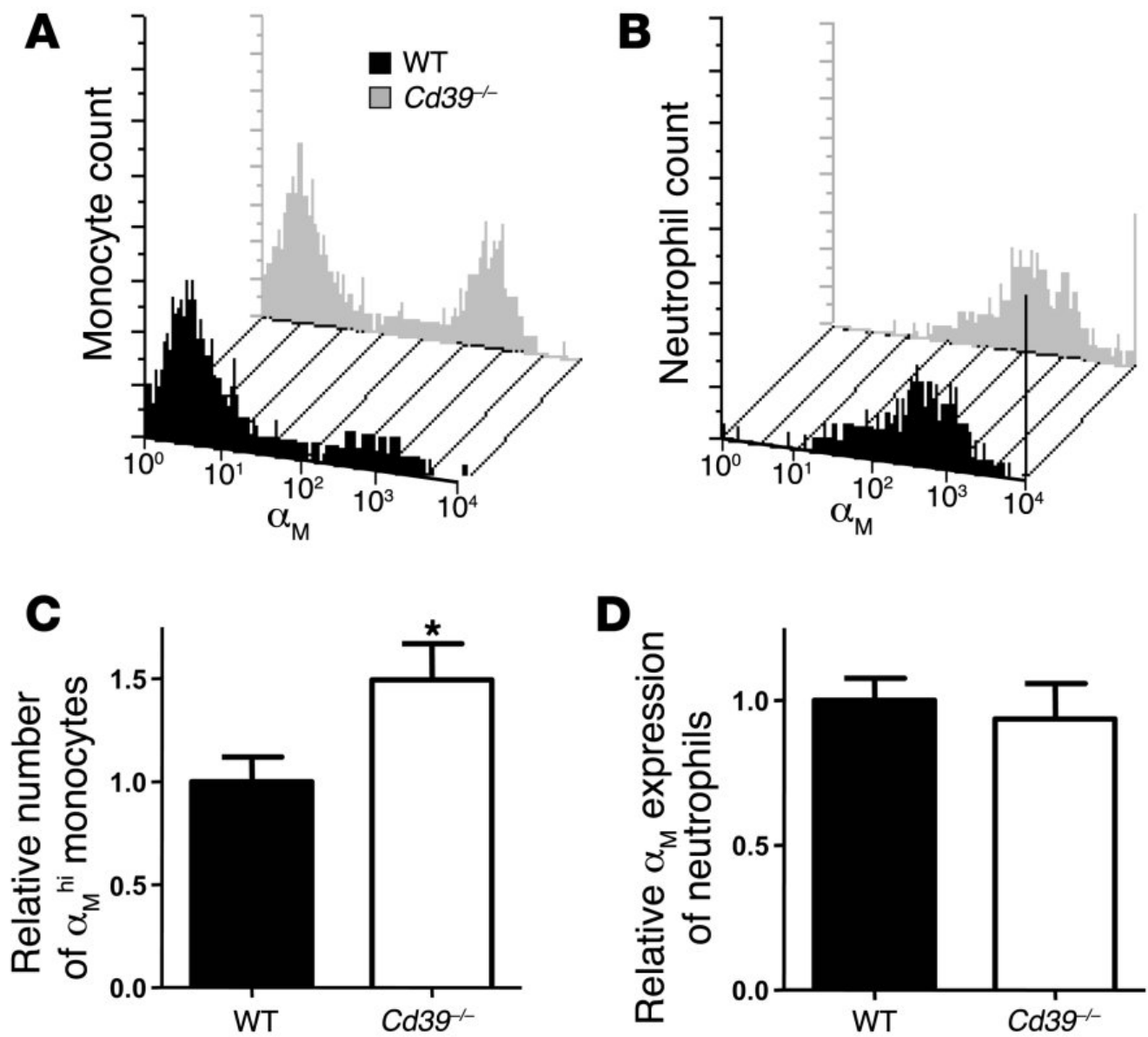
Figure 2.6

Figure 2.7 Apyrase treatment modulates monocyte $\alpha_M\beta_2$-integrin expression. WT and *Cd39*$^{-/-}$ mice were treated with soluble apyrase before examination of monocyte $\alpha_M\beta_2$-integrin expression. (**A**) Representative histogram shifts can be seen between vehicle-treated and apyrase-treated monocytes in WT and *Cd39*$^{-/-}$ mice. The aggregate effect of apyrase treatment on monocyte α_M expression can be seen in **B**. $n = 4$ per group; *$P <$ 0.01 versus all other columns.
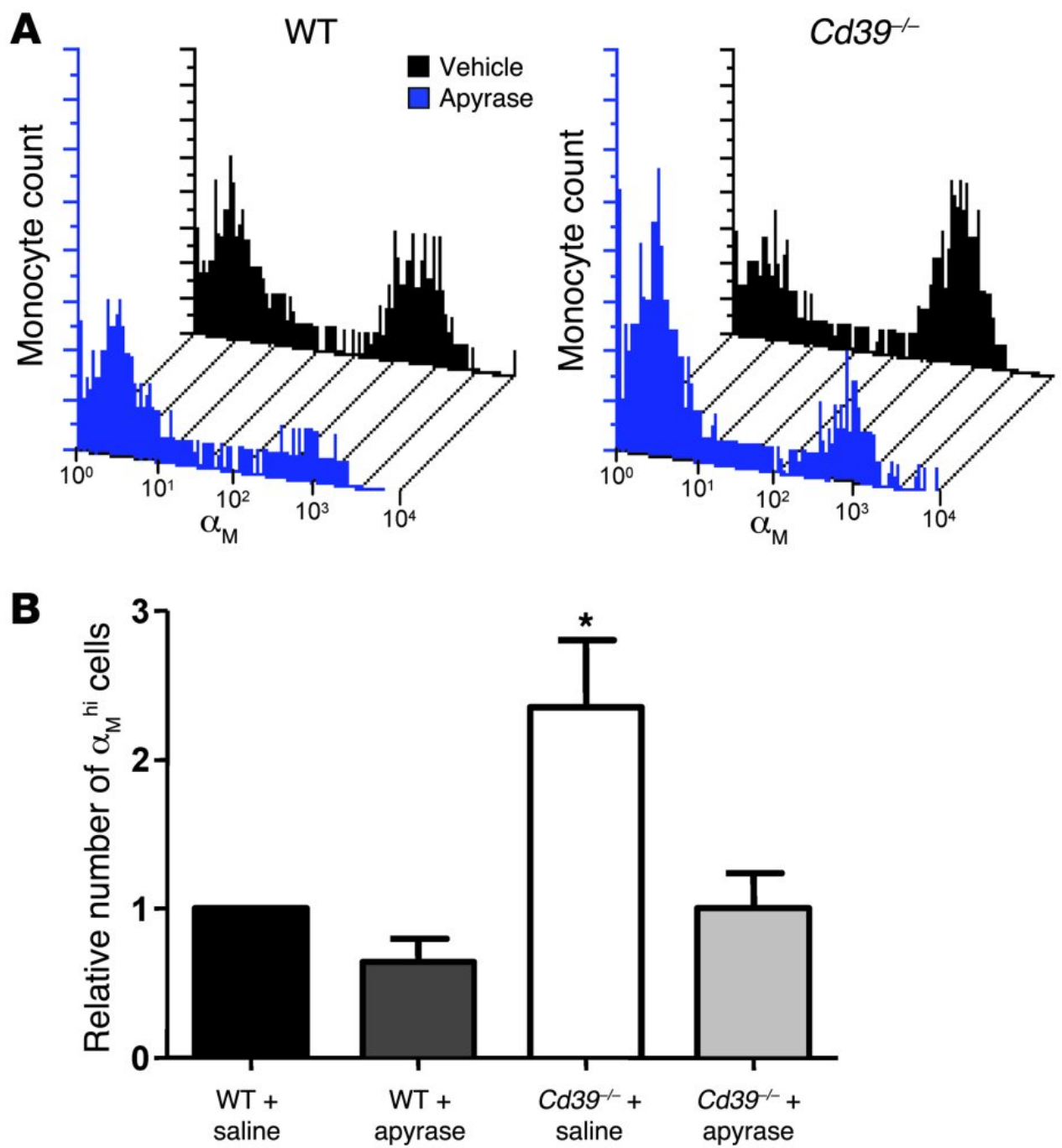
Figure 2.7

Figure 2.8 Regulation of $\alpha_M\beta_2$-integrin in RAW 264.7 macrophages. (**A**) Relative murine *Cd39* mRNA expression was measured using RT-PCR in empty vector–transfected and mCD39-overexpression vector–transfected macrophages. A representative immunoblot of membrane protein is shown. (**B**) Free ATP was measured in the medium of each cell line to assess the effect of altered CD39 expression on ambient ATP. (**C**) Representative histograms of α_M expression in empty vector–transfected (black overlay), mCD39-transfected (red) macrophages, and isotype control (orange overlay). (**D**) Empty vector– and mCD39 vector–transfected macrophages were modulated pharmacologically to determine the contribution of various P2 receptors and adenosine formation in the regulation of $\alpha_M\beta_2$-integrin. (**E**) bzATP, a specific $P2X_7$ receptor agonist, was used to treat macrophages to determine modulation of $\alpha_M\beta_2$-integrin. (**F**) Relative $P2X_7$ receptor mRNA was measured by quantitative PCR in macrophage cell lines that expressed either vector or mCD39 as well as either control shRNA or shRNA targeting the $P2X_7$ receptor. A representative $P2X_7$ receptor immunoblot of membrane protein is shown. (**G**) α_M expression following modulation of CD39 expression, $P2X_7$ receptor expression, or both. $n = 6$ per group; $*P < 0.01$ versus all other groups, $**P < 0.001$ versus all other groups, $***P < 0.001$.
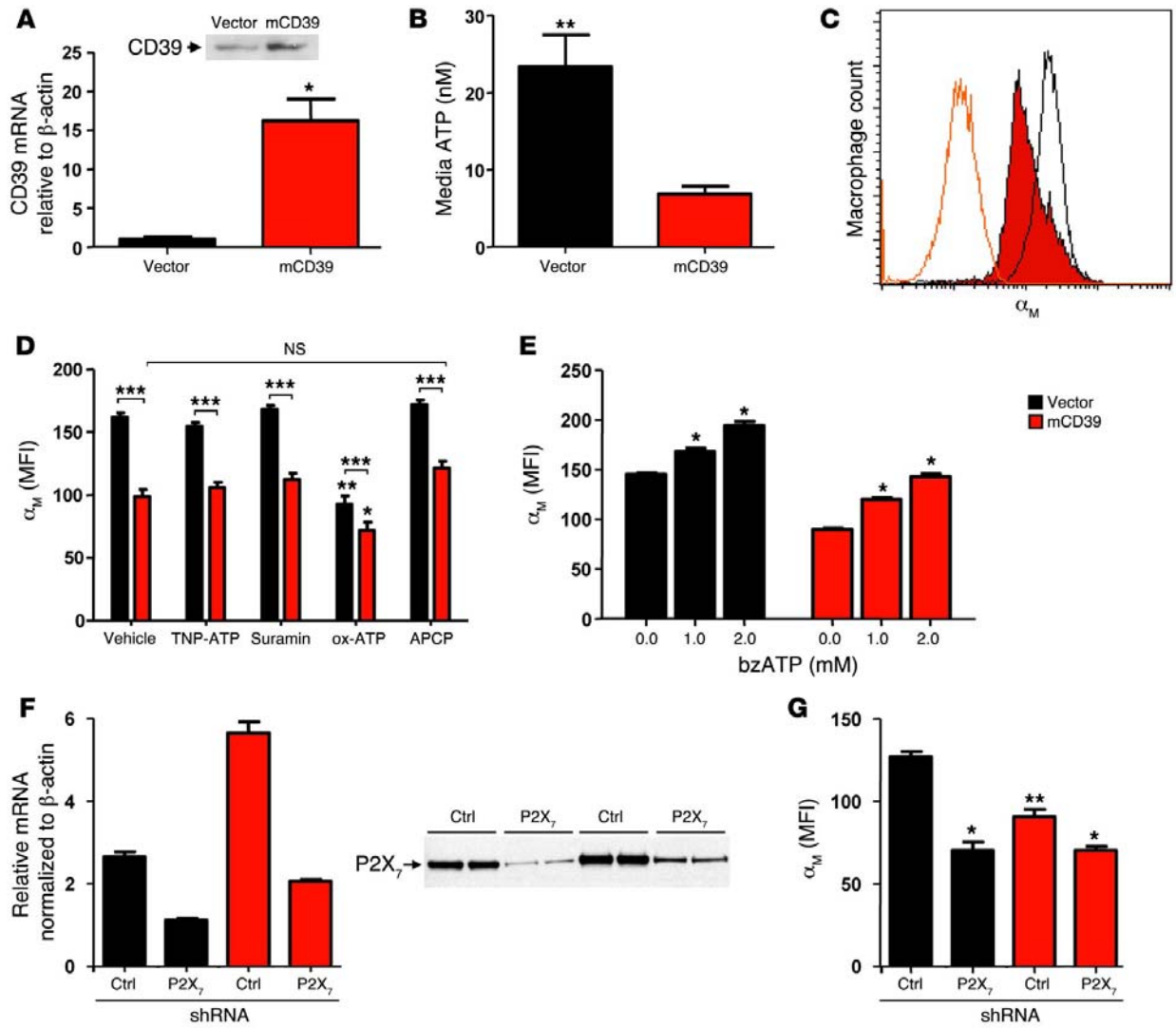
Figure 2.8

Figure 2.9 CD39 regulates leukocyte trafficking via $\alpha_M\beta_2$-integrin in vitro and in vivo. (**A**) Transmigration of WT or $Cd39^{-/-}$ peritoneal macrophages on fibrin(ogen)-coated Transwells. (**B**) Representative microscope field of transmigrated primary macrophages stained with F4/80 acquired with a 20× objective (0.325 μm/pixel). (**C**) Transmigration on fibrin(ogen)-coated Transwells was assessed using RAW 264.7 macrophages transfected with mCD39 or control vector. Some wells were treated with α_M functional blocking antibody or an isotype control. Migration was quantified relative to vehicle-treated, vector-transfected macrophages. In vivo studies examined leukocyte sequestration in WT and $Cd39^{-/-}$ mice treated with an $\alpha_M\beta_2$-integrin functional blocking antibody 48 hours after induction of cerebral ischemia. Flow cytometry was used to assess neutrophil (**D**) and macrophage (**E**) infiltration. (**F**) Quantification of MRI of infarcted ischemic hemispheres of mice treated with isotype control antibody or α_M-integrin functional blocking antibody. $n = 3$ per group in **A** and **B**, $n = 9$ per group in **C**, $n = 7$ per group in **D**–**F**. *$P < 0.001$ between indicated groups;
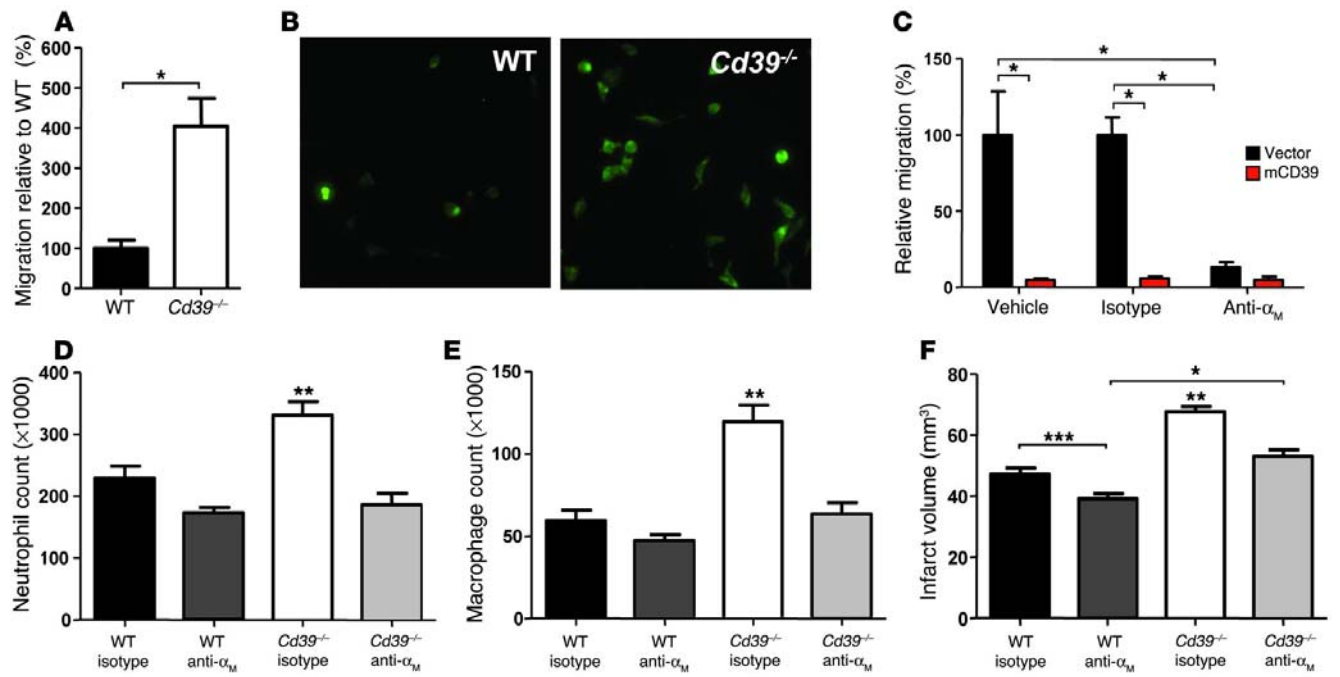
Figure 2.9

CHAPTER III

ECTO-ENZYMATIC SUPPRESSION OF ATHEROGENESIS

Abstract

The intracellular energy intermediaries ATP and ADP, released by activated or injured cells, act extracellularly to induce inflammation and thrombosis. To keep inflammation and coagulation in check, vascular cells express an ecto-enzyme (CD39/NTPDase-1) on their surface which effects the terminal phosphohydolysis of purine nucleotides released into flowing blood. Experiments tested the hypothesis that CD39, by mitigating local activation of platelets and monocytes, could protect against atherogenesis. Immunostaining of atherosclerotic murine aorta revealed CD39 to be absent from endothelium overlying plaque. Hypercholesterolemic mice lacking a CD39 allele, whose platelets showed increased sensitivity to ADP activation, had significantly greater atherosclerotic plaque burden than their hypercholesterolemic, wild-type counterparts. Concordantly, the CD39-deficient mice exhibited greater platelet deposition in plaque as well as elevated circulating levels of platelet-derived biomarkers soluble P-selectin and RANTES. *In vitro* experiments identify CD39 as a modulator of acetylated-LDL and oxidized-LDL transport in macrophages. CD39 suppressed foam cell formation by reducing the action the scavenger receptors CD36 and SRA-1 in a $P2X_7$-receptor-dependent fashion. These data are the first to demonstrate that through a

combination of inhibiting local platelet activation and macrophage foam cell formation, extracellular nucleotide metabolism suppress atherogenesis.

Introduction

Development of the atherosclerotic plaque is driven by dynamic interactions between the lipid milieu, cells of the vascular wall, and those recruited from the circulation. Endothelial cells, monocytes, T-cells, and platelets have all been implicated in atherogenesis[119]. Historically, the role of platelets in this process was principally defined by correlative evidence of increased platelet activation and local recruitment[120-122], and the notation of greater numbers of glycoprotein-mediated monocyte-platelet aggregates in the circulation of patients with cardiovascular disease[121,123-126]. However, more recent studies demonstrated that platelet activation likely plays an important role in the early stages of atherogenesis via transient endothelial and mononuclear cell interactions[127,128] and *in situ* release of bioactive mitogens and chemoattractants[127,129]. Moreover, activated platelets provide cholesterol that is scavenged by macrophages to form foam cells, which are key components of atherosclerotic plaques[130,131].

One of the principal regulators of platelet activation *in vivo* is CD39. This enzyme, a 70-100 kDa glycoprotein expressed on the surface of leukocytes and endothelial cells, is responsible for serial phosphohydrolysis of ATP to ADP and further to AMP, by virtue of its ecto-ATPDase (ATP diphosphohydrolase) activity[8,10,91,132,133]. Because ADP is a potent platelet agonist, endothelial CD39 serves as a critical negative regulator of platelet activation and recruitment,[8,10,11,91,133] and thereby maintains blood

fluidity. By metabolizing prothrombotic ADP, CD39 provides natural protection from nucleotides released from injured vasculature or activated platelets. Similarly, CD39 is thought to temper inflammation by catabolizing extracellular ATP[134,135] and by generating anti-inflammatory adenosine through downstream action of ecto-5'-nucleotidase (CD73; AMP $\rightarrow$ adenosine)[83]. The importance of inflammation and platelet activation in atherosclerosis and CD39's role in regulating both suggested a novel paradigm wherein endogenous regulation of endovascular purine levels modulate key cellular drivers of atherosclerosis.

RESULTS

As expression of CD39 changes dynamically with a cell's environment[136,137] we first sought to examine the presence of CD39 on endothelial cells of on healthy vessels to vessels with atherosclerotic plaques. Immunofluorescent staining of the $Apoe^{-/-}$ mouse aortas revealed a stark regionalization of CD39 expression. Robust CD39 expression was present on endothelial cells overlying non-atherosclerotic regions of the vascular wall, whereas CD39 was significantly diminished over atherosclerotic plaque (**Figure 3.1, A-B**). Cerium chloride staining of ATPase activity demonstrated a concordant loss of ATPase activity at sites of atherosclerotic plaque relative to vasculature without plaque in the same mouse (**Figure 3.1, C-D**).

To explore how a loss of CD39 may alter the course of atherosclerosis, $Cd39^{-/-}$ mice were crossed onto the hyperlipidemic $Apoe^{-/-}$ background to generate $Cd39^{+/+}Apoe^{-/-}$, $Cd39^{+/-}Apoe^{-/-}$, $Cd39^{-/-}Apoe^{-/-}$ mice. $Cd39^{+/-}Apoe^{-/-}$ mice model a state of diminished

CD39 enzyme activity, as CD39 protein expression and activity dose-dependently decrease with allele copy number (**Figure 3.2, A-C**). After 20 weeks on a high fat diet, mice missing a CD39 allele (*Cd39$^{+/-}$Apoe$^{-/-}$*) developed atherosclerotic lesions that were markedly larger than their *Cd39$^{+/+}$/Apoe$^{-/-}$* counterparts (**Figure 3.2, D-E**). This suggests that the partial loss of CD39 can strongly influence the course of atherogenesis. Somewhat paradoxically, a complete absence of CD39 had no significant effect on total plaque burden relative to controls. In all experiments, heart rate, blood pressures, and cholesterol levels did not vary significantly between control *Apoe$^{-/-}$* and CD39-deficient *Apoe$^{-/-}$* mice (data not shown).

We next examined the composition of atherosclerotic plaques in CD39-deficient mice. By identifying platelets with the constitutive surface marker CD41/glycoprotein IIb, platelet remnants appeared to localize to the surface and leading edges of atherosclerotic plaques (**Figure 3.2, F-H**). Histomorphometry revealed that *Cd39$^{+/-}$/Apoe$^{-/-}$* mice had 113% greater platelet deposition in their atherosclerotic plaques compared to *Cd39$^{+/+}$/Apoe$^{-/-}$*controls (**Figure 3.2I**). This implies that CD39-deficient mice are susceptible to chronic localized platelet deposition, and that circulating platelet-derived factors may also be elevated in these mice. Two of these, P-selectin (shed as soluble P-selectin) and RANTES, were found at 39% and 60% higher concentrations respectively in the plasma of *Cd39$^{+/-}$Apoe$^{-/-}$* mice compared to *Cd39$^{+/+}$Apoe$^{-/-}$* controls (**Figure 3.2, J-K**). These two biomarkers of platelet activation combined with the aortic root platelet deposition suggest that platelet activation may be driving the susceptibility to atherosclerosis phenotype of *Cd39$^{+/-}$Apoe$^{-/-}$* mice. In *Cd39$^{-/-}$Apoe$^{-/-}$* mice, both RANTES

and sP-Sel were found at moderately elevated levels (though not significantly) when compared to $Cd39^{+/+}Apoe^{-/-}$ controls.

The platelets of CD39-null mice, bombarded by elevated levels of extracellular nucleotides, become desensitized to stimulaton[11,15]. The ADP-sensitive receptors can be resensitized, though, by treatment with a soluble CD39 homolog[15]. Similarly, CD39 bearing leukocytes, when injected into CD39 null mice can restore ADP sensitivity to platelets[135,138]. This suggests that transcellular metabolism by CD39 plays an important role in the regulation of platelet activation. To explore platelet reactivity in CD39-deficient, hyperlipidemic mice, we used whole blood platelet aggregometry. This assay preserves the proximity of leukocyte-bound CD39 to platelets, unlike platelet rich plasma aggregometry, which assays platelet function in a preparation devoid of leukocytes. Consistent with previous studies, whole blood platelet aggregometry revealed that CD39 null mice were desensitized to ADP-mediated platelet activation (**Figure 3.3, A-B**)[11,15,135]. Physiologically, ADP acts in a paracrine fashion to activate platelets and is essential for the growth and stabilization of a thrombus[56]. ADP is an agonist for the G-protein coupled receptors (GPCRs) $P2Y_1$ and $P2Y_{12}$, the latter being the target of the anti-thrombotic thienopyridine class of drugs[60]. It is thought that chronic stimulation of these GPCRs leads to their transient downregulation and desensitization as seen in CD39-null mice[15].

As the sensitivity of mice heterozygous for CD39 had not been determined, we examined them using whole blood aggregometry. Interestingly, platelets from these mice

were not desensitized to ADP stimulation. In fact, platelets from these mice had slightly enhanced responses to ADP agonism. This increased ADP-induced aggregation was particularly pronounced at the lowest concentrations of ADP stimulation. When higher concentrations of ADP were used, there was no difference observed between the total aggregation of platelets in whole blood of $Cd39^{+/+}$ and $Cd39^{+/-}$ mice, implying that the maximal aggregation threshold of the two genotypes is not different. Instead, there is a saturable difference in sensitivity to ADP stimulation. In hyperlipidemia, the sensitivity of platelet activation from $Cd39^{+/-}Apoe^{-/-}$ mice persisted though maximal aggregation was achieved at an even lower dose of ADP than its normolipidemic counterpart (**Figure 3.3C**). Hyperlipidemia is known to enhance platelet reactivity through synergistic activation of the scavenger receptor CD36 on platelets[139]. These *ex vivo* responses support the hypothesis that lack of CD39 may promote atherosclerosis by exaggerating platelet activation at lesional sites and promoting platelet deposition on the atherosclerotic plaques of the same mice (**Figure 3.2I**). Historically, platelets or their remnants were seldom appreciated by histology and this was attributed to the transient nature of their interaction with endothelium[127]. Our data indicate that regional platelet activation is likely an important contributor to atherogenesis.

CD39 levels have been correlated with activation of multiple leukocyte subtypes[4,14,135] and recent work has shown enhanced ischemia-driven leukocyte trafficking in $Cd39^{-/-}$ mice[135]. Macrophages contribute to plaque growth by their profound tendency to scavenge circulating lipids via scavenger receptor mediated pinocytosis. These lipid-laden macrophages take on a foamy appearance when stuffed

with vesicular lipids, contributing to the lipid content of the growing plaque. Marophages could therefore contribute to atherogenesis by being recruited to nascent plaque in greater numbers, or by becoming more activated and lipid-avid. In $Cd39^{+/-}$ $Apoe^{-/-}$ or $Cd39^{-/-}Apoe^{-/-}$ mice, though, plaque macrophage numbers were not appreciably altered when compared to control $Cd39^{+/+}Apoe^{-/-}$ (data not shown). This does not preclude a relationship between CD39 and macrophages in the formation of atherosclerotic plaque as modulation of foam cell formation has profound effects on the formation of aortic plaque without altering plaque macrophage content[140]. CD39-deficient peritoneal macrophages took up significantly greater lipid than $Apoe^{-/-}$ controls (**Figure 3.4, A-B**). Concordantly, CD39 overexpression in macrophages[135] led to a 50% suppression of the scavenger receptors SRA-1 and CD36 (**Figure 3.4, C-D**). Consequently both AcLDL uptake and OxLDL uptake were reduced in CD39 overexpressing cells (**Figure 3.4, E-H**). To test the hypothesis that CD39- mediated dissipation of ATP reduces stimulation of ATP-sensitive receptors and thereby mitigate lipid scavenging, we employed a pharmacologic approach to selectively inhibit purinergic receptors to determine their contribution to foam cell formation. Neither OxLDL uptake nor AcLDL uptake were significantly affected by treatment with a $P2X_4$ receptor inhibitor (TNP-ATP) (**Figure 3.4, I-J**). Similarly, the pleotropic purine receptor inhibitor suramin had no effect on AcLDL uptake, but did suppress the uptake of OxLDL by 21%. The most striking effect was seen with OxATP (a selective $P2X_7$ receptor antagonist[99,100]), which strongly suppressed the uptake of both AcLDL and OxLDL. OxATP treatment of vector-transfected and mCD39-transfected cells did not completely abrogate the differences in lipid uptake between the two groups, though, suggesting that

other purine sensitive receptors may be involved as shown by suramin's inhibition of OxLDL uptake. Together, these data show that CD39 may act to reduce the uptake of modified-lipids by macrophages by reducing ATP mediated-stimulation of purine-receptors, thereby inhibiting foam cell formation and the atherogenic process by reducing local accumulaion of cholesterol esters.

Discussion

The increased plaque formation, platelet reactivity, and foam cell formation of CD39-deficient mice provides the first direct evidence linking CD39 expression to plaque formation. Furthermore, the loss of CD39 over atherosclerotic plaques shows that expression of CD39 is environmentally dependent; and that areas of higher and lower expression exist regionally in the same vessel of wild-type animals. Recent studies support this hypothesis, with investigators having noted abnormal leukocyte ADPase and ATPase activity[141] and smooth muscle cell CD39 expression[142] in patients with severe coronary artery disease. Another factor within the milieu of a plaque is oxidative stress, which can also affect CD39 by suppressing enzymatic activity independent of CD39 expression[143]. Free radicals and tumor necrosis factor-α both play a role in the development of atherosclerotic plaque and both of these factors can suppress the activity of endothelial CD39. One can envision a scenario whereby the loss of CD39 expression over a plaque (**Figure 3.1A**) synergizes with the local oxidative environment to suppress CD39 function. The end result would be an atherosclerotic plaque virtually devoid of ecto-apyrase activity on its surface, such as that seen in **Figure 3.1D**.

These focal losses of CD39 as seen over atherosclerotic plaque could be of greater consequence with respect to atherosclerosis than a global deficiency of CD39. The results presented here and elsewhere[11,15,135] indicate that in the absence of CD39, platelet ADP-receptors are overwhelmed by ambient nucleotides and become desensitized to further stimulation. Yet, our data suggest that partial expression of CD39 is sufficient to maintain platelet reactivity. Simultaneously, deficiency of CD39 predisposes macrophages to the formation of foam cells due to over-stimulation by ATP. Though desensitization of platelets and enhanced foam cell formation may balance each other in their effects on atherosclerosis (as in $Cd39^{-/-}Apoe^{-/-}$ mice), the summation of exaggerated platelet reactivity and foam cell formation in $Cd39^{+/-}Apoe^{-/-}$ mice leads to a profound increase in atherosclerotic plaque burden. In conclusion, these experiments demonstrate for the first time the importance of extracellular nucleotides in the development of atherogenesis and potential dose-dependent and regional effects of CD39 on plaque formation.

Materials and Methods

All animal experiments were conducted in accordance with protocols approved by the Institutional Animal Care and Use Committees at the University of Michigan.

Tissue Staining for CD39

$Apoe^{-/-}$ mice (Jackson Laboratories) were sacrificed after 32 weeks on a standard chow diet. The left ventricle was canulated and the mice were perfused with ice-cold saline (Gibco, Carlsbad, CA) followed by 10% buffered formalin (Fisher Scientific,

Pittsburgh, PA). The aortic arch was dissected free of the adventitial tissue and embedded in paraffin. Paraffin sections (5.0 μm) were made and antigen retrieved using citrate buffer (Vector Labs, Burlingame, CA, USA). Slides were stained with a rat anti-CD39 polyclonal antibody[144] and subsequently developed using a VECTASTAIN® ABC-Peroxidase Kit (Vector Labs, Burlingame, CA, USA) and developed using a TSA™ Tetramethylrhodamine Tyramide Reagent Pack (Perkin-Elmer,Wellesely, MA, USA). Nuclei were stained with 4',6-diamidino-2-phenylindole (DAPI). Images were acquired with a 40x objective with a 1.5x magnifying lens (0.107171 μm/pixel) using MetaMorph v7.0r3 software (Molecular Devices, Sunnyvale, CA, USA) on an Eclipse TE2000-E microscope (Nikon Instruments, Inc, Melville, NY, USA).

Cerium-chloride staining of ATPase activity

Twenty-six week-old *Apoe*^{-/-} mice and twelve week-old *Cd39*^{-/-} mice[11] were euthanized prior to cerium-chloride staining [145]. The left ventricle was perfused with ice-cold 0.05 M Na-cacodylate buffer, pH 7.2 (Electron Microscopy Sciences; Hatfield, PA, USA). Aortas were fixed for 5 minutes *in situ* with a mixture of ice-cold 2% paraformaldehyde (Electron Microscopy Sciences), 0.5% glutaraldehyde (Electron Microscopy Sciences), 0.25 mM sucrose, and 2 mM $MgCl_2$ in 0.05 M cacodylate buffer (pH 7.2). The aortic arch was dissected free and post-fixed for an additional 10 minutes in fixation buffer. Tissue was embedded in 7% low melting point agarose prior to sectioning with a Vibratome (70 mM). Tissue sections were washed overnight in cacodylate buffer and then rinsed briefly in Tris-maleate buffer (pH 7.2). Slides were incubated for 20 min at 37°C in reaction buffer: Tris-maleate (0.1 M, pH 7.2), ATP (2

mM), $MgCl_2$ (2 mM), KCl (20 mM), $CeCl_3$ (2 mM), 2 mM levamisole, 100 mM ouabain, and 50 μM a,b-methylene-ADP, and 0.0001% Triton X-100. Samples were rinsed in Tris-maleate buffer (pH 6.0) and cacodylate buffer (pH 7.2) prior to post-fixation with 1% OsO_4 (Electron Microscopy Sciences). After rinses in distilled water, tissue slices were dehydrated in graded ethanol, processed with propylene oxide, and embedded in Epon (Fluka; Buchs, Switzerland). Ultrathin 40 nM sections were cut using a Reichert Ultracut-E (Leica Microsystems Inc., Bannockburn, IL, USA) and imaged with a Philips CM-100 transmission electron microscope.

Generation of Cd39^{-/-}Apoe^{-/-} and Cd39[+/-]Apoe^{-/-} Mice

To investigate the *in vivo* effects of *Cd39* gene-deletion on atherogenesis, mice null in the enzymatically active apyrase-conserved regions 2-4 of the *Cd39* gene[11] were bred with *Apoe^{-/-}* mice[146] on a C57BL/6 background (Jackson Laboratories). *Cd39^{-/-}* mice were previously backcrossed a minimum of 6 generations onto the C57BL/6 background. Animals were backbred for 6 generations to produce *Cd39*-deficient-*Apoe*-deficient (*Cd39^{-/-}Apoe^{-/-}*) and *Cd39*-heterozygous-*Apoe*-deficient (*Cd39[+/-]Apoe^{-/-}*) littermates. At 4 weeks of age male littermates were placed on a diet containing 42% calories from fat (Harlan Teklad, Madison, WI). At 20 weeks of age, animals were euthanized after a 12-hour fast.

Cellular Membrane Preparations from Tissue Homogenates

WT, *Cd39^{+/-}*, *Cd39^{-/-}* mice were euthanized and perfused with ice-cold saline via a right ventricular cannula (Gibco, Langley, OK). To obtain cell membrane preparations

from a rich vascular source, murine lungs were excised and placed in 2 ml of ice-cold hypotonic lysis buffer (50 mM sucrose, 10 mM Hepes, pH 7.4, with 1 μg/ml aprotinin, 1 μg leupeptin, 1 mM PMSF). The lungs were minced using a Tissuemizer tissue homogenizer (Fisher Scientific). Following the addition of 132 μl of 65% sucrose [(w/w) in 10 mM Hepes, pH 7.4], 4 μl of 0.5 M $MgCl_2$ into 2 ml of hypotonic lysis buffer, the homogenate was subjected to two 20-min spins at 2,000 x g at 4°C to pellet nuclei, mitochondria, and unlysed cells. Crude membranes were pelleted from the resulting supernatant by centrifugation at 100,000g for 30 min at 4°C, washed quickly in 2 ml of hypotonic lysis buffer, and resuspended in the same buffer. The membranes were flash frozen in aliquots and stored at -80°C. Protein concentration was determined by Bio-Rad protein assay (Bio-Rad, Hercules, CA).

Measurement of CD39 expression and function

For immunoblotting, purified membrane fractions were resolved with a non-reducing Bis-Tris gel in LDS buffer (Invitrogen, Carlsbad, CA). Murine CD39 was recognized with a rat anti-mouse CD39 polyclonal antibody. Rabbit anti-rat heavy and light chain IgG conjugated to horseradish peroxidase was used as a secondary antibody (Sigma) and developed using ECL Detection Reagent (GE Amersham, Piscataway, NJ). Apyrase activity of the purified mouse membrane fraction was assayed with a Malachite Green Phosphate Assay Kit (BioAssay Systems, Hayward, CA) per the manufacturer's instructions, and analyzed using a VersaMax Tunable Microplate Reader (Molecular Devices, Sunnyvale, CA).

Measurement of atherosclerotic lesion size of Apoe-/- mice

The aortas of $Cd39^{+/+}Apoe^{-/-}$, $Cd39^{+/-}Apoe^{-/-}$, and $Cd39^{-/-}Apoe^{-/-}$ mice that had been fed a 42% calories from fat diet for 20 weeks were collected and stained with oil red O as described[147]. Images were taken using a DP12 Olympus Microscope Digital Camera and the percent surface areas occupied by oil red O−stained lesions were determined using Image-Pro Plus v.4.5 analysis software (Media Cybernetics, Inc).

Whole blood aggregometry

Heparinized murine blood was drawn from the retro-orbital plexus of $Cd39^{+/+}$, $Cd39^{+/-}$, and $Cd39^{-/-}$ mice, at 12 weeks of age. Whole blood was then allowed to sit for 25 minutes prior to being diluted 4-fold with a 1:1 mixture of normal saline and a lactated Ringer's that had been prewarmed to 37°C. The blood/electrolyte mixture was allowed to equilibrate for 5 minutes in the cuvette of the Chrono-log 560CA whole blood aggregometry machine (Chronolog, Havertown, PA). The whole blood samples were then treated with either 0.75 μM, 5.0 μM, or 10 μM ADP, and aggregation was recorded using the 810 Aggrolink Interface. An identical set of aggregation experiments were performed on $Cd39^{+/+} Apoe^{-/-}$, $Cd39^{+/-} Apoe^{-/-}$, and $Cd39^{-/-} Apoe^{-/-}$ mice that had been fed a 42% calories from fat diet for 20-24 weeks.

Measurement of plasma cytokines and lipids

Whole blood was drawn into citrated syringes via the inferior *vena cava* from mice that had been fasted overnight (~12 hours). The citrated blood was promptly centrifuged at 1000g after which the plasma fraction was removed. This was followed by a second centrifugation at 10,000g to remove containment red blood cells and platelet

fragments. Plasma was analyzed per the manufacturer's protocol using a Mouse CCL5/RANTES Quantikine ELISA kit (R&D Systems Inc., Minneapolis, MN), Mouse sP-Selectin/CD62P Quantikine ELISA Kit (R&D Systems Inc.), and an Amplex Red Cholesterol Assay Kit (Molecular Probes, Eugene, OR), using a VersaMax Tunable Microplate Reader (Molecular Devices).

Flow cytometric analysis of circulating monocyte-platelet aggregates

Citrated whole blood was drawn from the retro-orbital plexus 24 hours after cerebral ischemia induction in wild type and *Cd39^{-/-}* mice. The blood was mixed with Fc receptor as well as CD62p blocking antibodies (BD) and immediately fixed with 5% buffered formalin. Following fixation, the red blood cells were lysed using water. The cells were stained with antibodies against the platelet marker GPIIb conjugated to FITC (BD), and monocytes were gated based on their coexpression of CD115 and F4/80 as described earlier[148,149]. Monocytes were examined for coexpression of the platelet marker GPIIb.

Preparation and staining of cryosections

Frozen sections of the aortic root sinus were prepared as previously described[150]. Aortic sinus sections (5.0 μM) were briefly fixed with acetone. Platelet remnants were identified by staining for CD41/GP11b (AbD Serotec) at a dilution of 1:300. Primary antibody was detected using a TSA™ Tetramethylrhodamine System (Perkin-Elmer,Wellesely, MA, USA). Macrophages were stained with CD68 (AbD Serotec) at a dilution of 1:300 and detected with an AlexaFluor 488 preconjugated secondary antibody

(Molecular Probes). Nuclei were stained with 4',6-diamidino-2-phenylindole (DAPI). Images were acquired using MetaMorph v7.0r3 software (Molecular Devices) on an Eclipse TE2000-E microscope (Nikon Instruments, Inc.).

Data analysis

Values are expressed as mean ± standard error of the mean, with the number of experiments performed provided in the figure legends. For experiments in which two variables were compared, unpaired Student *t* tests were used. For experiments in which more than two variables were compared, one-way ANOVA was used, with Tukey's *post hoc* test used to test for significant differences. Data were considered significantly different when $p<0.05$.

Acknowledgements

Figure 3.1 CD39 function and expression over atherosclerotic plaque. Coronal sections of an *Apoe*$^{-/-}$ aorta are shown via brightfield (**A**) and immunofluorescent (**B**) microscopy. CD39 is shown in red and nuclei are blue (bar is equal to 10 μm). Transmission electron micrographs were made of the cerium-chloride stained ATPase activity in *Apoe*$^{-/-}$ aorta at sites of healthy (**C**) and atherosclerotic (**D**) vascular wall. Black cerium precipitate denotes sites of ATPase activity. (34,000x magnification)
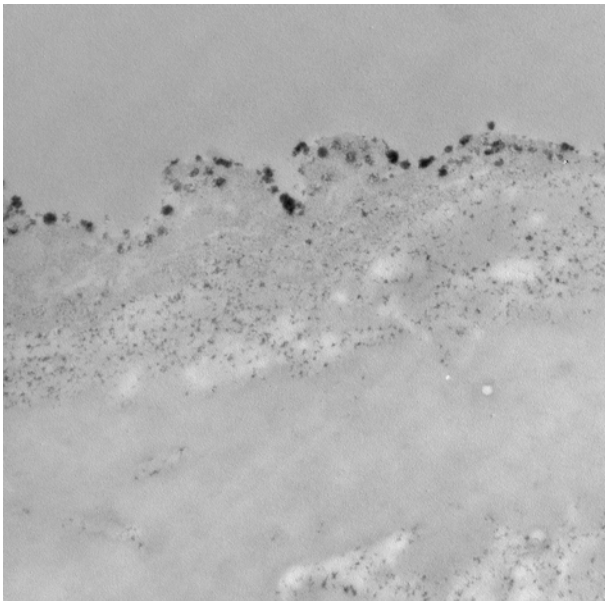
A

B

C

D
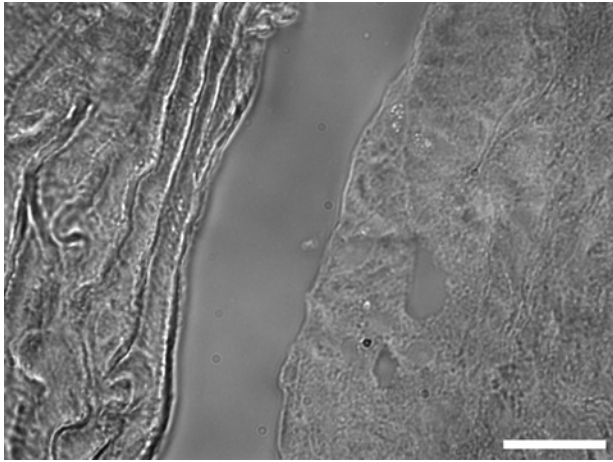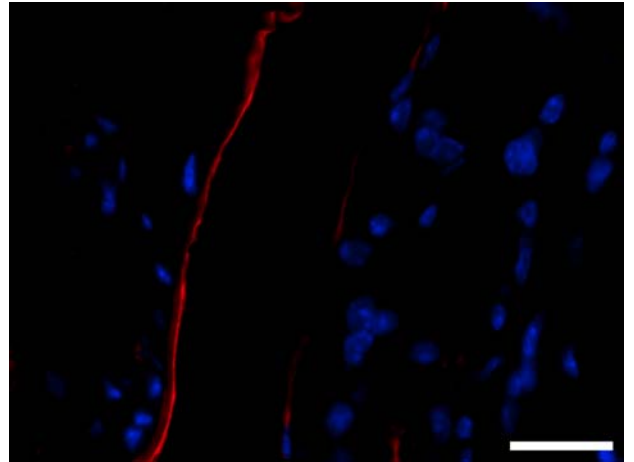
Figure 3.1

Figure 3.2 CD39-deficiency alters the course of atherogenesis. The membrane protein fraction was isolated from tissue taken from $Cd39^{+/+}$, $Cd39^{+/-}$, and $Cd39^{-/-}$ mice. Isolated protein was immunoblotted to examine CD39 expression (**A**) and examined with a Malachite green assay for ATPase activity (**B**) and ADPase activity (**C**). $Cd39^{+/+}$, $Cd39^{+/-}$, and $Cd39^{-/-}$ mice were crossed to an $Apoe^{-/-}$ background and fed a fat enriched diet for 20 weeks. Aortas were stained for plaque and pinned *en face* to allow quantification of aortic plaque burden. Representative vessels (**D**) and summed quantifications (**E**) are shown. Platelet deposition was examined by staining for the platelet surface marker CD41 in atherosclerotic plaques of $Cd39^{+/+}$ $Apoe^{-/-}$ (**F**), $Cd39^{+/-}$ $Apoe^{-/-}$ (**G**), and $Cd39^{-/-}$ $Apoe^{-/-}$ (**H**) mice, and then later quantified (**I**). Red indicates CD41 and blue indicates nuclei. Circulating levels of platelet-related biomarkers P-selectin and (**J**) and RANTES (**K**) were measured in the blood of fasting $Cd39^{+/+}$ $Apoe^{-/-}$, $Cd39^{+/-}$ $Apoe^{-/-}$, and $Cd39^{-/-}$ $Apoe^{-/-}$ mice via ELISA. $n=3$ for panels **A**-**C**, $n=6$ for panel **I**, $n=7$ for panels **J**-**K**; *p<0.01, **p<0.05
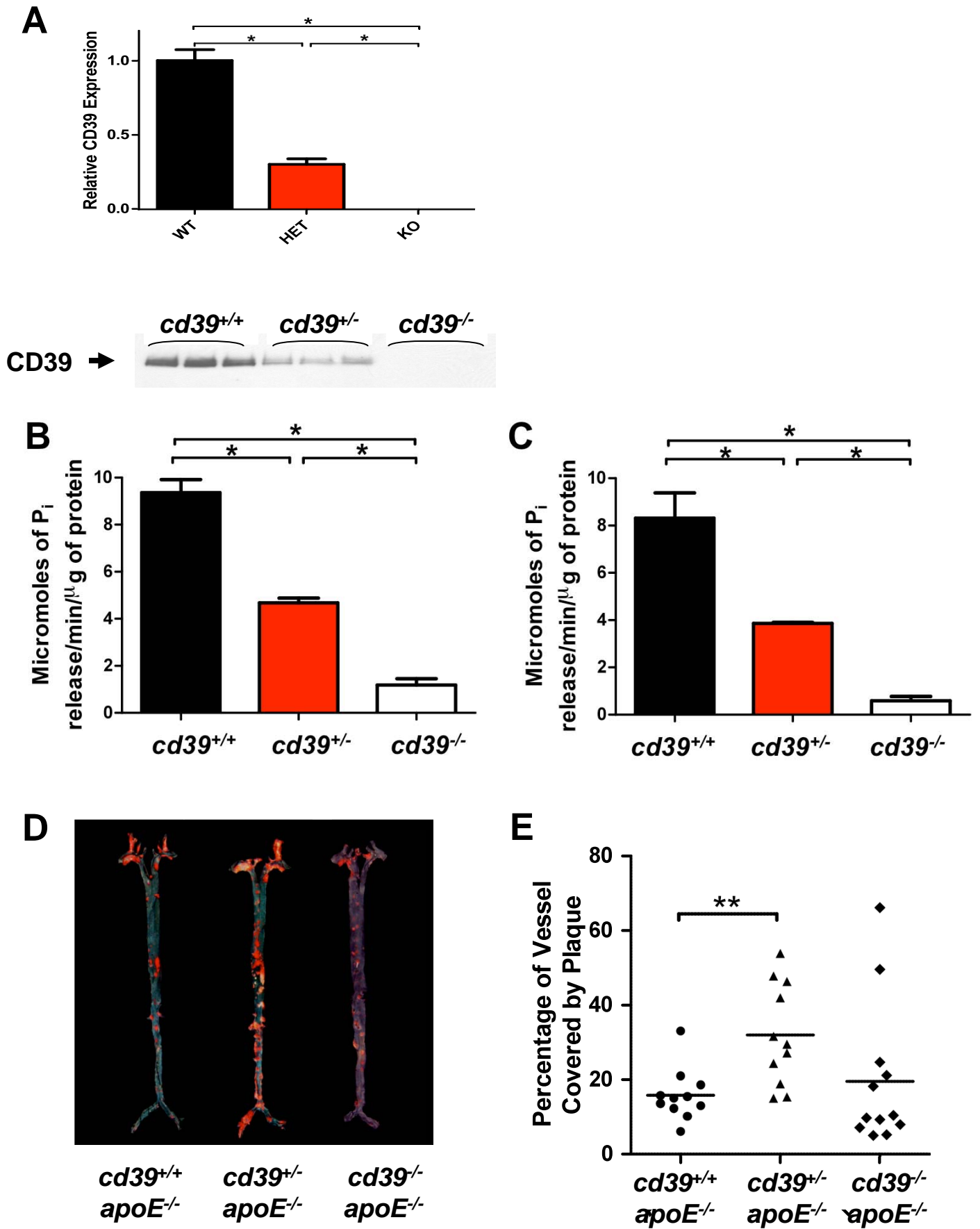
A
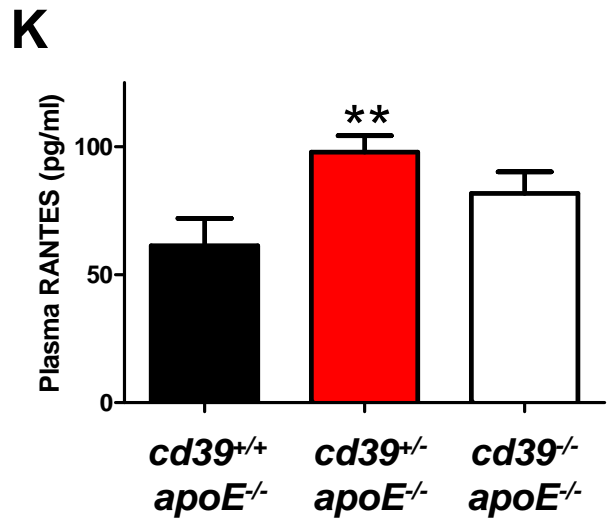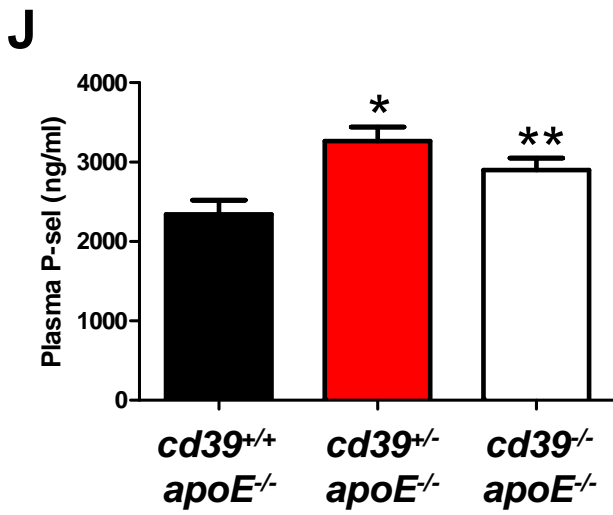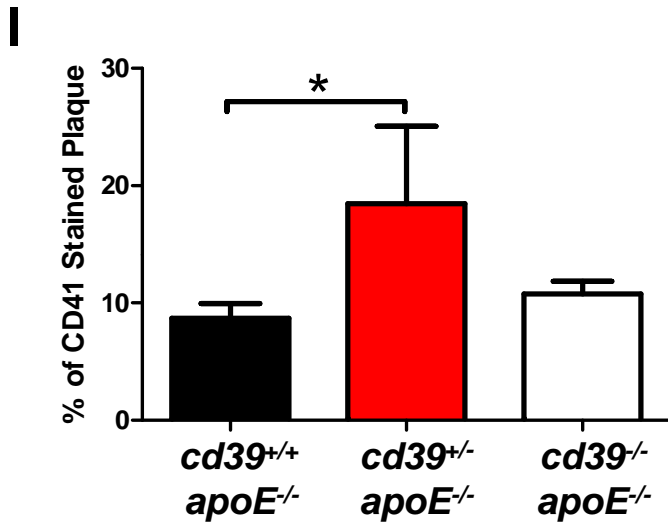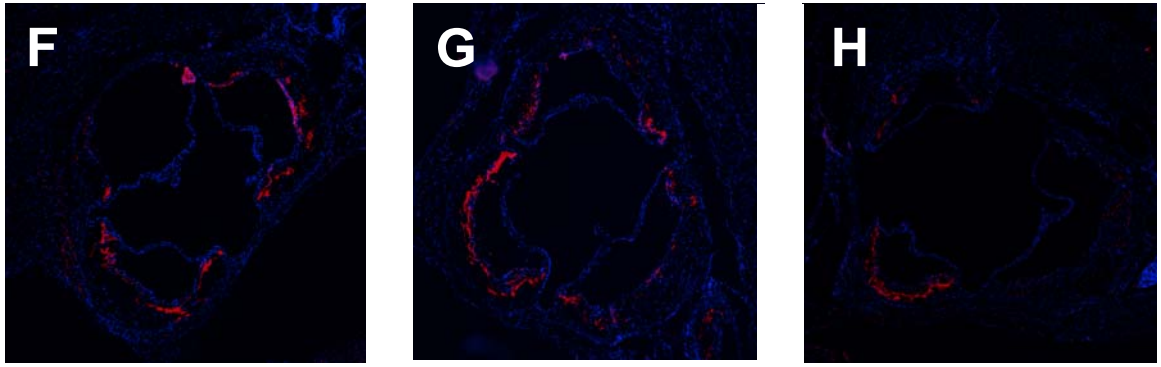
B

C

D

E

Figure 3.2

Figure 3.2

Figure 3.3 Modulation of whole blood platelet aggregometry by CD39. Whole blood was drawn from $Cd39$, $Cd39^{+/-}$, and $Cd39^{-/-}$ mice to test for ADP sensitivity. Representative aggregometry responses were taken at different concentrations of ADP stimulation (**A**). Summed aggregometry data is shown for normolipidemic $Cd39^{+/+}$, $Cd39^{+/-}$, and $Cd39^{-/-}$ mice (**B**) as well as hyperlipidemic $Cd39^{+/+}$ $Apoe^{-/-}$, $Cd39^{+/-}$ $Apoe^{-/-}$, and $Cd39^{-/-}$ $Apoe^{-/-}$ mice (**C**). n=3 per group, *p<0.05, **p<0.01
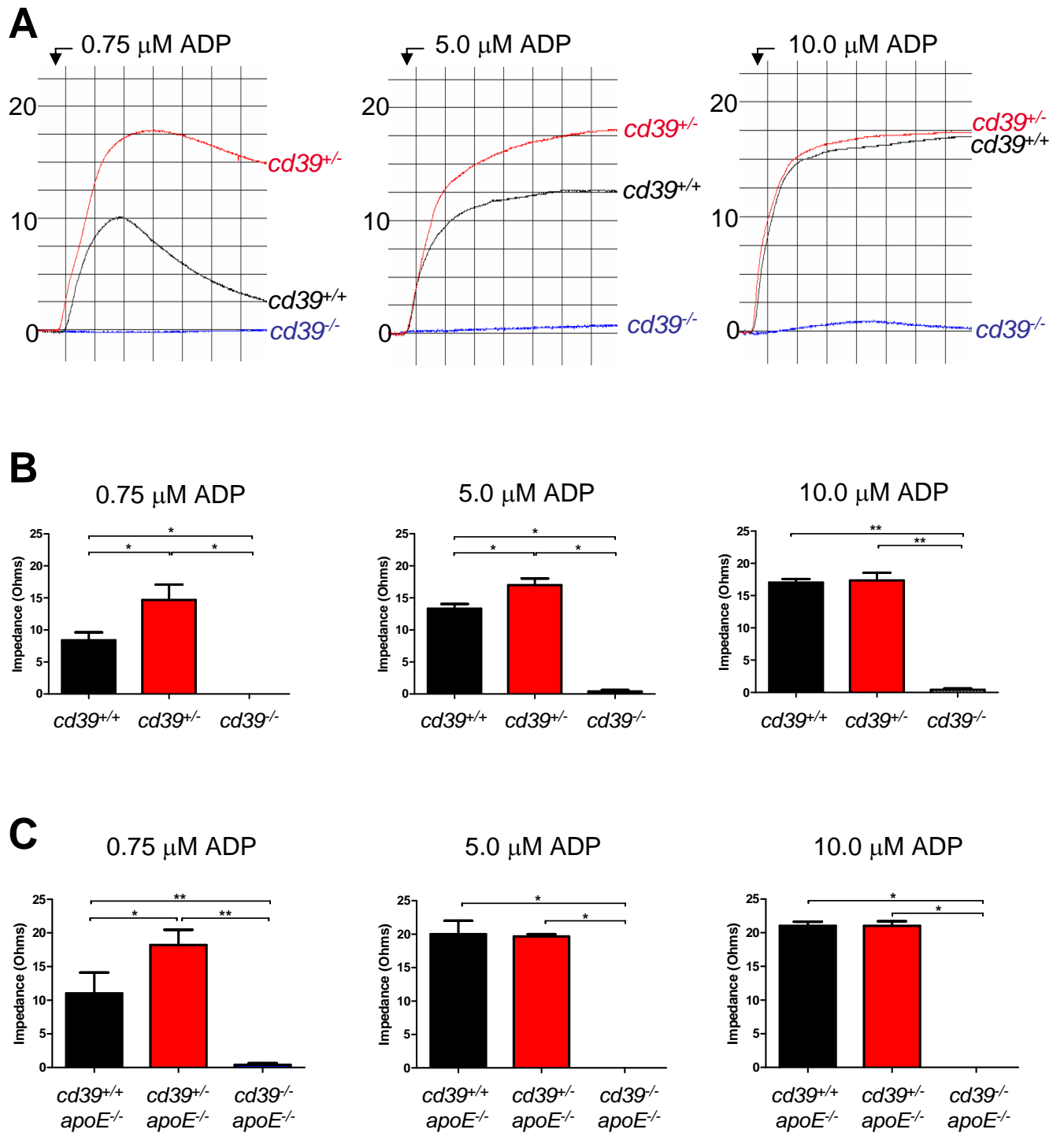
Figure 3.3

Figure 3.4 CD39 suppresses lipid uptake in macrophages. Peritoneal macrophages isolated from $Cd39^{+/+}$ $Apoe^{-/-}$, $Cd39^{+/-}$ $Apoe^{-/-}$, and $Cd39^{-/-}$ $Apoe^{-/-}$ mice were exposed to Di-labeled AcLDL (**A**) or Di-labeled OxLDL (**B**) and lipoprotein uptake was measured as a corollary for foam cell formation. The RAW 264.7 macrophage cell line was transfected to overexpress murine CD39 (mCD39) or "empty" pcDNA3. Quantitative PCR was used to measure the effect CD39 has on the expression of the scavenger receptors SRA-1 (**C**) and CD36 (**D**). Representative images of pcDNA3 transfected (**E**) and mCD39 transfected (**F**) RAW cells 2 hours after exposure to Di-AcLDL. Representative images of pcDNA3-transfected (**G**) and mCD39-transfected (**H**) RAW cells 2 hours after exposure to Di-OxLDL. Di-AcLDL (**I**) and Di-OxLDL (**J**) uptake was measured in pcDNA3-transfected and mCD39-transfected RAW macrophages. $n=12$ panels **A-B**, $n=5$ panels **C-D**, $n=12$ panels **I-J**; *$p<0.05$, **$p<0.01$, ***$p<0.001$, #$p<0.001$, $^{\theta}p<0.05$ versus groups transfected with the same vector, $^{\phi}p<0.01$ versus groups transfected with the same vector, $^{\varsigma}p<0.01$ versus Vehicle and TNP-ATP of groups transfected with the same vector, $^{\Psi}p<0.05$ versus Vehicle and TNP-ATP of groups transfected with the same vector.
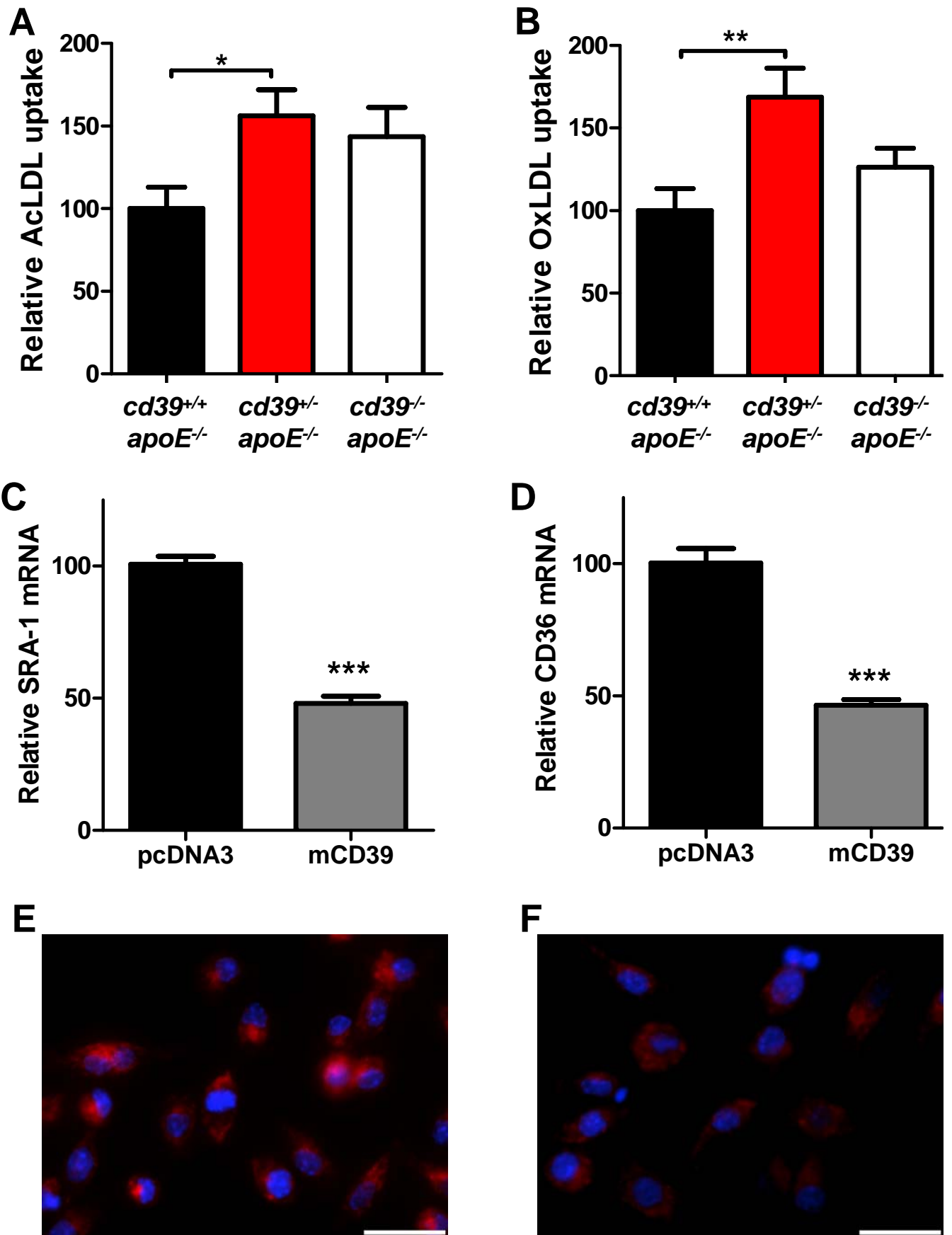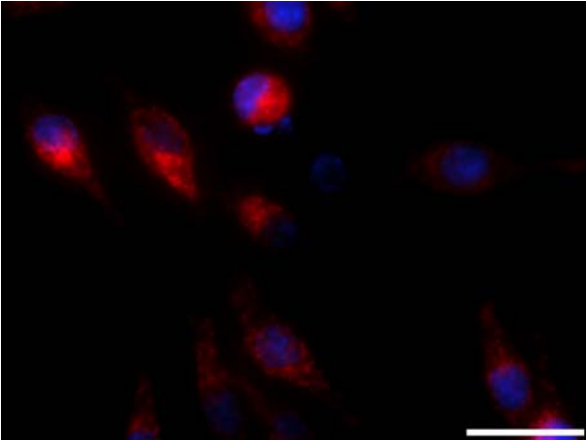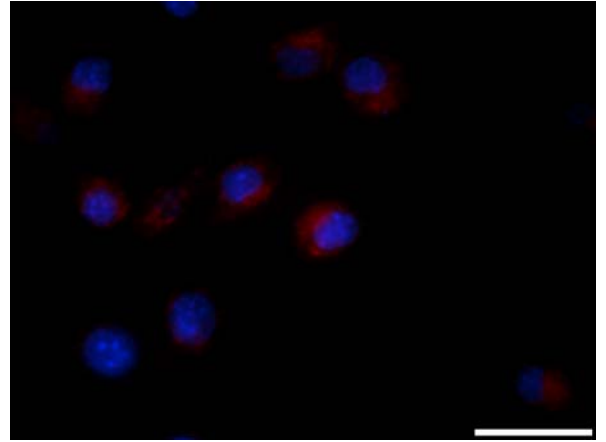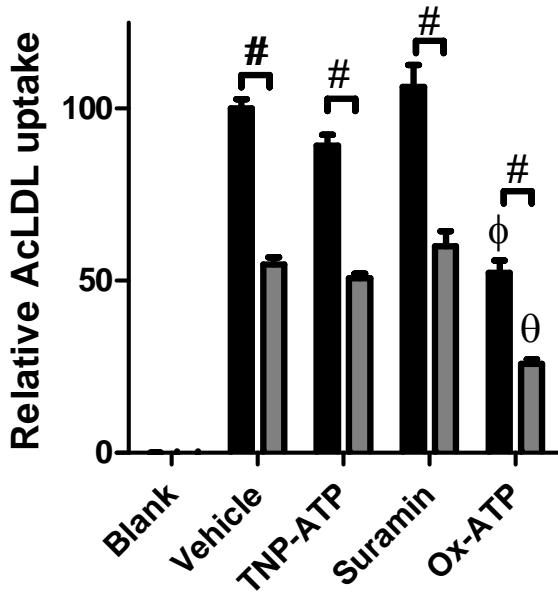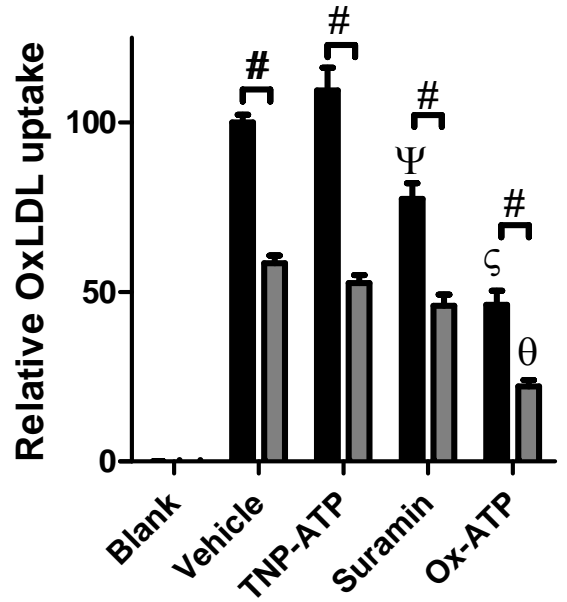
Figure 3.4

Figure 2.4

CHAPTER IV

INDUCTION OF THE ECTO-ENZYME CD39 BY LAMINAR SHEAR FORCES

Abstract

Fluid phase shear forces alter the expression of vascular endothelial genes thereby dictating the localization of atherosclerotic plaque. Laminar shear forces promote the expression of anti-inflammatory and anti-coagulant genes in healthy endothelium, whereas turbulent flow suppresses their expression in vascular regions predisposed to plaque formation. Our recent work has identified CD39, a key regulator of thrombosis and inflammation, as profoundly diminished on endothelium overlying atherosclerotic plaque. This suggested that CD39 could be regulated in a dynamic fashion by the prevailing blood flow. We show here that CD39 is potently induced by laminar shear, but not turbulent shear patterns. The transcription factor KLF2, induced by laminar shear itself, binds to the CD39 promoter to drive its expression under conditions of high laminar shear. To determine whether modulating KLF2 could alter the CD39 response to changes in shear stress, a strategy of genetic and pharmacologic manipulation of KLF2 was undertaken. These experiments demonstrated that CD39 expression is closely linked to the expression of KLF2. As HMG-CoA reductase inhibitors were shown to activate KLF2 and thereby strongly induce CD39, these findings implicate statin-induced CD39 expression as a novel means to limit thrombosis and inflammation in areas of turbulent shear.

Introduction

The interface between the blood and the vascular endothelium is a site of dynamic exchange where individual cells adapt rapidly to their environment. Endothelial cells respond to the prevailing fluid flows and the mechanical shear forces they impart to effect widespread changes in gene expression, cellular morphology, and function[151,152]. These changes result in region-specific patterning of the endothelium and a subsequent resistance or predisposition to inflammation and atherosclerosis[153-155].

Our recent work has identified CD39 as a gene that displays stark regionalization throughout the vasculature [156]. Under normal conditions, CD39 is a primary regulator of vascular homeostasis due to its avid catabolism of ATP and ADP[7,8,11,15,91]. By limiting purine-driven thrombosis and inflammation, CD39 is able to suppress atherogenesis [74,135,156]. Consequently, when CD39 expression is reduced by 50%, atherosclerotic plaque burden is more than doubled[156].

Results

Staining of murine aortas showed that CD39 is preferentially lost from endothelium overlying atherosclerotic plaque, but is intact in adjacent healthy endothelial cells (**Figure 4.1 A-B**). To determine whether CD39 is differentially expressed depending on vascular location, which may contribute to the formation and regionalization of atherosclerotic plaque, we quantified the heterogeneity of CD39 expression in the vasculature. We first explored whether a mechanism involving the oxidative milieu [143] of an atherosclerotic plaque could account for the focal loss of CD39.

Surprisingly, aortas from both normolipidemic and hyperlipidemic/atherosclerotic mice displayed a similar regionalized expression of CD39. This suggests that the driving force behind vascular CD39 heterogeneity was not the atherosclerotic plaque per se (**Figure 4.1 A-D**). Furthermore, we noted that when examining the greater curvature and branch points of the aortic arch, there was a defined and consistent pattern: from proximally to a branch point, CD39 was diminished, but from aorta distal to that point, there was very strong staining (**Figure 4.1 E-F**). This same pattern of expression is found for other endothelial genes, where branch points exhibit diminished expression but linear stretches have higher expression. These results suggested regions of high shear stress showed marked lower CD39 gene expression. Mechanical shear stresses (fluid phase frictional forces) are likely to mediate these changes by turning on and off entire gene ontologies [154,155]. This led to the hypothesis that CD39 is a shear stress-responsive gene, with areas of laminar fluid flow inducing and disturbed fluid flow suppressing the expression of this gene.

To further confirm this finding, we examined aortic endothelial staining *en face*. In the greater curvature of the aorta CD39 staining was strongest at the apical aspect of the endothelial membrane, however CD39 staining was largely absent in the lesser curvature of the aortic arch (**Figure 4.1 G-H**). As CD39 function does not always coincide with protein expression [143], we tested CD39's ATPase activity using a technique where cerium-chloride is used to scavenge phosphates liberated by ATP phosphohydrolysis to produce a stain. Electron micrographs of the aortic branch points

show strong CD39 activity in areas associated with high laminar shear, and significantly diminished staining in areas of disturbed blood flow (**Figure 4.1 I-J**) [157].

To determine if laminar shear stress is sufficient to regulate CD39 gene expression, we modeled shear stresses *in vitro* using a cone-plate viscometer that creates either laminar fluid flow (by rotating the cone uni-directionally), or disturbed flow (by oscillating the cone bi-directionally). Human umbilical vein endothelial cells (HUVEC) were exposed to both forms of shear to determine if laminar shear was sufficient to regulate CD39 expression *in vitro*. Following exposure to prolonged laminar shear (15 dyne/cm^2), CD39 was upregulated 15-fold compared to static control (**Figure 4.2 A**). Oscillatory shear had no effect on endothelial CD39 expression, demonstrating that shear forces themselves are insufficient to induce CD39. The nature of the shear stress is critical, i.e. it must be laminar to regulate CD39 expression. This response was specific for CD39, as gene expression of other ecto-nucleotidease family members (ENTPD3-8) were not induced by laminar shear (**Figure 4.2B**). Flow cytometric analysis of HUVEC confirmed that cell surface CD39 protein was increased following laminar shear (**Figure 4.2 C-D**).

Laminar shear induces families of genes with convergent mechanisms and biological effects while at the same time suppressing families of genes that counteract them. Laminar shear, for example, is anti-thrombotic: inducing endothelial nitric oxide synthase [158,159] and thrombomodulin [160], while suppressing plasminogen activator inhibitor-1 [160,161] and tissue factor [160]. The underlying mechanism responsible for driving

these anti-thrombotic genes is the transcription factor Kruppel-like factor 2 (KLF2). KLF2 is a zinc finger DNA-binding transcription factor that is critical for maintenance of vascular morphology and endothelial homeostasis [158,162,163]. It is potently induced by laminar shear, which causes it to bind to the promoter of numerous genes such as thromobomodulin and eNOS, thereby inducing their expression [160,163,164]. We hypothesized that the laminar shear induction of CD39 could similarly be a response to KLF2 induction. This idea was strengthened by *in silico* analysis of the first 1 kb of the CD39 promoter, which revealed three putative binding sites clustered between -85 and -55 bp upstream of the CD39 transcriptional start site: one canonical KLF2 binding site and two Sp1 sites. To test whether this transcription factor has a role in the regulation of CD39, we used a lentiviral shRNA construct to silence KLF2. Treatment with control virus did not have a significant effect on the induction of CD39 by laminar shear (**Figure 4.3**). By comparison, CD39 was significantly less responsive to laminar shear when KLF2 was silenced. In these experiments, KLF2 was inhibited 87%, with a consequent 77% suppression of CD39. Interestingly, silencing of KLF2 leads to a significant suppression of unstimulated endothelial CD39 expression as well. This implies that KLF2 plays a critical role in maintaining the basal expression of CD39. It is of note that the expression of related ecto-enzymes such as CD73 and other CD39 family members were not suppressed by KLF silencing, again suggesting specificity for CD39 induction by shear stress.

3-hydroxyl-3-methyglutaryl coenzyme A inhibitors (statins) exert anti-atherogenic effects that are greater than can be explained by lipid lowering alone [165].

There is emerging evidence that many of the pleiotropic anti-inflammatory and anti-thrombotic effects of statins are dependent upon KLF2 [166,167]. CD39 is a potent repressor of both atherogenesis [156] and platelet activation [7,91] which led to the hypothesis that the anti-atherosclerotic and anti-thrombotic effects of statins may be due in part to induction of CD39. To test this, endothelial cells were treated with a panel of statins. Independent of chemical formulation, statins as a drug class are able to potently induce CD39 expression at the mRNA and protein level (**Figure 4.4 A-B**). Furthermore, when KLF2 is silenced in statin treated cells, the induction of CD39 is muted (**Figure 4.4 C**). This finding suggest that statins may be used as a pharmacologic means to induce CD39 *in vivo* to capitalize on CD39's anti-thrombotic and anti-atherogenic effects. Interestingly, KLF2 silencing does not completely abrogate the statin-mediated induction of CD39 suggesting that other pathways may also be involved in this response. It still remains unclear whether these alternate pathways are the same as those activated by shear stress.

Discussion

Findings presented here show that even before a plaque has formed, areas of regional CD39-abundance and CD39-deficiency exist in healthy wild-type individuals. This local CD39-deficiency may contribute to regional inflammation and coagulation at sites predisposed to atherogenesis. Furthermore, numerous ischemic conditions such as stroke[11,135], intestinal [13], and renal ischemia reperfusion [12] are ameliorated by bolstering levels of CD39. In each of these situations, pharmacologic induction of CD39 may be therapeutically beneficial. CD39, if induced therapeutically, also has the advantage of being self-limiting in its actions, as it does not act directly on platelets, leukocytes or

endothelium but instead on the purinergic agonists ATP and ADP. This principal is derived from observations made with a soluble form of recombinant CD39 protein that has been used therapeutically with great success in animal models to treat ischemic stroke [63].

In conclusion, we show for the first time that CD39 on the surface of endothelial cells is regulated in a dynamic fashion by the mechanical shear stresses imparted by the flowing blood. The induction of CD39 by both shear and statins has both KLF2-dependent and independent components, which suggests, teleologically speaking, that this pathway for inducing thrombosis-limiting genes is of fundamental importance to the maintenance of vascular homeostasis.

Materials and Methods

All animal experiments were conducted in accordance with protocols approved by the Institutional Animal Care and Use Committee at the University of Michigan.

Tissue Staining for CD39

Twenty-six week old *Apoe^-/-* mice or 12 week old wild-type mice were euthanized (Jackson Laboratories), perfused with ice-cold saline (Gibco, Carlsbad, CA), and then 10% buffered formalin (Fisher Scientific, Pittsburgh, PA). The aortic arch was removed, post-fixed in formalin overnight and serially dehydrated before embedding in paraffin. Citrate buffer (Vector Labs, Burlingame, CA, USA) was used for antigen retrieval in paraffin sections (5.0 mm). Slides were stained with rat anti-CD39 polyclonal antibody

[135] and a [VECTASTAIN® ABC-Peroxidase Kit](#) (Vector Labs, Burlingame, CA, USA) that was developed with a TSA™ Tetramethylrhodamine Tyramide Reagent Pack (Perkin-Elmer,Wellesely, MA, USA). Nuclei were stained with 4',6-diamidino-2-phenylindole (DAPI). Images were acquired with a 20x objective (0.32520057 mm/pixel) using MetaMorph v7.0r3 software (Molecular Devices, Sunnyvale, CA, USA) on an Eclipse TE2000-E microscope (Nikon Instruments, Inc, Melville, NY, USA).

Confocal Microscopy

Aortas from 12 week old wild-type mice islolated following perfusion with ice-cold saline, and buffered formalin as described above. Aortic ringlets were stained with rat anti-CD39 polyclonal antibody [135] and a [VECTASTAIN® ABC-Peroxidase Kit](#) (Vector Labs, Burlingame, CA, USA) that was developed with a TSA™ Tetramethylrhodamine Tyramide Reagent Pack (Perkin-Elmer,Wellesely, MA, USA). Nuclei were stained with 4',6-diamidino-2-phenylindole (DAPI). Images were acquired with a 40x objective (0.5 mm slice thickness) using a Zeiss LSM 510-META Laser Scanning Confocal Microscope.

Cerium-chloride staining of ATPase activity

Twelve week old wild-type and $Cd39^{-/-}$ [11] mice were euthanized prior to cerium-chloride staining [145]. The left ventricle was perfused with ice-cold 0.05 M Na-cacodylate buffer, pH 7.2 (Electron Microscopy Sciences; Hatfield, PA, USA). Aortas were fixed for 5 minutes *in situ* with a mixture of ice-cold 2% paraformaldehyde (Electron

Microscopy Sciences), 0.5% glutaraldehyde (Electron Microscopy Sciences), 0.25 mM sucrose, and 2 mM $MgCl_2$ in 0.05 M cacodylate buffer (pH 7.2). The aortic arch was dissected free and fixed for 10 additional minutes in fixation buffer. Tissue was embedded in 7% low melting point agarose prior to sectioning with a Vibratome (70 µM). Tissue sections were washed overnight in cacodylate buffer and then rinsed briefly in Tris-maleate buffer (pH 7.2). Slides were incubated for 20 min at 37°C in reaction buffer: Tris-maleate (0.1 M, pH 7.2), ATP (2 mM), $MgCl_2$ (2 mM), KCl (20 mM), $CeCl_3$ (2 mM), 2 mM levamisole, 100 mM ouabain, and 50 µM α,β-methylene-ADP, and 0.0001% Triton X-100. Samples were rinsed in Tris-maleate buffer (pH 6.0) and cacodylate buffer (pH 7.2) prior to post-fixation with 1% OsO_4 (Electron Microscopy Sciences). After rinses in distilled water, tissue slices were dehydrated in graded ethanol, processed through propylene oxide, and embedded in Epon (Fluka; Buchs, Switzerland). Ultrathin 40 nM sections were cut using a Reichert Ultracut-E (Leica Microsystems Inc., Bannockburn, IL, USA) and imaged with a Philips CM-100 transmission electron microscope.

In vitro shear stress

Primary human umbilical vein endothelial cells freshly isolated from umbilical cords or human aortic endothelial cells (Lonza, Walkersville, MD, USA) were grown to confluency in either 60 mm or 100 mm tissue culture dishes, and exposed to laminar shears of 10 dyn/cm^2 or 15 dyn/cm^2 respectively. Laminar shear was imparted by spinning a previously described Teflon cone (0.5° cone angle) uni-directionally [168]. Disturbed fluid flow patterns were mimicked by oscillating the Teflon cone bi-

directionally with a 1 Hz cycle (± 5 dyn/cm^2) using a stepping motor (Servo Motor) and a computer program (DC Motor Company, Atlanta, GA).

Acknowledgements

Figure 4.1 Regional expression of CD39 in the murine aorta. Coronal sections of an *Apoe*$^{-/-}$ aorta at the branch of the left common carotid are shown staining for CD39 in red immunofluorescence (**A**). CD39 staining is an overlay with the brightfield image of the aortic branch point (**B**). CD39 staining (**C**) and overlay (**D**) were also acquired from a wild-type mouse without atherosclerosis in its vasculature. Analysis of the whole aorta of a wild type mouse showed a stark regionalization to CD39 expression (red) and a consistent pattern centering on aortic branch points as shown in (**E**) and the overlay (**F**). Microscope images in panels **A** – **F** were acquired with a 20x objective. Confocal microscopy of *en face* vessel preparations examined CD39 staining (red) in the lesser curvature (**G**) and greater curvature (**H**) of the aortic arch. Nuclei are stained with DAPI (blue). Confocal images were acquired at 40x magnification. Transmission electron micrographs were made of cerium-chloride staining for ATPase activity in areas of the left common carotid artery branch proximal (**I**) and distal (**J**) to the carotid ostium. Black cerium precipitate denotes sites of ATPase activity. (19,000x magnification)
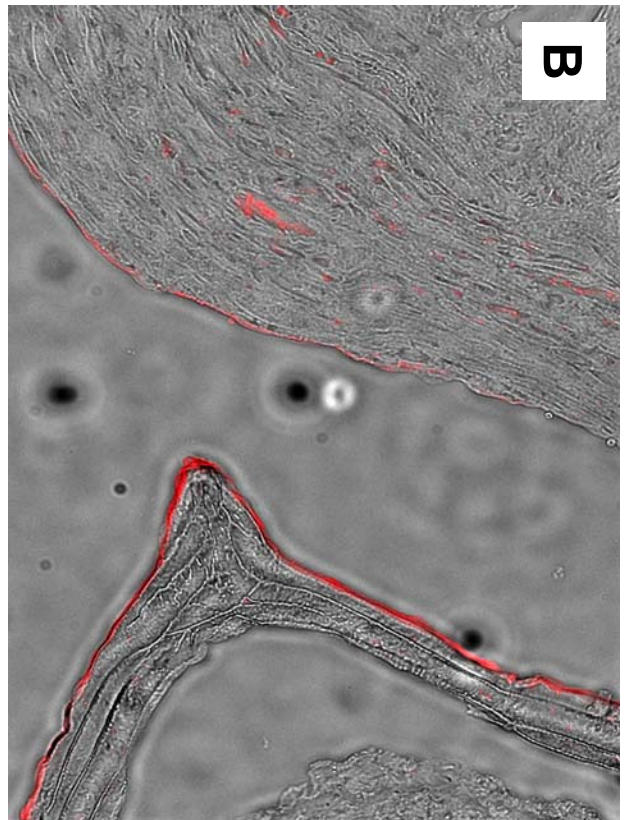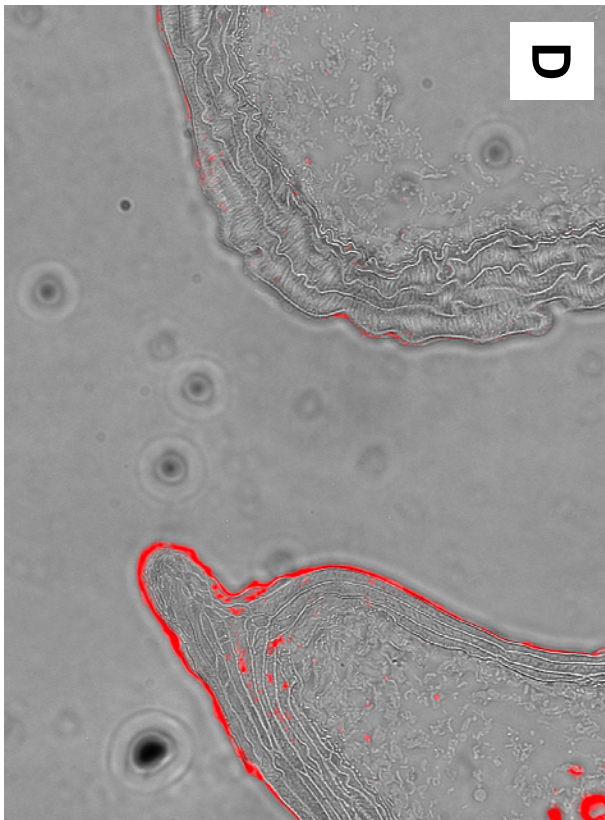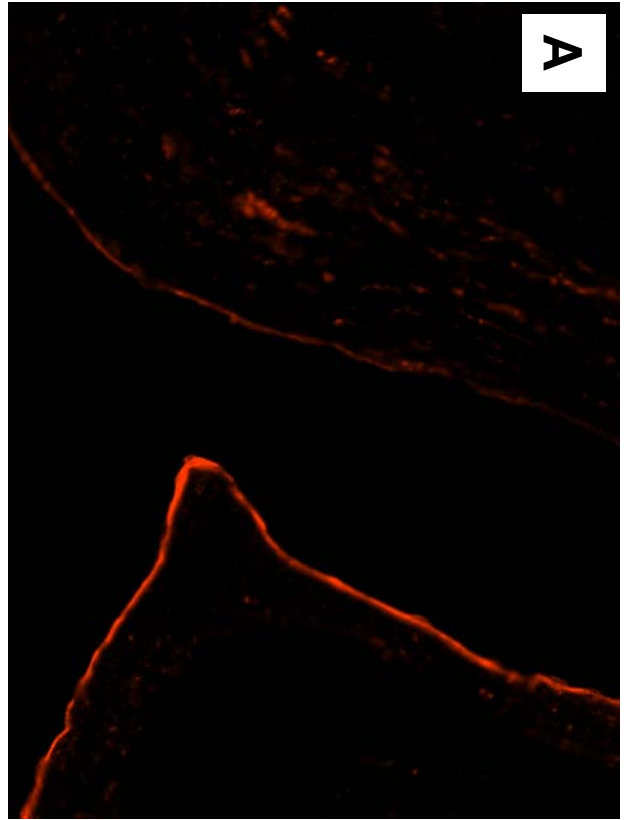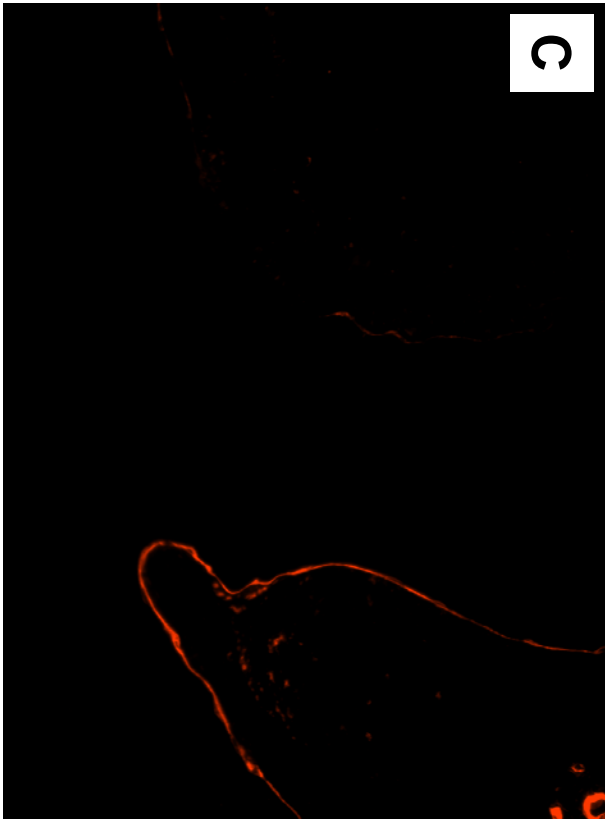
Figure 4.1
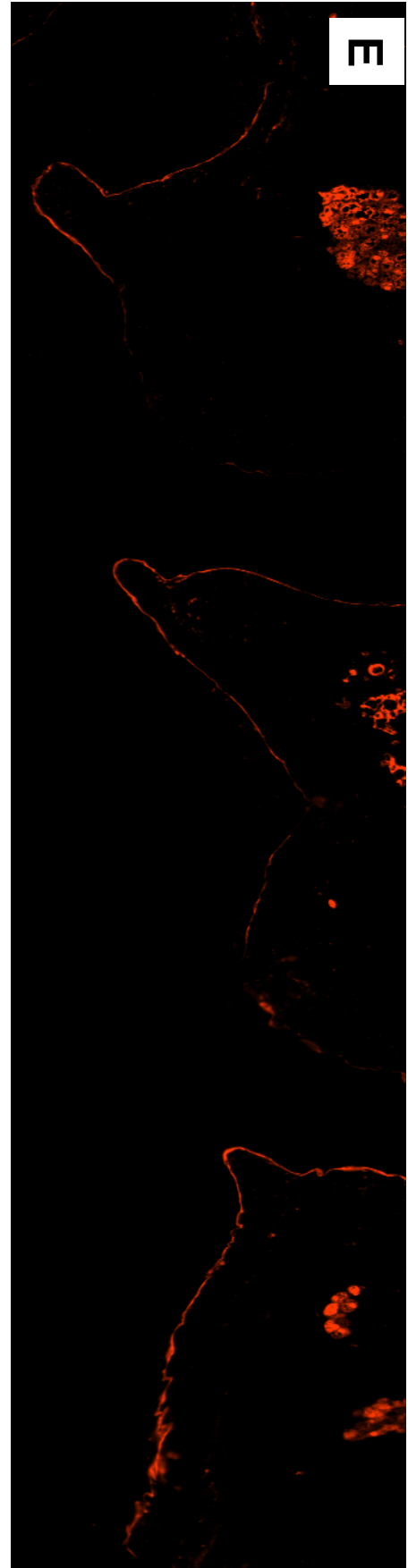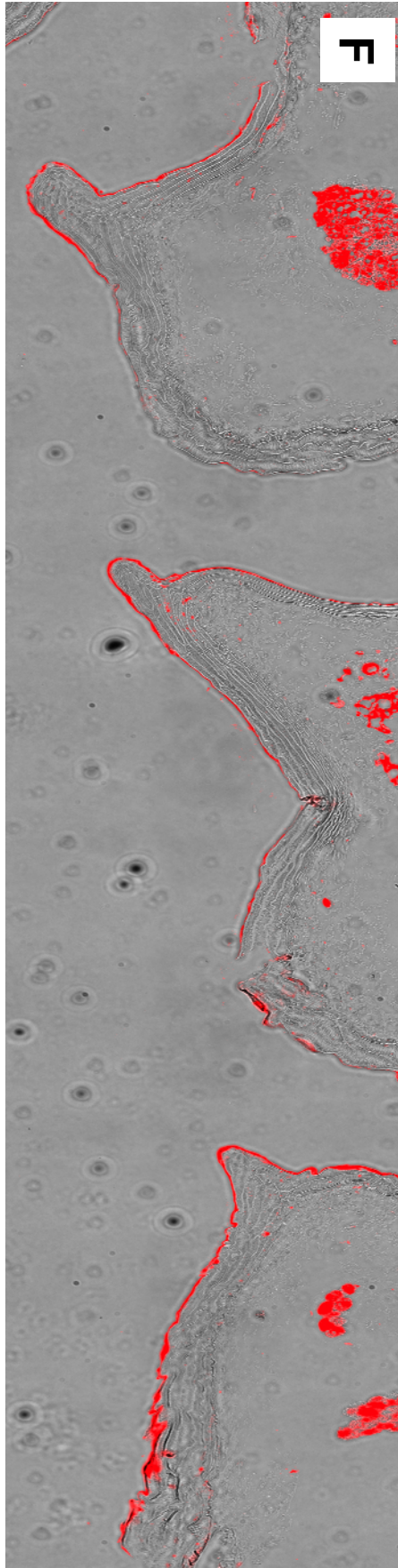
Figure 4.1

Figure 1 (continued)
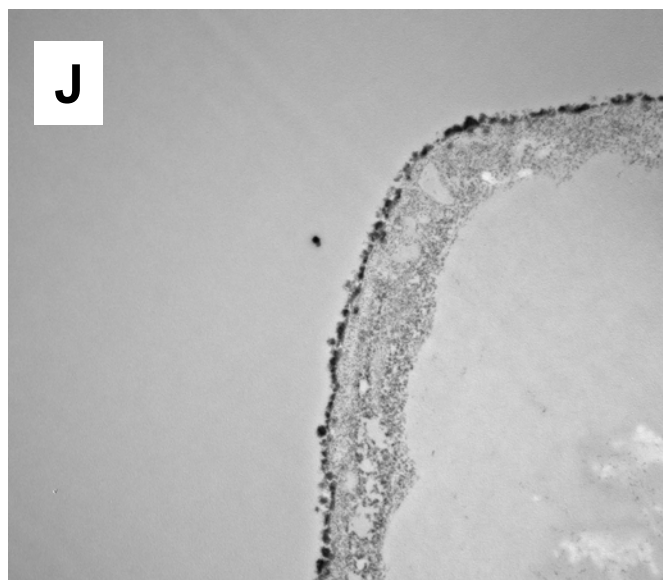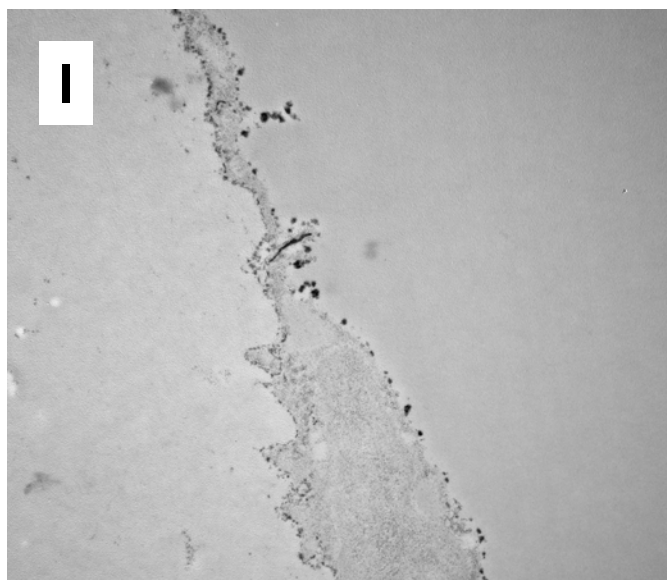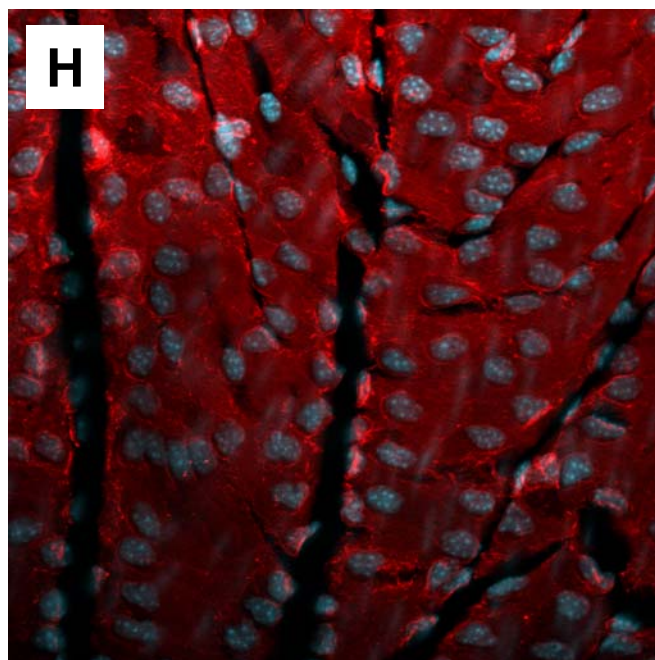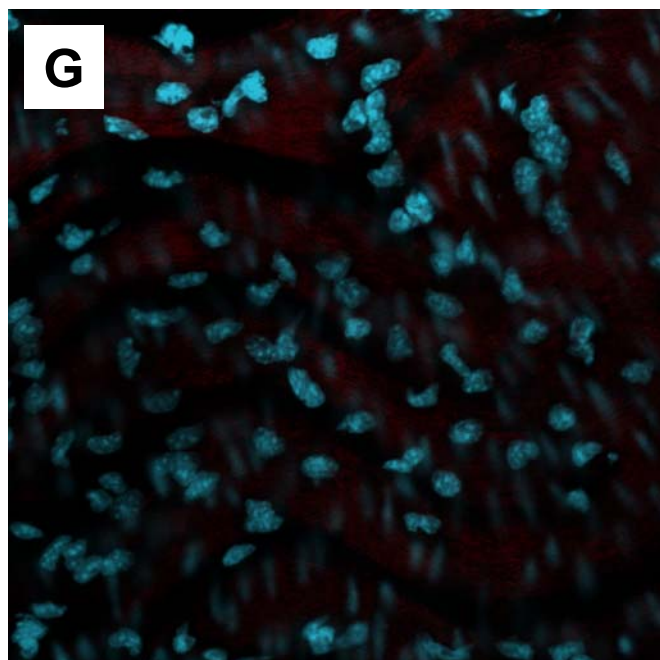
Figure 4.1

Figure 4.2 Laminar shear stress induces CD39 expression *in vitro*. Laminar shear stress (15 dyne/cm^2) and oscillatory shear stress (±5 dyne/cm^2 at 1 Hz) were applied to human umbilical endothelial cells for 24 hours. CD39 mRNA was quantified using qPCR (**A**). The CD39 protein expression of cells exposed to laminar shear stress was compared with cells in a static dish, via flow cytometry (**B**) and quantified (**C**). *n*=5 panel **A**, *n*=2 panels **B** and **C**; *p<0.001.
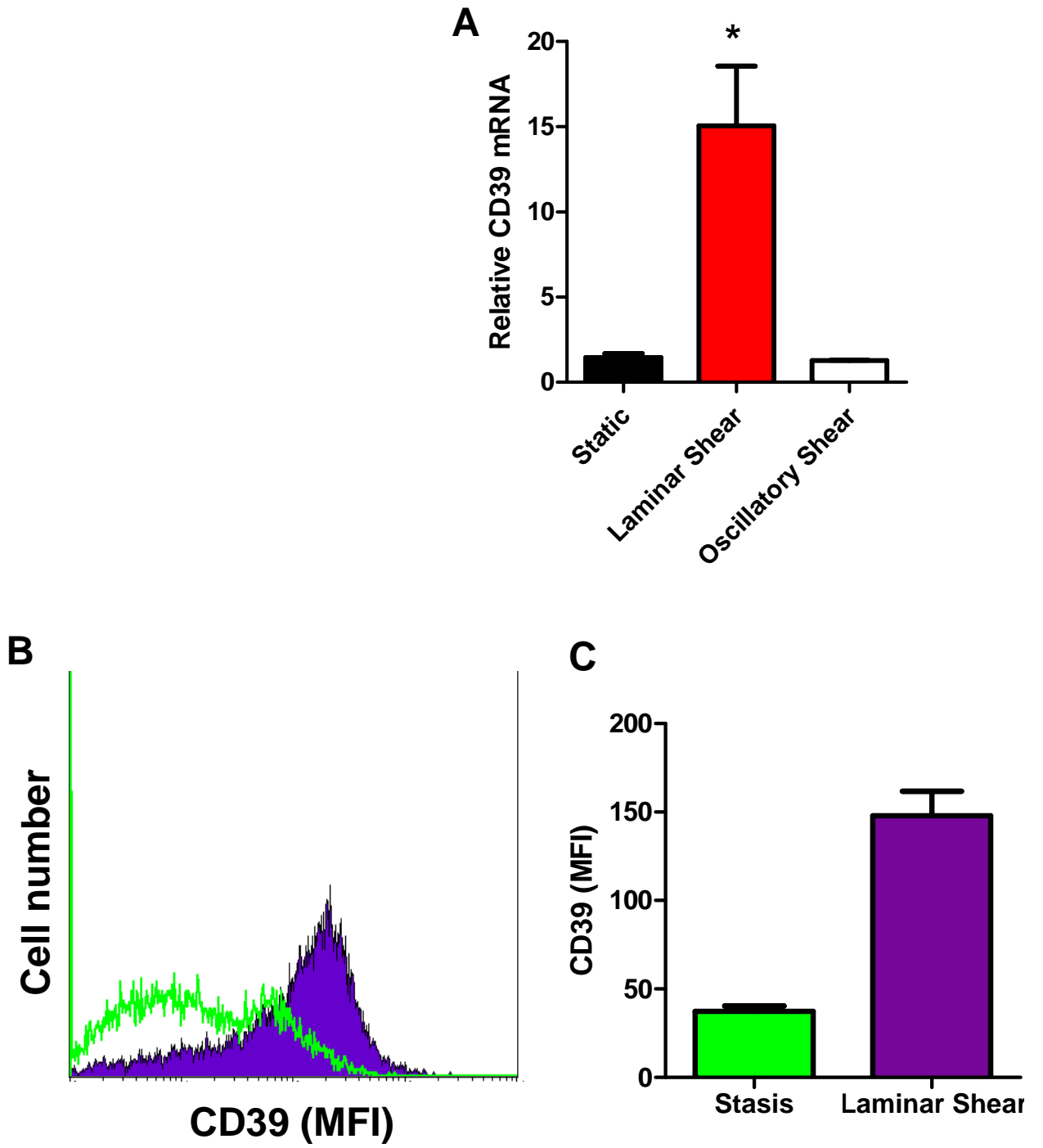
Figure 4.2

Figure 4.3 Silencing of KLF2 suppresses CD39 expression. Endothelial cells were treated with either a lentiviral construct that expressed a hairpin sequence that targeted KLF2 or a control (scramble sequence). Cells were then subjected to either laminar shear stress or static conditions prior to quantification of both KLF2 (**A**) and CD39 mRNA (**B**). $n=5$ for static conditions and $n=2$ for laminar shear conditions, *p<0.01.

A

KLF2 (1° HUVEC)

B

CD39 (1° HUVEC)

Figure 4.3

-115-
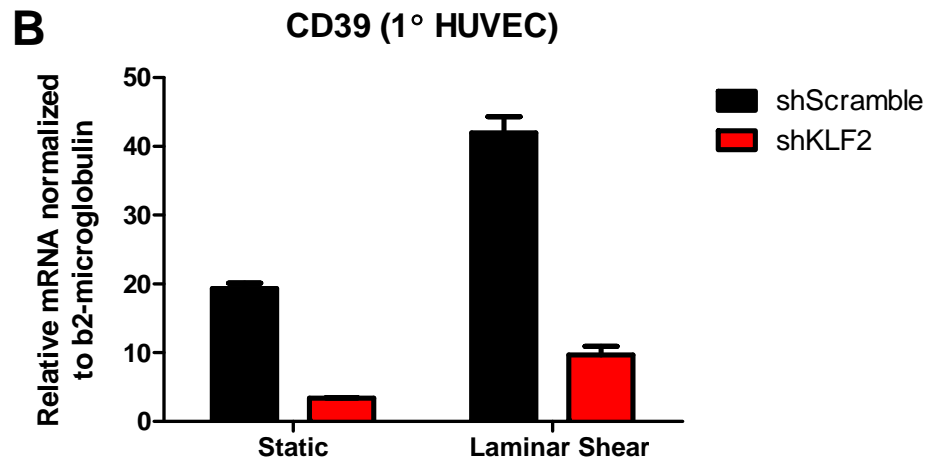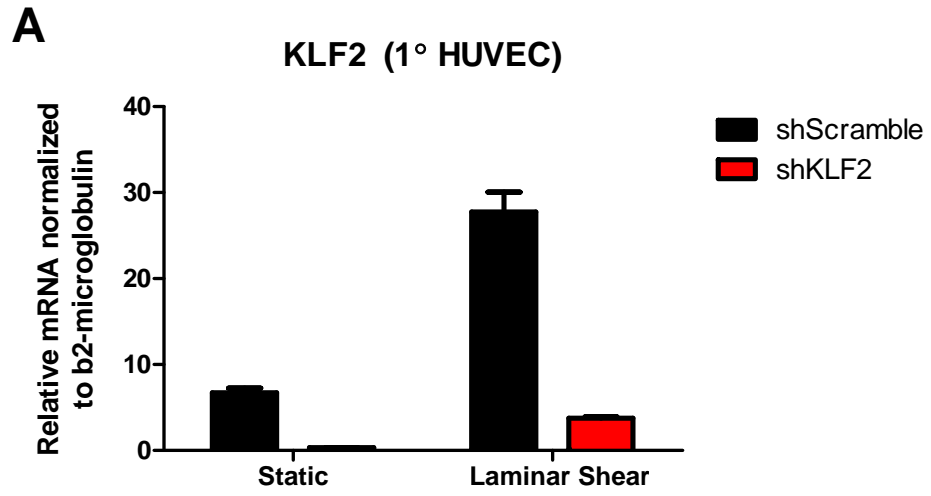
Figure 4.4 Simvastatin induction of CD39 in primary endothelial cells. Endothelial cells were treated with either simvastatin (10 mM) or vehicle for 24 hours. CD39 mRNA and protein was quantified by qPCR (**A**) and flow cytometry (**B**). KLF2 silencing virus was used to test whether the induction of CD39 by simvastatin was dependent upon the presence of KLF2 (**C**). *n*=3 all groups; *p<0.001.

A

B

B
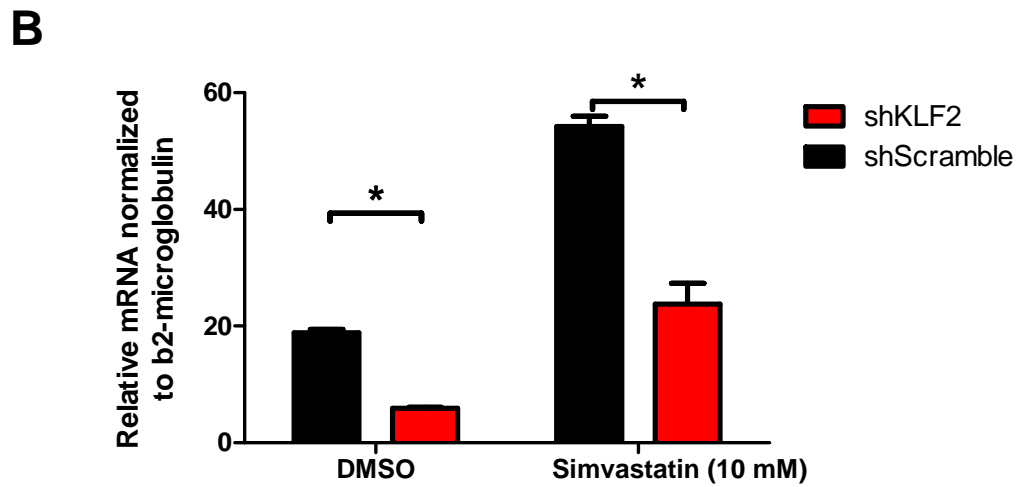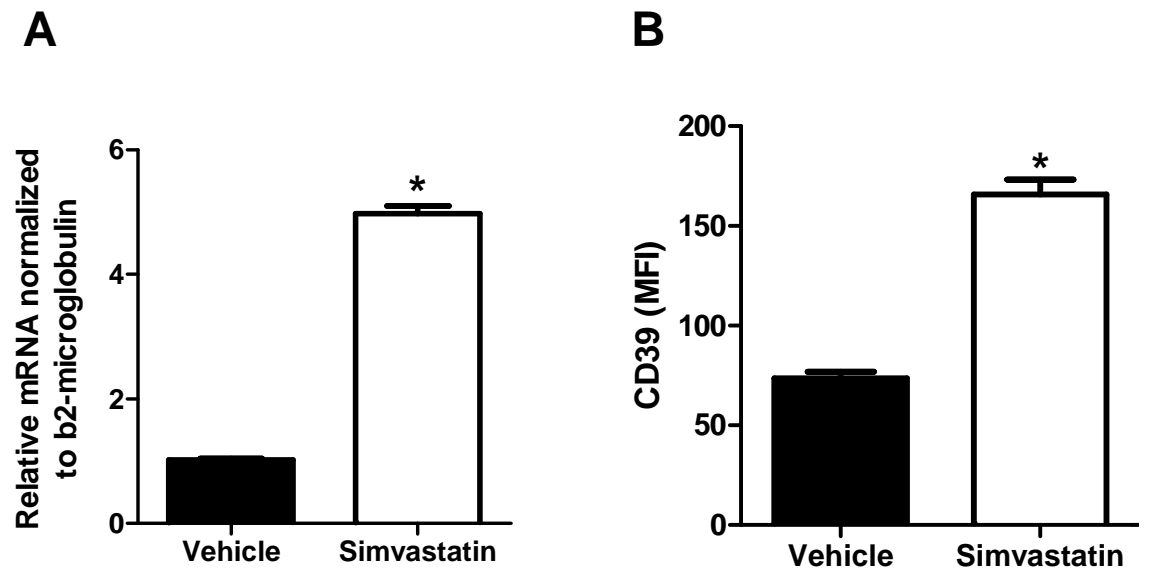
Figure 4.4

CHAPTER V

CONCLUSIONS

Summary

The work presented in this thesis explores our evolving understanding of the role of extracellular nucleotides and their metabolism in cardiovascular disease. The primary focus is on the principal regulator of extracellular ATP and ADP catabolism[11,15], CD39/ENTPDase1, and its modulation of disease pathologies that have an inflammatory component driven by extracellular nucleotides. ATP and ADP are potent signaling molecules that act in both autocrine and paracrine fashions to activate numerous cell types through the engagement of cell surface purine-sensitive receptors[74]. CD39, located in close proximity to these same receptors[169,170], competes for and dissipates the same ATP/ADP substrate, and thereby acts as an endogenous inhibitor of purinergic signaling. Thus, the principal goal of this work was to elucidate how the competing nucleotide avidities of CD39 and purine receptors interact in the setting of inflammation.

Chapter II begins by exploring the role of CD39 in limiting the inflammation associated with ischemic brain injury. It has long been known that injured neurons and parenchyma release ATP and ADP into the extracellular space, but how and whether this release was important remained unclear. This work demonstrated that ambient nucleotides are able stimulate monocytes to adopt a pro-adhesive state. Furthermore,

CD39 is able to prevent this stimulation by catabolizing ATP before it can activate the cell surface purine receptor, $P2X_7$. Agonism of the $P2X_7$ receptor leads to a potent induction of the $\alpha_M\beta_2$-integrin adhesion molecule and is responsible for heightened integrin expression in CD39-null mice. We further explored if this proclivity for adhesion would have functional consequences *in vivo* using an ischemia-driven inflammatory model of cerebral infarction. In this model, we saw a profound increase in inflammation in ischemic $Cd39^{-/-}$ brains. This inflammation was α_M-integrin dependent as shown by antibody-mediated functional-blockade. In total, this work demonstrated that CD39 on leukocytes is an endogenous regulator of leukocyte activation and extravasation.

Chapter III is an extension of the initial work in acute injury and inflammation to the chronic injury and inflammation of atherosclerosis. Atherosclerosis is a polygenic disease that involves a complex interplay between many heterogenous cells types. Two of these cell types, platelets and monocytes, are modulated by the enzymatic activity of CD39, as shown in Chapter II and elsewhere[7,91], yet the role of ecto-enyzmes in the etiology of atherosclerosis was unknown. Experiments found that a partial deficiency of CD39 was more deleterious than a complete loss of the enzyme. Surprisingly, mice missing one allele of CD39 had a near doubling of atherosclerotic plaque burden, while CD39-null mice had similar plaque burden as controls. The explanation for this paradox lay in the summed atherosclerotic contributions of monocytes and platelets. CD39-deficiency in macrophages (heterozygous or homozygous null) leads to heightened scavenger receptor expression on their surface and an enhanced ability to form foam cells

compared to controls. Yet, CD39-deficiency has dichotomous effects on platelet activation. CD39 heterozygous mice have enhanced stimulation of platelet purine receptors and greater platelet aggregation. *Cd39*-null mice have even greater platelet purine receptor stimulation, but chronically high levels of stimulation ultimately lead to the desensitization of these purine receptors. Thus $Cd39^{+/-}$ mice have enhanced platelet aggregation due to increased sensitivity, while $Cd39^{-/-}$ mice are refractory to ADP-induced aggregation. These phenomena suggest a mechanism where in greater platelet activation and enhanced foam cell formation leads to larger plaque in $Cd39^{+/-}$ mice, whereas loss of platelet reactivity and enhanced foam cell formation leads to no appreciable change in atherosclerotic plaque burden in $Cd39^{-/-}$ mice. This work shows that many of the cellular factors that CD39 influences can act in a summative fashion to produce pro-atherogenic and anti-atherogenic effects.

Chapter IV expanded upon the findings of Chapter III to identify the gene environment interactions between CD39 and the atherosclerotic plaque. This project was precipitated by the startling observation that endothelium overlying atherosclerotic plaque is devoid of CD39. We hypothesized that either the oxidative milieu or other local factors were suppressing CD39 in a region specific fashion and thereby influencing the localization and growth of plaque. Interestingly, examination of wild-type mice demonstrated that the CD39 enzyme was missing from endothelium in areas pre-disposed to atherosclerosis even though a plaque had not yet formed. This led to the idea that that the prevailing mechanical forces from the blood (shear stresses) could be mediating the vascular patterning of CD39 expression. *In vitro* application of laminar shear stress (as

seen in athero-resistant areas of the aorta) where able to potently induce CD39 expression. By comparison, oscillatory shear (as seen in athero-susceptible regions of the aorta) had no significant effect on CD39 expression. This laminar shear specific response begins to explain the regionalization of CD39 expression in the vasculature. Fluid flow induction of CD39 was partially dependent upon Kruppel-like factor 2 (KLF2), a transcription factor known to play a role regulating the shear responsiveness of other genes. Of note, KLF2 is also induced by the widely-prescribed, cardiotherapeutic drug class known as statins suggesting that off label use of this medicine may be a potential means to ameliorate local CD39 deficiencies in the vasculature.

CD39 and leukocyte autonomy

In Chapter II we explore the migratory fate of peripheral leukocytes in $Cd39^{-/-}$ and wild-type animals. Up to this point, numerous studies had demonstrated the importance of cell surface CD39 in models of ischemic injury[11-13] with broad endpoints such as infarct volume or death. Furthermore, in each of these studies, CD39-null mice were looked at as a whole (endogenous wild-type expression or whole animal ablation). Given that CD39 is expressed on a variety of cell types, this limited the interpretation of the role played by individual cells and/or subpopulations in developing a deeper understanding of CD39's ischemia protection. This restriction was due in large part to a paucity of reagents with which to explore this gene limited to recombinant proteins[33,63] and full animal genetic ablations[11,15]. In the absence of other techniques, the protection afforded

by CD39 in these studies was attributed to endothelial CD39, which can powerfully limit platelet activation and thrombosis[11-13].

In Chapter II, I sought to test whether endothelial CD39 was sufficient for conferring protection from cerebral ischemia by separating the blood-borne CD39 from the tissue-derived CD39 via bone marrow transplantation. By employing this technique we were able to individually analyze these two compartments and identify a novel immunomodulatory role for CD39 on monocytes. Perhaps the most interesting finding was that CD39 on a leukocyte regulates the stimulation of that very same cell. Thus this work demonstrated a "cell-autonomous" control of leukocyte migration, i.e., monocytes do not appear to be passive participants in the inflammatory response. Instead, leukocytes appear to regulate their extravasation into tissue through enzymatic catabolism of inflammatory stimuli. This paradigm is somewhat unique for leukocyte trafficking in a classical sense. Traditional stimuli (such as cytokines) are only passively degraded and rarely by the leukocyte itself.

CD39's autonomous regulation of leukocytes and inflammation can be paired with statins to suggest a novel therapeutic approach. The work of our lab and others has previously shown that exogenous supplementation of CD39 is profoundly protective in ischemic stroke[11,64]. Furthermore, it is has also been shown that in addition to inducing KLF2 in endothelium, statins can induce this transcription factor at high levels in macrophages as well[171]. This presents a tantalizing idea that patients in ischemic stress may be given a statin in conjunction with the current aspirin regimen prescribed now.

Only recently it has been shown that early statin therapy for patients suffering from acute myocardial infarction significantly decreases patient mortality[172]. The mechanism for this protection remains unclear. It is possible, though, that some of the statin-mediated protection is due to the induction of CD39 on macrophages and endothelium, thereby limiting post-ischemic inflammation and coagulation.

With the techniques employed in this work, we have begun to parse the effects of one CD39-bearing subpopulation from another. Yet, the tools used here are relatively coarse. Ablation of CD39 from an entire tissue or organ (as in marrow reconstitution) is assured of having effects and compensations beyond those that we intended to test in our experiments. Thus we have tried to guard against drawing our conclusions too firmly. It is well known, for example, that bone marrow derived cells can integrate into tissue as endothelium and that long lasting recipient derived blood cells may still be present after marrow reconstitution. We developed a novel quantitative PCR technique to measure bone marrow reconstitution efficiency and used flow cytometry to examine the reconstitution of individual cell populations to guard against this possibility, but some confounding by the transplant procedure itself cannot be ruled out. Furthermore, the leukocentric focus taken in these studies was not meant to preclude the idea that CD39 can also confer ischemia protection through regulation of platelet activation. In fact, the answer likely lies somewhere in the middle; a potential synergy may exist between the populations of leukocytes and platelets leading to co-activation and hetero-aggregation[125,126]. Ultimately to address these two questions effectively, new molecular tools and genetic mouse models will need to be developed.

CD39 and atherogenesis

One person dies every 34 seconds from atherosclerosis and its associated comorbidities, making cardiovascular disease the leading cause of death and disability in the world[173]. Despite great advancements in the treatment and prevention of cardiovascular disease in the twentieth century, the burden of this disease is increasing. Identification of new mechanisms, which contribute to atherogenesis or endogenous mechanisms that retard its development could lead to new insights into its disease pathogenesis and new therapeutic options. With this concept in mind, Chapters III and IV explored the endogenous protection afforded to the body by cell surface enzymes that mitigate inflammatory stimuli. In doing so, we identify a novel approach for combating cardiovascular disease.

This work was significant for being the first to link an endogenous regulation of extracellular nucleotide signaling with atherosclerosis. Platelet activation has recently emerged as a therapeutic target for limiting cardiovascular disease[127,128]. Thus it is not surprising that CD39's regulation of platelet activation may play a large role in disease pathogenesis. Furthermore, work in Chapter II and elsewhere[16] has highlighted the $P2X_7$ receptor as particularly sensitive to CD39's regulatory action. For many purine-sensitive receptors, like the P2Y family of G protein coupled receptors, chronic stimulation leads to downregulation and desensitization (e.g., the $P2Y_{12}$ receptor on platelets). Chronic stimulation occurs because $Cd39^{-/-}$ mice have approximately 90% less vascular ecto-enzyme activity than their wild-type counterparts allowing local accumulation of

nucleotides[75,76]. By comparison, the P2X$_7$ receptor, is known to be resistant to desensitization, allowing for a close interrelationship between CD39 activity and P2X$_7$ receptor engagement. In the setting of atherosclerosis this interrelationship manifested as an enhanced scavenger receptor expression and consequent increase in lipid avidity on CD39-deficient marophages. This finding was the first identification of ATP-driven foam cell formation. In conjunction with the regulation of adhesion molecule expression in Chapter II, ecto-enzyme regulation of foam cell formation highlights an important pathway for macrophage activation. The CD39-macrophage-P2X$_7$ receptor axis may extend deeper as the P2X$_7$ receptor was originally identified for its role in inducing cellular apoptosis[107]. Recent evidence has shown that CD39 is able to limit apoptosis of natural killer cells[174] and endothelium[16] suggesting that the same may hold true for macrophages as well. The deleterious effects of macrophage apoptosis in atherosclerosis has been well documented[175].

One of the major limitations of this work lies in reconciling the multi-factorial nature of atherosclerosis with the multi-cellular expression of CD39. Further compounding the issue is the relatively ubiquitous nature of purinergic signaling and its pervasive effects. A microcosm of this is clearly evident in *Cd39*$^{+/-}$ and *CD39*$^{-/-}$ mice which both have lipid-avid macrophages, but have very different responses to ADP-induced platelet aggregation. The only clear way to dissect the mechanisms that underly the atherosclerotic phenotype of CD39-deficient animals is to design experiments that have only one cellular variable at a time. This does not diminish the value of the current studies, which were critical for demonstrating that extracellular nucleotide metabolism is

a powerful endogenous protector against atherosclerosis, and identifying this field as an area of future study. In the future, development of novel reagents should allow for targeted ablations and overexpressions of CD39 that will enable study of the role CD39 plays on individual subpopulations in the etiology of this complex disease.

We think these CD39 and atherosclerosis findings combined with the subsequent shear stress work may ultimately be of therapeutic benefit. Numerous current purine-based pharmacologic therapies, such as the thienopyridine class of anti-coagulants, function by irreversibly antagonizing their cognate receptors. This can lead to permanent blockade of a pathway and consequently unwanted side effects such as hemorrhage. As CD39 does not act directly on the cells or receptors themselves, its effects are self-limiting and may theoretically be used with fewer adverse events[63]. As lipid lowering drugs are already a first-line therapy in preventing heart disease, preferential prescription of statins may be all that is necessary to capitalize on CD39's anti-atherogenic effects.

Future Directions

Throughout this thesis (and in this chapter in particular) I have highlighted the limitations of our methods and the gaps that remain in our knowledge. At the point where this thesis research concludes, there are a number of exciting and important questions that remain to be answered. Three of the most pressing to me are outlined below:

1) *What are the individual roles of CD39 bound macrophages and endothelium in suppressing atherogenesis?* The multilayered phenotypes presented by CD39 heterozygous and homozygous null mice were a reflection of the divergent responses of different cell populations to CD39-deficiency. To explore these phenotypes further, we need to use more precise tools that utilize targeted manipulations of CD39. A CD39 flox ablation mouse should allow for CD39's platelet effects to be separated from those of the monocyte effects. A conditionally inducible CD39 transgenic mouse would then serve as an ideal complement to the CD39 conditional ablation mouse to examine the inverse scenario. As monocyte CD39 accounts for only a very small percentage of blood born CD39[67], it is unlikely that platelet function and desensitization would be affected in either of these models.

Bone marrow transplantation could be used as an initial technique to selectively overexpress or ablate CD39 expression, but there are several limitations to using this model in a chronic injury setting like atherosclerosis. One of primary goals of a targeted ablation is to separate monocyte responses from that of the platelets. As shown in Chapter II, however, bone marrow reconstitution and the bone marrow compartment as a whole have significant effects on platelet function. Thus in a transplant scenario, the role of platelets and monocytes could not be fully separated. Secondly, the contributions of the innate and adaptive immune responses could not be parsed with a transplant as both originate within the marrow. Finally, endothelial progenitor cells emigrate from the bone marrow and can engraft in the vascular wall over time. This phenomenon is thought to be particularly important as an endogenous reparative mechanism that combats

atherogenesis[176]. This blending of cellular origin (and in this case genotype) would ultimately make attribution of tissue-derived effects and leukocyte-derived effects difficult.

As part of the work for this thesis, I have already begun to make the mouse that conditionally ablates CD39 (*Cd39$^{flx/flx}$*). The *Cd39$^{flx/flx}$* mouse was generated using a strategy targeting the first exon of CD39 (**Figure 5.1**). Excision of this exon has previously been shown to disrupt endogenous expression of CD39[15]. A representative Southern blot demonstrating successful targeting of the floxed allele is shown in (**Figure 5.2**). Backcrossing is unnecessary as these mice were generated with the Bruce 4 stem cell line (C57Bl/6 background). Currently the *Cd39$^{flx/flx}$* mice have been bred to homozygosity and crossed to a pleiotropic CRE (EIIA) to demonstrate that CD39 can be successfully excised in all tissues (*Cd39$^{\Delta/\Delta}$*). By crossing *Cd39$^{flx/flx}$* to mice that express CRE in specific cell lineages or tissues we should be able to assess the contribution of CD39 on individual cells to whole animal physiology.

To generate the conditional overexpression of CD39, murine CD39 cDNA could be inserted into a vector with a highly expressed promoter like β-actin followed by a floxed LacZ and stop codon (**Figure 5.3**). Murine CD39 cDNA can be taken from the same overexpression construct used to generate a CD39 overexpression in macrophages (Chapters II and III). The proposed transgenic expression strategy has been used before and allows for rapid screening of ES cells and founder mice by staining for transgenic expression of LacZ[177]. With this construct CD39 could be induced in specific cell types

by breeding the transgenic mouse to the desired CRE expressing mouse. Successful recombination can be confirmed by testing for the loss of LacZ staining and consequent overexpression of CD39.

2) *How do shear stress, Kruppel-like factor 2, and CD39 intersect?* Work in this thesis has shown a relationship exists between mechanical shear forces on an endothelial cell and a KLF2 dependent induction of CD39. Yet to this point, we still do not know what role KLF2 plays in effecting a change in CD39 mRNA. It is critical that future experiments focus on how shear stress activates CD39's promoter. A stepwise, "promoter bashing" approach would be the ideal method. Technically this would be challenging, as primary endothelial cells are required for optimal shear stress responses, yet primary endothelial cells are notoriously hard to transfect due to their delicate nature. Once the method is established, however, particular attention should be paid to the segment of CD39 promoter between -85 bp and -55 bp as our *in silico* study identified 3 putative KLF2 binding sites in this region (one canonical KLF2 site and 2 SP1 sites). When a region of interest has been identified, site-directed mutagensis could be used to identify with certainty the binding sequence of interest. At this point electrophoretic shift mobiliy assays and chromatin immunoprecipiation assays should be used to confirm its functional and *in vitro* relevance.

It is also possible that CD39, like many other genes, is regulated post transcriptionally by laminar shear. The mRNA of cyclooxygenase-2, e.g., is stabilized by laminar shear in addition to its transcriptional activation[178]. RNA stability assays that

utilize Actinomycin D would enable us to examine if post-transcriptional phenomena were involved. Actinomycin D is a chemical isolated from *Streptomyces* which binds to DNA at the transcriptional start complex preventing RNA transcription. Thus the effects of shear stress on CD39 mRNA without the confounding of effects of transcription can be examined. Ideally, this experiment would be done with two parallel sets of sheared cells (to induce maximal CD39), then both would be treated with Actinomycin D and one set returned to shear while the other remained stationary. This would allow direct comparison of the effects of shear stress alone.

Finally, as mentioned in Chapter I, work from Guidotti's lab has shown that the biomechanics of the cell membrane can directly influence CD39's function. By regulating tetramer formation and interactions as well as regulating the ecto-enzyme's flexibility, the cell membrane is able to heavily influence CD39's ability to accommodate and thereby degrade nucleotides. Cholesterol is an integral part of the cell membrane that heavily influences membrane fluidity and thereby controls CD39 activity[48,49]. Underscoring this is the fact that CD39 resides in cholesterol rich micro-domains known as caveolae and that perturbations of these cholesterol domains can alter CD39 activity[26,48,170]. Our observation that simvastatin, a drug that inhibits cholesterol biosynthesis profoundly suppresses CD39 expression, appears to highlight the convergence of multiple homologous regulatory mechanisms on one pathway. It would be of great interest to explore how statins and cholesterol are interacting to directly alter CD39 activity independent of protein induction. This would best be accomplished by transfecting CD39 into a KLF2 and CD39 deficient cell line like Chinese hamster ovary

cells or COS-7 cells. Choosing a CD39- and KLF2-deficient cell line would completely separate transcriptional effects from biomechanical and structural ones. Transfection of CD39 into COS-7, e.g., results in normal targeting of CD39 to the cell membrane and correct localization within caveolar micro-domains making it an ideal system for exploring this question[132].

3) Knowing that shear stress modulates CD39, can CD39 in turn modulate shear stress? Time and again we have seen in this work and elsewhere that CD39 is indiscriminant in its catabolism of ATP and ADP. If a nucleotide is present within the local microenvironment of a CD39 molecule, it will be degraded. This raises the question of how CD39 and shear are interacting. Shear stress applied to an endothelial cell induces bolus release of ATP from submembrane compartments through pores such as connexins[179]. This ATP can circle back in both an autocrine and paracrine fashion to activate the endothelial cell and its neighbors. Though there are many mechanisms of shear stress sensing by endothelial cells, this release and subsequent engagement of ATP on the endothelial surface[179] is the most likely to be regulated by CD39. To explore this question further, endothelial cells isolated from $Cd39^{-/-}$ and WT mice should be isolated and exposed to both laminar and turbulent shear stresses to produce varied types of ATP release. A cone-plate viscometer, could be compared with a parallel plate system as well. The critical difference between the two being that the cone-plate system does not employ media exchange, whereas a parallel plate system has continuous media exchange and thus less local accumulation of released metabolites. After a prescribed period of time, RNA should be isolated from these cells and a gene array run to determine shear stress

responses that are susceptible to modulation by CD39. This would be an interesting question in the field as CD39 could be one of the first identified modifiers of shear stress's outside-in signal transduction.

Figure 5.1 Molecular strategy for ablating CD39 in specific tissues. The native CD39 gene is shown in parallel with the targeting construct. The targeting construct is identical to the native gene with the exception of two loxP sites that flank the first exon of CD39 as well as a reverse neomycin cassette that is flanked by two FRT sites. The diagram shows how successive breeding to a FLP recombinase-expressing mouse followed by a CRE recombinase expressing mouse can be used to ablate CD39 in a targeted fashion.
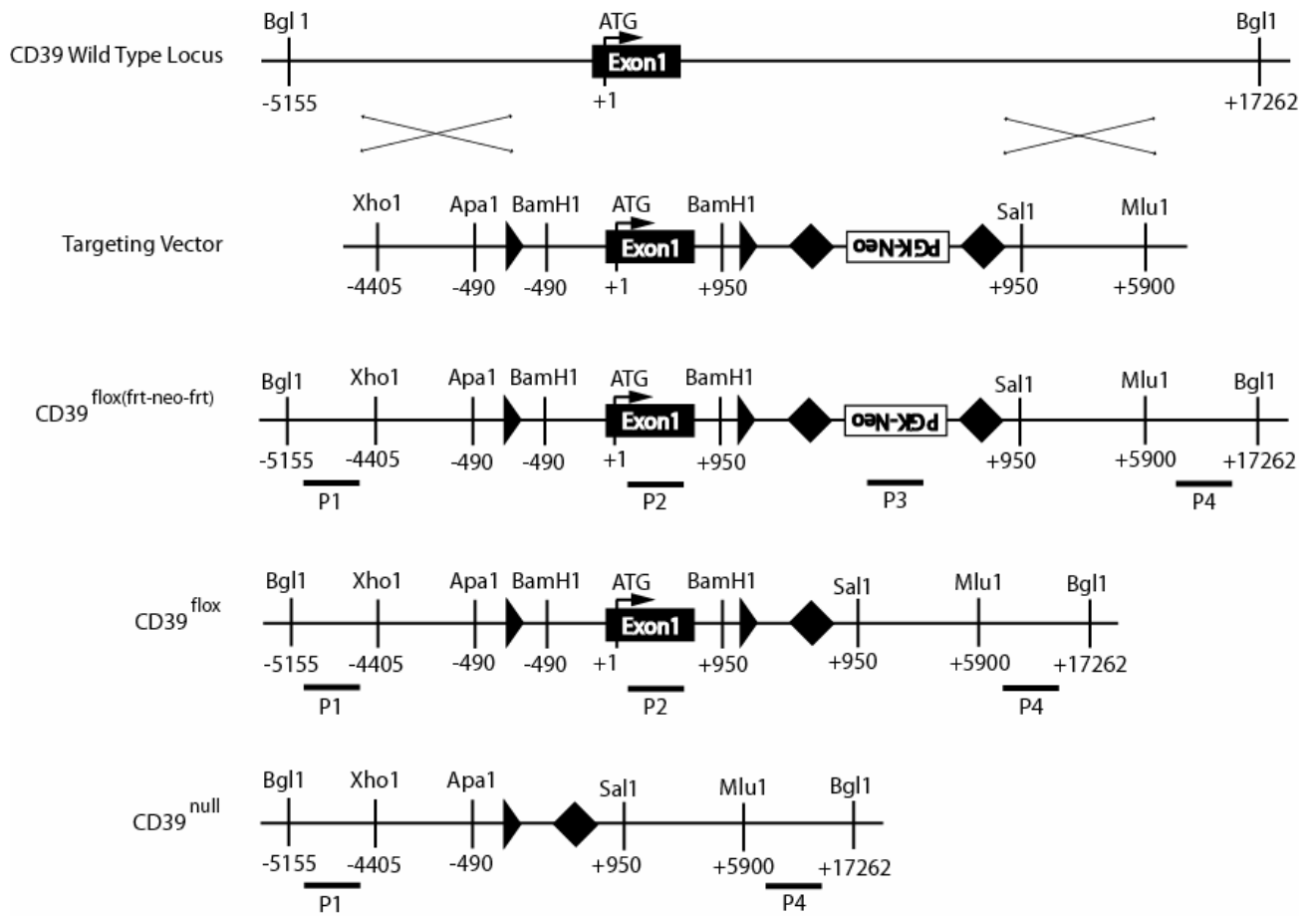
Figure 5.1

Figure 5.2 Southern blot analysis of *CD39*^{*flx/+*} heterozygous mice. Probes were designed to detect the 5' end (P1 in **Figure 5.1**) and 3' end (P4 in **Figure 5.1**) of the DNA targeted for homologous recombination in transfected stem cell lines. These 5' (**A**) and 3' (**B**) probes were radiolabeled and hybridized with genomic DNA purified from untransfected stem cells, to yield a successfully transfected stem cell line, and an F1 generation mouse.
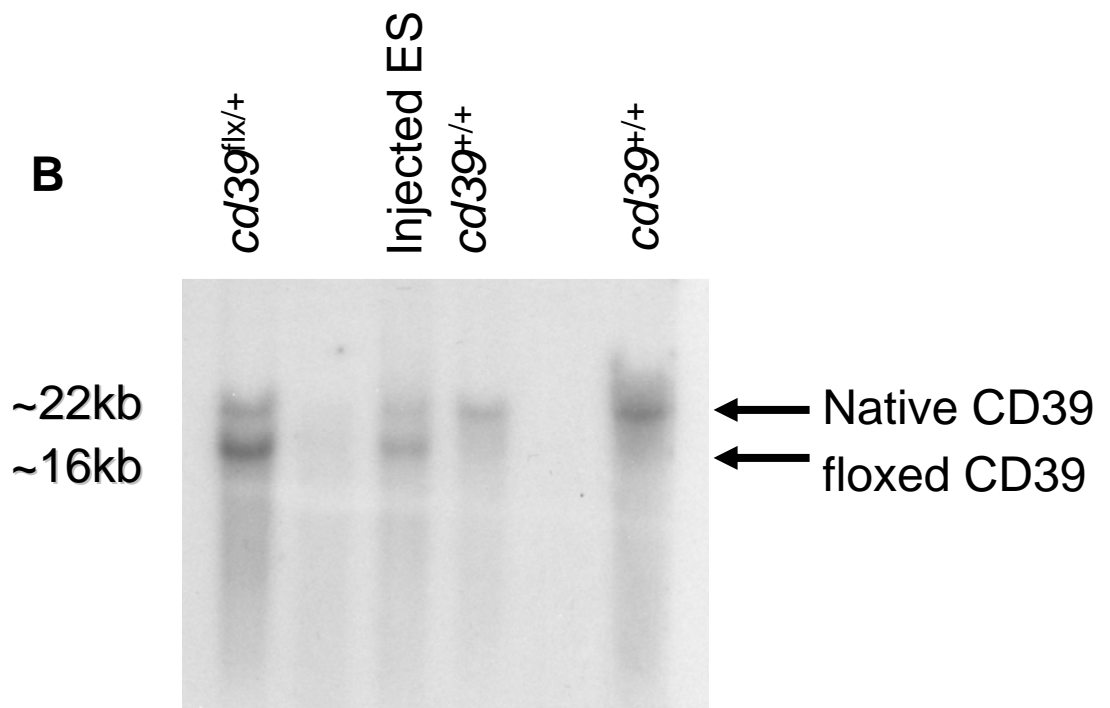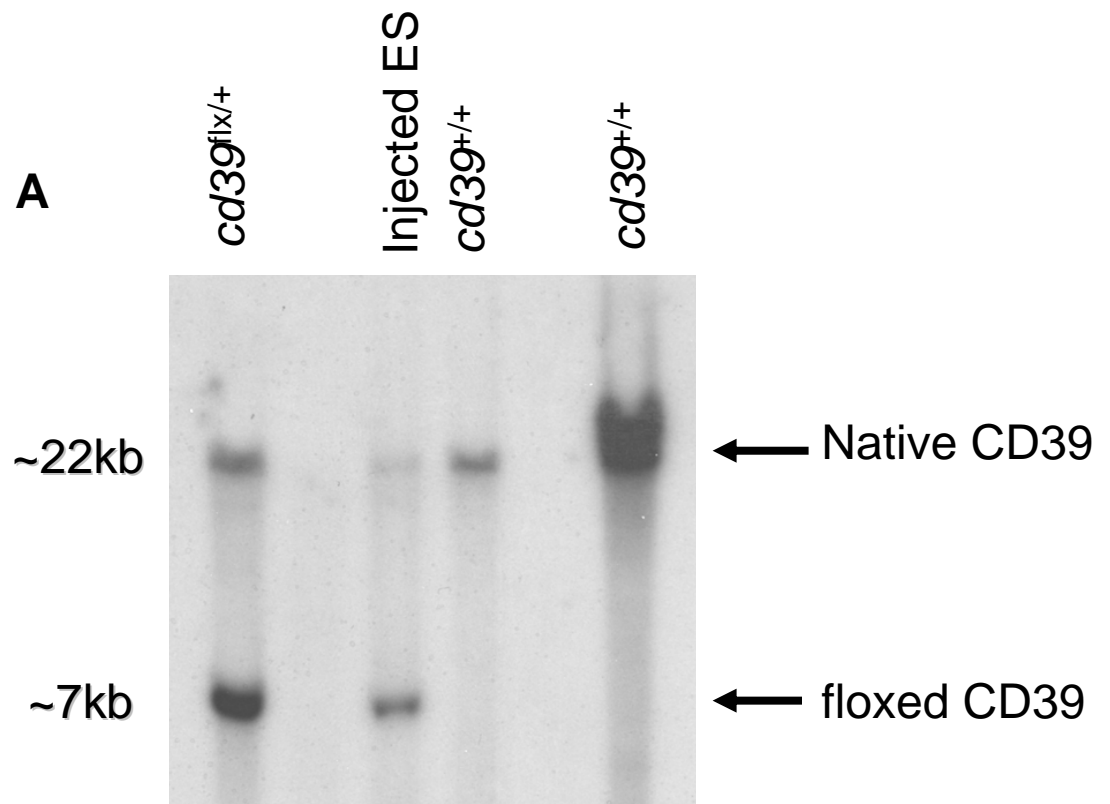
Figure 5.2

Figure 5.3 Molecular strategy for overexpressing CD39 in specific tissues. A targeting construct using a previously validated strategy is diagrammed. A ubiquitous promoter (β-actin) drives LacZ expression in all tissues. When CRE recombinase is introduced to this system, recombination occurs at the two LoxP sites. This results in excision of both LacZ and the stop codon that were preventing transcription of the CD39 transgene.
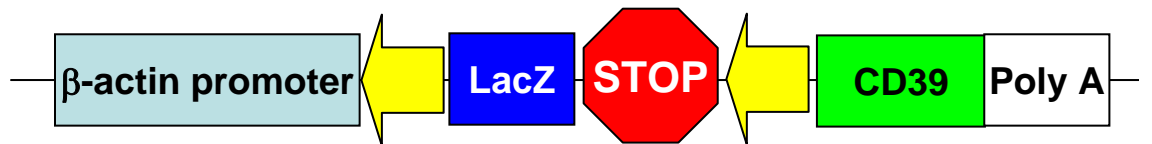
Figure 5.3

Literature Referenced

1.   Boeynaems, J.M., Communi, D., Gonzalez, N.S. & Robaye, B. Overview of the P2 receptors. *Semin Thromb Hemost* **31**, 139-149 (2005).

2.   Freyer, D.R., Boxer, L.A., Axtell, R.A. & Todd, R.F., 3rd. Stimulation of human neutrophil adhesive properties by adenine nucleotides. *J Immunol* **141**, 580-586 (1988).

3.   Wong, C.W.*, et al.* Connexin37 protects against atherosclerosis by regulating monocyte adhesion. *Nat Med* **12**, 950-954 (2006).

4.   Deaglio, S.*, et al.* Adenosine generation catalyzed by CD39 and CD73 expressed on regulatory T cells mediates immune suppression. *J Exp Med* **204**, 1257-1265 (2007).

5.   Coade, S.B. & Pearson, J.D. Metabolism of adenine nucleotides in human blood. *Circ Res* **65**, 531-537 (1989).

6.   Marcus, A.J.*, et al.* The Endothelial Cell Ecto-ADPase Responsible for Inhibition of Platelet Function is CD39. *J. Clin. Invest.* **99**, 1351-1360 (1997).

7.   Marcus, A.J.*, et al.* Inhibition of platelet function by an aspirin-insensitive endothelial cell ADPase. Thromboregulation by endothelial cells. *J Clin Invest* **88**, 1690-1696 (1991).

8.   Kaczmarek, E.*, et al.* Identification and characterization of CD39/vascular ATP diphosphohydrolase. *J.Biol.Chem.* **271**, 33116-33122 (1996).

9.   Sevigny, J.*, et al.* Differential catalytic properties and vascular topography of murine nucleoside triphosphate diphosphohydrolase 1 (NTPDase1) and NTPDase2 have implications for thromboregulation. *Blood* **99**, 2801-2809 (2002).

10.   Marcus, A.J.*, et al.* Role of CD39 (NTPDase-1) in thromboregulation, cerebroprotection, and cardioprotection. *Semin Thromb Hemost* **31**, 234-246 (2005).

11.   Pinsky, D.J.*, et al.* Elucidation of the thromboregulatory role of CD39/ectoapyrase in the ischemic brain. *J Clin Invest* **109**, 1031-1040 (2002).

12.   Grenz, A.*, et al.* Contribution of E-NTPDase1 (CD39) to renal protection from ischemia-reperfusion injury. *FASEB J* **21**, 2863-2873 (2007).

13.   Guckelberger, O.*, et al.* Beneficial effects of CD39/ecto-nucleoside triphosphate diphosphohydrolase-1 in murine intestinal ischemia-reperfusion injury. *Thromb Haemost* **91**, 576-586 (2004).

14. Mizumoto, N.*, et al.* CD39 is the dominant Langerhans cell-associated ecto-NTPDase: Modulatory roles in inflammation and immune responsiveness. *Nature Medicine* **8**, 358-365 (2002).

15. Enjyoji, K.*, et al.* Targeted disruption of cd39/ATP diphosphohydrolase results in disordered hemostasis and thromboregulation. *Nature Medicine* **5**, 1010-1017 (1999).

16. Goepfert, C.*, et al.* CD39 modulates endothelial cell activation and apoptosis. *Mol Med* **6**, 591-603 (2000).

17. Imai, M., Goepfert, C., Kaczmarek, E. & Robson, S.C. CD39 Modulates IL-1 Release from Activated Endothelial Cells. *Biochemical and Biophysical Research Communications* **270**, 272-278 (2000).

18. Maliszewski, C.R.*, et al.* The CD39 lymphoid cell activation antigen. Molecular cloning and structural characterization. *J Immunol* **153**, 3574-3583 (1994).

19. Rowe, M., Hildreth, J.E., Rickinson, A.B. & Epstein, M.A. Monoclonal antibodies to Epstein-Barr virus-induced, transformation-associated cell surface antigens: binding patterns and effect upon virus-specific T-cell cytotoxicity. *Int J Cancer* **29**, 373-381 (1982).

20. Ling, N.R.*, et al.* A phenotypic study of cells from Burkitt lymphoma and EBV-B-lymphoblastoid lines and their relationship to cells in normal lymphoid tissues. *Int J Cancer* **43**, 112-118 (1989).

21. Kansas, G., Wood, G. & Tedder, T. Expression, distribution, and biochemistry of human CD39. Role in activation-associated homotypic adhesion of lymphocytes. *Journal of Immunology* **146**, 2235-2244 (1991).

22. Koziak, K., Sevigny, J., Robson, S.C., Siegel, J. & Kaczmarek, E. Analysis of CD39/ATP diphophohydrolase (ATPDase) expression in endothelial cells, platelets, and leukocytes. *Thrombosis and Haemostasis* **82**, 1538-1544 (1999).

23. Sevigny, J., Levesque, F.P., Grondin, G. & Beaudoin, A.R. Purification of the blood vessel ATP diphosphohydrolase, identification and localisation by immunological techniques. *Biochim Biophys Acta* **1334**, 73-88 (1997).

24. Wang, T.F. & Guidotti, G. CD39 is an ecto-(Ca2+,Mg2+)-apyrase. *J Biol Chem* **271**, 9898-9901 (1996).

25. Heine, P., Braun, N., Heilbronn, A. & Zimmermann, H. Functional characterization of rat ecto-ATPase and ecto-ATP diphosphohydrolase after heterologous expression in CHO cells. *Eur J Biochem* **262**, 102-107 (1999).

26. Koziak, K.*, et al.* Palmitoylation targets CD39/endothelial ATP diphosphohydrolase to caveolae. *J Biol Chem* **275**, 2057-2062 (2000).

27. Kittel, A. & Bacsy, E. Ecto-ATPases and 5′-nucleotidases in the caveolae of smooth muscle. Enzyme-histochemical evidence may indicate a role for caveolae in neurotransmission. *Cell Biology International* **18**, 875-880 (1994).

28. Kittel, A., Csapo, Z., Csizmadia, E., Jackson, S. & Robson, S.C. Co-localization of P2Y1 receptor and NTPDase1/CD39 within caveolae in human placenta. *European Journal of Histochemistry* **48**, 253-259 (2004).

29. Khakh, B.S. & North, R.A. P2X receptors as cell-surface ATP sensors in health and disease. *Nature* **442**, 527-532 (2006).

30. Sitkovsky, M.V.*, et al.* Physiological Control of Immune Response and Inflammatory Tissue Damage by Hypoxia-Inducible Factors and Adenosine A2A Receptors. *Annual Review of Immunology* **22**, 657-682 (2004).

31. Bermudes, D., Peck, K.R., Afifi, M.A., Beckers, C.J. & Joiner, K.A. Tandemly repeated genes encode nucleoside triphosphate hydrolase isoforms secreted into the parasitophorous vacuole of Toxoplasma gondii. *J Biol Chem* **269**, 29252-29260 (1994).

32. Champagne, D.E., Smartt, C.T., Ribeiro, J.M. & James, A.A. The salivary gland-specific apyrase of the mosquito Aedes aegypti is a member of the 5'-nucleotidase family. *Proc Natl Acad Sci U S A* **92**, 694-698 (1995).

33. Handa, M. & Guidotti, G. Purification and cloning of a soluble ATP-diphosphohydrolase (apyrase) from potato tubers (Solanum tuberosum). *Biochem Biophys Res Commun* **218**, 916-923 (1996).

34. Chadwick, B.P. & Frischauf, A.M. The CD39-like gene family: identification of three new human members (CD39L2, CD39L3, and CD39L4), their murine homologues, and a member of the gene family from Drosophila melanogaster. *Genomics* **50**, 357-367 (1998).

35. Grinthal, A. & Guidotti, G. Transmembrane domains confer different substrate specificities and adenosine diphosphate hydrolysis mechanisms on CD39, CD39L1, and chimeras. *Biochemistry* **41**, 1947-1956 (2002).

36. Schoenborn, M.A.*, et al.* Gene structure and chromosome location of mouse Cd39 coding for an ecto-apyrase. *Cytogenet Cell Genet* **81**, 287-289 (1998).

37. Smith, T.M. & Kirley, T.L. Site-directed mutagenesis of a human brain ecto-apyrase: evidence that the E-type ATPases are related to the actin/heat shock 70/sugar kinase superfamily. *Biochemistry* **38**, 321-328 (1999).

38. Bork, P., Sander, C. & Valencia, A. An ATPase domain common to prokaryotic cell cycle proteins, sugar kinases, actin, and hsp70 heat shock proteins. *Proc Natl Acad Sci U S A* **89**, 7290-7294 (1992).

39.	Drosopoulos, J.H., *et al.* Site-directed mutagenesis of human endothelial cell ecto-ADPase/soluble CD39: requirement of glutamate 174 and serine 218 for enzyme activity and inhibition of platelet recruitment. *Biochemistry* **39**, 6936-6943 (2000).

40.	Yang, F., Hicks-Berger, C.A., Smith, T.M. & Kirley, T.L. Site-directed mutagenesis of human nucleoside triphosphate diphosphohydrolase 3: the importance of residues in the apyrase conserved regions. *Biochemistry* **40**, 3943-3950 (2001).

41.	Smith, T.M., Lewis Carl, S.A. & Kirley, T.L. Mutagenesis of two conserved tryptophan residues of the E-type ATPases: inactivation and conversion of an ecto-apyrase to an ecto-NTPase. *Biochemistry* **38**, 5849-5857 (1999).

42.	Grinthal, A. & Guidotti, G. Substitution of His59 converts CD39 apyrase into an ADPase in a quaternary structure dependent manner. *Biochemistry* **39**, 9-16 (2000).

43.	North, R.A. Families of ion channels with two hydrophobic segments. *Curr Opin Cell Biol* **8**, 474-483 (1996).

44.	Wang, T.F., Ou, Y. & Guidotti, G. The transmembrane domains of ectoapyrase (CD39) affect its enzymatic activity and quaternary structure. *J Biol Chem* **273**, 24814-24821 (1998).

45.	Grinthal, A. & Guidotti, G. Dynamic motions of CD39 transmembrane domains regulate and are regulated by the enzymatic active site. *Biochemistry* **43**, 13849-13858 (2004).

46.	Hicks-Berger, C.A. & Kirley, T.L. Expression and characterization of human ecto-ATPase and chimeras with CD39 ecto-apyrase. *IUBMB Life* **50**, 43-50 (2000).

47.	Grinthal, A. & Guidotti, G. Bilayer mechanical properties regulate the transmembrane helix mobility and enzymatic state of CD39. *Biochemistry* **46**, 279-290 (2007).

48.	Papanikolaou, A., *et al.* Cholesterol-dependent lipid assemblies regulate the activity of the ecto-nucleotidase CD39. *J Biol Chem* **280**, 26406-26414 (2005).

49.	Robson, S.C., *et al.* Modulation of vascular ATP diphosphohydrolase by fatty acids. *Blood Coagul Fibrinolysis* **8**, 21-27 (1997).

50.	Wu, Y., *et al.* RanBPM associates with CD39 and modulates ecto-nucleotidase activity. *Biochem J* **396**, 23-30 (2006).

51.	Zhong, X., Malhotra, R., Woodruff, R. & Guidotti, G. Mammalian plasma membrane ecto-nucleoside triphosphate diphosphohydrolase 1, CD39, is not

active intracellularly. The N-glycosylation state of CD39 correlates with surface activity and localization. *J Biol Chem* **276**, 41518-41525 (2001).

52.   Zhong, X., Kriz, R., Kumar, R. & Guidotti, G. Distinctive roles of endoplasmic reticulum and golgi glycosylation in functional surface expression of mammalian E-NTPDase1, CD39. *Biochim Biophys Acta* **1723**, 143-150 (2005).

53.   Wu, J.J., Choi, L.E. & Guidotti, G. N-linked oligosaccharides affect the enzymatic activity of CD39: diverse interactions between seven N-linked glycosylation sites. *Mol Biol Cell* **16**, 1661-1672 (2005).

54.   Kansas, G. & Tedder, T. Transmembrane signals generated through MHC class II, CD19, CD20, CD39, and CD40 antigens induce LFA-1-dependent and independent adhesion in human B cells through a tyrosine kinase-dependent pathway. *J Immunol* **147**, 4094-4102 (1991).

55.   Bodas, E*., et al.* ATP crossing the cell plasma membrane generates an ionic current in xenopus oocytes. *J Biol Chem* **275**, 20268-20273 (2000).

56.   Born, G.V. Aggregation of blood platelets by adenosine diphosphate and its reversal. *Nature* **194**, 927-929 (1962).

57.   Smyth, S.S*., et al.* G-protein-coupled receptors as signaling targets for antiplatelet therapy. *Arterioscler Thromb Vasc Biol* **29**, 449-457 (2009).

58.   Gachet, C. Regulation of platelet functions by P2 receptors. *Annu Rev Pharmacol Toxicol* **46**, 277-300 (2006).

59.   Gachet, C. P2 receptors, platelet function and pharmacological implications. *Thromb Haemost* **99**, 466-472 (2008).

60.   Hollopeter, G*., et al.* Identification of the platelet ADP receptor targeted by antithrombotic drugs. *Nature* **409**, 202-207 (2001).

61.   Leon, C*., et al.* The P2Y1 receptor is an ADP receptor antagonized by ATP and expressed in platelets and megakaryoblastic cells. *FEBS Lett* **403**, 26-30 (1997).

62.   Hechler, B*., et al.* The P2Y1 receptor is necessary for adenosine 5'-diphosphate-induced platelet aggregation. *Blood* **92**, 152-159 (1998).

63.   Gayle, R.B., 3rd*, et al.* Inhibition of platelet function by recombinant soluble ecto-ADPase/CD39. *J Clin Invest* **101**, 1851-1859 (1998).

64.   Belayev, L*., et al.* Neuroprotective effect of SolCD39, a novel platelet aggregation inhibitor, on transient middle cerebral artery occlusion in rats. *Stroke* **34**, 758-763 (2003).

65. Wolff, K. & Winkelmann, R.K. Ultrastructural localization of nucleoside triphosphatase in Langerhans cells. *J Invest Dermatol* **48**, 50-54 (1967).

66. Granstein, R.D. The skinny on CD39 in immunity and inflammation. *Nat Med* **8**, 336-338 (2002).

67. Pulte, E.D.*, et al.* CD39/NTPDase-1 activity and expression in normal leukocytes. *Thromb Res* **121**, 309-317 (2007).

68. Goepfert, C.*, et al.* Disordered Cellular Migration and Angiogenesis in cd39-Null Mice. *Circulation* **104**, 3109-3115 (2001).

69. Huang, J.*, et al.* Neuronal protection in stroke by an sLex-glycosylated complement inhibitory protein. *Science* **285**, 595-599 (1999).

70. Choudhri, T.F.*, et al.* Reduced microvascular thrombosis and improved outcome in acute murine stroke by inhibiting GP IIb/IIIa receptor-mediated platelet aggregation. *J Clin Invest* **102**, 1301-1310 (1998).

71. Salmi, M. & Jalkanen, S. Cell-surface enzymes in control of leukocyte trafficking. *Nat Rev Immunol* **5**, 760-771 (2005).

72. Ralevic, V. & Burnstock, G. Receptors for purines and pyrimidines. *Pharmacol Rev* **50**, 413-492 (1998).

73. Di Virgilio, F.*, et al.* Nucleotide receptors: an emerging family of regulatory molecules in blood cells. *Blood* **97**, 587-600 (2001).

74. Khakh, B.S. & North, R.A. P2X receptors as cell-surface ATP sensors in health and disease. *Nature* **442**, 527-532 (2006).

75. Pinsky, D.J.*, et al.* Elucidation of the thromboregulatory role of CD39/ectoapyrase in the ischemic brain. *J. Clin. Invest.* **109**, 1031-1040 (2002).

76. Enjyoji, K.*, et al.* Targeted disruption of cd39/ATP diphosphohydrolase results in disordered hemostasis and thromboregulation. *Nat Med* **5**, 1010-1017 (1999).

77. Zimmermann, H. Nucleotides and cd39: principal modulatory players in hemostasis and thrombosis. *Nat Med* **5**, 987-988 (1999).

78. Chen, Y.*, et al.* ATP release guides neutrophil chemotaxis via P2Y2 and A3 receptors. *Science* **314**, 1792-1795 (2006).

79. Gorini, S. & la Sala, A. Hydrolysis of extracellular ATP and immune suppression: humans versus mice. *Blood* **111**, 964-965 (2008).

80. Linden, J. Cell biology. Purinergic chemotaxis. *Science* **314**, 1689-1690 (2006).

81.   Eltzschig, H.K.*, et al.* Coordinated adenine nucleotide phosphohydrolysis and nucleoside signaling in posthypoxic endothelium: role of ectonucleotidases and adenosine A2B receptors. *J Exp Med* **198**, 783-796 (2003).

82.   Thompson, L.F.*, et al.* Crucial Role for Ecto-5'-Nucleotidase (CD73) in Vascular Leakage during Hypoxia. *J. Exp. Med.* **200**, 1395-1405 (2004).

83.   Eltzschig, H.K.*, et al.* Endogenous adenosine produced during hypoxia attenuates neutrophil accumulation: coordination by extracellular nucleotide metabolism. *Blood* **104**, 3986-3992 (2004).

84.   Su, E.J.*, et al.* Activation of PDGF-CC by tissue plasminogen activator impairs blood-brain barrier integrity during ischemic stroke. *Nat Med* **14**, 731-737 (2008).

85.   Austyn, J.M. & Gordon, S. F4/80, a monoclonal antibody directed specifically against the mouse macrophage. *Eur J Immunol* **11**, 805-815 (1981).

86.   Jander, S., Kraemer, M., Schroeter, M., Witte, O.W. & Stoll, G. Lymphocytic infiltration and expression of intercellular adhesion molecule-1 in photochemically induced ischemia of the rat cortex. *J Cereb Blood Flow Metab* **15**, 42-51 (1995).

87.   Hassan, N.F., Rifat, S., Campbell, D.E., McCawley, L.J. & Douglas, S.D. Isolation and flow cytometric characterization of newborn mouse brain-derived microglia maintained in vitro. *J Leukoc Biol* **50**, 86-92 (1991).

88.   Stirling, D.P. & Yong, V.W. Dynamics of the inflammatory response after murine spinal cord injury revealed by flow cytometry. *J Neurosci Res* **86**, 1944-1958 (2008).

89.   Yu, L.*, et al.* Selective inactivation or reconstitution of adenosine A2A receptors in bone marrow cells reveals their significant contribution to the development of ischemic brain injury. *Nat Med* **10**, 1081-1087 (2004).

90.   Dwyer, K.M.*, et al.* Thromboregulatory manifestations in human CD39 transgenic mice and the implications for thrombotic disease and transplantation. *J. Clin. Invest.* **113**, 1440-1446 (2004).

91.   Marcus, A.J.*, et al.* The endothelial cell ecto-ADPase responsible for inhibition of platelet function is CD39. *J.Clin.Invest* **99**, 1351-1360 (1997).

92.   Freyer, D.R., Morganroth, M.L., Rogers, C.E., Arnaout, M.A. & Todd, R.F., 3rd. Modulation of surface CD11/CD18 glycoproteins (Mo1, LFA-1, p150,95) by human mononuclear phagocytes. *Clin Immunol Immunopathol* **46**, 272-283 (1988).

93. Morabito, L*., et al.* Methotrexate and sulfasalazine promote adenosine release by a mechanism that requires ecto-5'-nucleotidase-mediated conversion of adenine nucleotides. *J Clin Invest* **101**, 295-300 (1998).

94. Soto, F., Garcia-Guzman, M. & Stuhmer, W. Cloned ligand-gated channels activated by extracellular ATP (P2X receptors). *J Membr Biol* **160**, 91-100 (1997).

95. Haines, W.R., Torres, G.E., Voigt, M.M. & Egan, T.M. Properties of the novel ATP-gated ionotropic receptor composed of the P2X(1) and P2X(5) isoforms. *Mol Pharmacol* **56**, 720-727 (1999).

96. Communi, D., Robaye, B. & Boeynaems, J.M. Pharmacological characterization of the human P2Y11 receptor. *Br J Pharmacol* **128**, 1199-1206 (1999).

97. Tsuda, M*., et al.* P2X4 receptors induced in spinal microglia gate tactile allodynia after nerve injury. *Nature* **424**, 778-783 (2003).

98. Inoue, K., Tsuda, M. & Koizumi, S. ATP- and adenosine-mediated signaling in the central nervous system: chronic pain and microglia: involvement of the ATP receptor P2X4. *J Pharmacol Sci* **94**, 112-114 (2004).

99. Murgia, M., Hanau, S., Pizzo, P., Rippa, M. & Di Virgilio, F. Oxidized ATP. An irreversible inhibitor of the macrophage purinergic P2Z receptor. *J Biol Chem* **268**, 8199-8203 (1993).

100. Michel, A.D., Kaur, R., Chessell, I.P. & Humphrey, P.P. Antagonist effects on human P2X(7) receptor-mediated cellular accumulation of YO-PRO-1. *Br J Pharmacol* **130**, 513-520 (2000).

101. Arumugam, T.V*., et al.* Contributions of LFA-1 and Mac-1 to brain injury and microvascular dysfunction induced by transient middle cerebral artery occlusion. *Am J Physiol Heart Circ Physiol* **287**, H2555-2560 (2004).

102. Marcus, A.J*., et al.* Formation of leukotrienes and other hydroxy acids during platelet-neutrophil interactions in vitro. *Biochem Biophys Res Commun* **109**, 130-137 (1982).

103. Freedman, J.E. & Loscalzo, J. Platelet-monocyte aggregates: bridging thrombosis and inflammation. *Circulation* **105**, 2130-2132 (2002).

104. Guckelberger, O*., et al.* Beneficial effects of CD39/ecto-nucleoside triphosphate diphosphohydrolase-1 in murine intestinal ischemia-reperfusion injury. *Thrombosis and Haemostasis* **91**, 576-586 (2004).

105. Hentzen, E.R*., et al.* Sequential binding of CD11a/CD18 and CD11b/CD18 defines neutrophil capture and stable adhesion to intercellular adhesion molecule-1. *Blood* **95**, 911-920 (2000).

106. Lambrecht, G. Agonists and antagonists acting at P2X receptors: selectivity profiles and functional implications. *Naunyn Schmiedebergs Arch Pharmacol* **362**, 340-350 (2000).

107. Di Virgilio, F. Liaisons dangereuses: P2X(7) and the inflammasome. *Trends Pharmacol Sci* **28**, 465-472 (2007).

108. Soriano, S.G.*, et al.* Mice deficient in Mac-1 (CD11b/CD18) are less susceptible to cerebral ischemia/reperfusion injury. *Stroke* **30**, 134-139 (1999).

109. Hata, R.*, et al.* A reproducible model of middle cerebral artery occlusion in mice: hemodynamic, biochemical, and magnetic resonance imaging. *J Cereb Blood Flow Metab* **18**, 367-375 (1998).

110. Yegutkin, G.G., Samburski, S.S. & Jalkanen, S. Soluble purine-converting enzymes circulate in human blood and regulate extracellular ATP level via counteracting pyrophosphatase and phosphotransfer reactions. *FASEB J* **17**, 1328-1330 (2003).

111. Thompson, L.F.*, et al.* Ecto-5'-nucleotidase activity in T and B lymphocytes from normal subjects and patients with congenital X-linked agammaglobulinemia. *J Immunol* **123**, 2475-2478 (1979).

112. Day, S.M.*, et al.* Macrovascular thrombosis is driven by tissue factor derived primarily from the blood vessel wall. *Blood* **105**, 192-198 (2005).

113. Michelson, A., Barnard, M., Krueger, L., Valeri, C. & Furman, M. Circulating monocyte-platelet aggregates are a more sensitive marker of in vivo platelet acivation than platelet surface P-selectin: studies in baboons, human coronary intervention, and human acute myocardial infarction. *Circulation* **104**, 1533-1537 (2001).

114. Jackson Labs Molecular Genotyping Laboratory. Tg(pPGKneobpA)3Ems, Quantitative PCR, Version 1. in *JAX®Mice Protocol Index* (http://jaxmice.jax.org/pub-cgi/protocols/protocols.sh?objtype=protocol&protocol_id=1646, 2008).

115. Soliman, G.A.*, et al.* A simple qPCR-based method to detect correct insertion of homologous targeting vectors in murine ES cells. *Transgenic Res* **16**, 665-670 (2007).

116. Coppi, M.V. & Guidotti, G. Intracellular localization of Na,K-ATPase alpha2 subunit mutants. *Arch Biochem Biophys* **346**, 312-321 (1997).

117. Cao, C., Lawrence, D.A., Strickland, D.K. & Zhang, L. A specific role of integrin Mac-1 in accelerated macrophage efflux to the lymphatics. *Blood* **106**, 3234-3241 (2005).

118. Chopp, M.*, et al.* Postischemic administration of an anti-Mac-1 antibody reduces ischemic cell damage after transient middle cerebral artery occlusion in rats. *Stroke* **25**, 869-875; discussion 875-866 (1994).

119. Ross, R. Atherosclerosis--an inflammatory disease. *N Engl J Med* **340**, 115-126 (1999).

120. Fitzgerald, D.J., Roy, L., Catella, F. & FitzGerald, G.A. Platelet activation in unstable coronary disease. *N Engl J Med* **315**, 983-989 (1986).

121. Rinder, C.S.*, et al.* Cardiopulmonary bypass induces leukocyte-platelet adhesion. *Blood* **79**, 1201-1205 (1992).

122. van Zanten, G.H.*, et al.* Increased platelet deposition on atherosclerotic coronary arteries. *J Clin Invest* **93**, 615-632 (1994).

123. Silverstein, R.L. & Nachman, R. Thrombospondin binds to monocytes-macrophages and mediates platelet-monocyte adhesion. *Journal of Clinical Investigation* **79**, 867-874 (1987).

124. Silverstein, R.L., Asch, A. & Nachman, R. Glycoprotein IV mediates thrombospondin-dependent platelet-monocyte and platelet-U937 cell adhesion. *Journal of Clinical Investigation* **84**, 546-552 (1989).

125. Michelson, A.D., Barnard, M.R., Krueger, L.A., Valeri, C.R. & Furman, M.I. Circulating monocyte-platelet aggregates are a more sensitive marker of in vivo platelet activation than platelet surface P-selectin: studies in baboons, human coronary intervention, and human acute myocardial infarction. *Circulation* **104**, 1533-1537 (2001).

126. Furman, M.I.*, et al.* Circulating monocyte-platelet aggregates are an early marker of acute myocardial infarction. *J Am Coll Cardiol* **38**, 1002-1006 (2001).

127. Huo, Y.*, et al.* Circulating activated platelets exacerbate atherosclerosis in mice deficient in apolipoprotein E. **9**, 61-67 (2003).

128. Massberg, S.*, et al.* A critical role of platelet adhesion in the initiation of atherosclerotic lesion formation. *J Exp Med* **196**, 887-896 (2002).

129. Schober, A.*, et al.* Deposition of platelet RANTES triggering monocyte recruitment requires P-selectin and is involved in neointima formation after arterial injury. *Circulation* **106**, 1523-1529 (2002).

130. Mendelsohn, M.E. & Loscalzo, J. Role of platelets in cholesteryl ester formation by U-937 cells. *J Clin Invest* **81**, 62-68 (1988).

131. Kockx, M.M.*, et al.* Phagocytosis and macrophage activation associated with hemorrhagic microvessels in human atherosclerosis. *Arterioscler Thromb Vasc Biol* **23**, 440-446 (2003).

132. Wang, T.F. & Guidotti, G. CD39 is an ecto-(Ca2+,Mg2+)-apyrase. *J.Biol.Chem.* **271**, 9898-9901 (1996).

133. Gayle, R.B., III*, et al.* Inhibition of platelet function by recombinant soluble ecto-ADPase/CD39. *J.Clin.Invest* **101**, 1851-1859 (1998).

134. Labasi, J.M.*, et al.* Absence of the P2X7 Receptor Alters Leukocyte Function and Attenuates an Inflammatory Response. *J Immunol* **168**, 6436-6445 (2002).

135. Hyman, M.C.*, et al.* Self-regulation of inflammatory cell trafficking in mice by the leukocyte surface apyrase CD39. *J Clin Invest* (2009).

136. Kittel, A., Kiss, A.L., Mullner, N., Matko, I. & Sperlagh, B. Expression of NTPDase1 and caveolins in human cardiovascular disease. *Histochemical Cell Biology* **124**, 53-61 (2005).

137. Kohler, D.*, et al.* CD39/ectonucleoside triphosphate diphosphohydrolase 1 provides myocardial protection during cardiac ischemia/reperfusion injury. *Circulation* **116**, 1784-1794 (2007).

138. Dwyer, K.M.*, et al.* Thromboregulatory manifestations in human CD39 transgenic mice and the implications for thrombotic disease and transplantation. *J Clin Invest* **113**, 1440-1446 (2004).

139. Podrez, E.A.*, et al.* Platelet CD36 links hyperlipidemia, oxidant stress and a prothrombotic phenotype. *Nat Med* **13**, 1086-1095 (2007).

140. Ricci, R.*, et al.* Requirement of JNK2 for scavenger receptor A-mediated foam cell formation in atherogenesis. *Science* **306**, 1558-1561 (2004).

141. El-Omar, M.M.*, et al.* The ratio of ADP- to ATP-ectonucleotidase activity is reduced in patients with coronary artery disease. *Thromb Res* **116**, 199-206 (2005).

142. Hatakeyama, K.*, et al.* Relation of CD39 to plaque instability and thrombus formation in directional atherectomy specimens from patients with stable and unstable angina pectoris. *Am J Cardiol* **95**, 632-635 (2005).

143. Robson, S.C.*, et al.* Loss of ATP diphosphohydrolase activity with endothelial cell activation. *J Exp Med* **185**, 153-163 (1997).

144. Hyman, M. BMT Stroke. *dunno* (2009).

145.   Kittel, A. Lipopolysaccharide treatment modifies pH- and cation-dependent ecto-ATPase activity of endothelial cells. *J Histochem Cytochem* **47**, 393-400 (1999).

146.   Piedrahita, J.A., Zhang, S.H., Hagaman, J.R., Oliver, P.M. & Maeda, N. Generation of mice carrying a mutant apolipoprotein E gene inactivated by gene targeting in embryonic stem cells. *Proc Natl Acad Sci U S A* **89**, 4471-4475 (1992).

147.   Nunnari, J.J., Zand, T., Joris, I. & Majno, G. Quantitation of oil red O staining of the aorta in hypercholesterolemic rats. *Exp Mol Pathol* **51**, 1-8 (1989).

148.   Qu, C.*, et al.* Role of CCR8 and other chemokine pathways in the migration of monocyte-derived dendritic cells to lymph nodes. *J Exp Med* **200**, 1231-1241 (2004).

149.   Geissmann, F., Jung, S. & Littman, D.R. Blood monocytes consist of two principal subsets with distinct migratory properties. *Immunity* **19**, 71-82 (2003).

150.   Kraemer, R.*, et al.* Decreased neurotrophin TrkB receptor expression reduces lesion size in the apolipoprotein E-null mutant mouse. *Circulation* **112**, 3644-3653 (2005).

151.   Resnick, N. & Gimbrone, M.A., Jr. Hemodynamic forces are complex regulators of endothelial gene expression. *FASEB J* **9**, 874-882 (1995).

152.   Davies, P.F. Flow-mediated endothelial mechanotransduction. *Physiol Rev* **75**, 519-560 (1995).

153.   Jongstra-Bilen, J.*, et al.* Low-grade chronic inflammation in regions of the normal mouse arterial intima predisposed to atherosclerosis. *J Exp Med* **203**, 2073-2083 (2006).

154.   Dai, G.*, et al.* Distinct endothelial phenotypes evoked by arterial waveforms derived from atherosclerosis-susceptible and -resistant regions of human vasculature. *Proc Natl Acad Sci U S A* **101**, 14871-14876 (2004).

155.   Ku, D.N., Giddens, D.P., Zarins, C.K. & Glagov, S. Pulsatile flow and atherosclerosis in the human carotid bifurcation. Positive correlation between plaque location and low oscillating shear stress. *Arteriosclerosis* **5**, 293-302 (1985).

156.   Hyman, M.C. Ecto-enzymatic suppression of atherogensis. *?* (?).

157.   Suo, J.*, et al.* Hemodynamic shear stresses in mouse aortas: implications for atherogenesis. *Arterioscler Thromb Vasc Biol* **27**, 346-351 (2007).

158.   SenBanerjee, S.*, et al.* KLF2 Is a novel transcriptional regulator of endothelial proinflammatory activation. *J Exp Med* **199**, 1305-1315 (2004).

159.   Topper, J.N., Cai, J., Falb, D. & Gimbrone, M.A., Jr. Identification of vascular endothelial genes differentially responsive to fluid mechanical stimuli: cyclooxygenase-2, manganese superoxide dismutase, and endothelial cell nitric oxide synthase are selectively up-regulated by steady laminar shear stress. *Proc Natl Acad Sci U S A* **93**, 10417-10422 (1996).

160.   Lin, Z.*, et al.* Kruppel-like factor 2 (KLF2) regulates endothelial thrombotic function. *Circ Res* **96**, e48-57 (2005).

161.   Dekker, R.J.*, et al.* KLF2 provokes a gene expression pattern that establishes functional quiescent differentiation of the endothelium. *Blood* **107**, 4354-4363 (2006).

162.   Kuo, C.T.*, et al.* The LKLF transcription factor is required for normal tunica media formation and blood vessel stabilization during murine embryogenesis. *Genes Dev* **11**, 2996-3006 (1997).

163.   Parmar, K.M.*, et al.* Integration of flow-dependent endothelial phenotypes by Kruppel-like factor 2. *J Clin Invest* **116**, 49-58 (2006).

164.   Dekker, R.J.*, et al.* Prolonged fluid shear stress induces a distinct set of endothelial cell genes, most specifically lung Kruppel-like factor (KLF2). *Blood* **100**, 1689-1698 (2002).

165.   Schonbeck, U. & Libby, P. Inflammation, immunity, and HMG-CoA reductase inhibitors: statins as antiinflammatory agents? *Circulation* **109**, II18-26 (2004).

166.   Parmar, K.M.*, et al.* Statins exert endothelial atheroprotective effects via the KLF2 transcription factor. *J Biol Chem* **280**, 26714-26719 (2005).

167.   Sen-Banerjee, S.*, et al.* Kruppel-like factor 2 as a novel mediator of statin effects in endothelial cells. *Circulation* **112**, 720-726 (2005).

168.   Sorescu, G.P.*, et al.* Bone morphogenic protein 4 produced in endothelial cells by oscillatory shear stress stimulates an inflammatory response. *J Biol Chem* **278**, 31128-31135 (2003).

169.   Kittel, A., Csapo, Z.S., Csizmadia, E., Jackson, S.W. & Robson, S.C. Co-localization of P2Y1 receptor and NTPDase1/CD39 within caveolae in human placenta. *Eur J Histochem* **48**, 253-259 (2004).

170.   Kittel, A.*, et al.* CD39 as a caveolar-associated ectonucleotidase. *Biochem Biophys Res Commun* **262**, 596-599 (1999).

171.   Tuomisto, T.T.*, et al.* Simvastatin has an anti-inflammatory effect on macrophages via upregulation of an atheroprotective transcription factor, Kruppel-like factor 2. *Cardiovasc Res* **78**, 175-184 (2008).

172. Stenestrand, U. & Wallentin, L. Early statin treatment following acute myocardial infarction and 1-year survival. *JAMA* **285**, 430-436 (2001).

173. Association, A.H. Heart Disease and Stroke Statistics - 2005 Update. *Dallas, Texas. American Heart Association* (2005).

174. Beldi, G.*, et al.* Natural killer T cell dysfunction in CD39-null mice protects against concanavalin A-induced hepatitis. *Hepatology* **48**, 841-852 (2008).

175. Seimon, T.A.*, et al.* Macrophage deficiency of p38alpha MAPK promotes apoptosis and plaque necrosis in advanced atherosclerotic lesions in mice. *J Clin Invest* **119**, 886-898 (2009).

176. Goldschmidt-Clermont, P.J.*, et al.* Atherosclerosis 2005: recent discoveries and novel hypotheses. *Circulation* **112**, 3348-3353 (2005).

177. Roh, M., Kim, J., Song, C., Wills, M. & Abdulkadir, S.A. Transgenic mice for Cre-inducible overexpression of the oncogenes c-MYC and Pim-1 in multiple tissues. *Genesis* **44**, 447-453 (2006).

178. Inoue, H.*, et al.* Transcriptional and posttranscriptional regulation of cyclooxygenase-2 expression by fluid shear stress in vascular endothelial cells. *Arterioscler Thromb Vasc Biol* **22**, 1415-1420 (2002).

179. Yamamoto, K.*, et al.* Impaired flow-dependent control of vascular tone and remodeling in P2X4-deficient mice. *Nat Med* **12**, 133-137 (2006).